# KALMAN FILTER BASED APPLICATIONS FOR HELICOPTERS

A THESIS SUBMITTED TO
THE GRADUATE SCHOOL OF NATURAL AND APPLIED SCIENCES
OF
MIDDLE EAST TECHNICAL UNIVERSITY

BY

MERVE OKATAN

IN PARTIAL FULFILLMENT OF THE REQUIREMENTS
FOR
THE DEGREE OF MASTER OF SCIENCE
IN
AEROSPACE ENGINEERING

SEPTEMBER 2014

Approval of the thesis:

**KALMAN FILTER BASED APPLICATIONS FOR HELICOPTERS**

submitted by **MERVE OKATAN** in partial fulfillment of the requirements for the degree of **Master of Science in Aerospace Engineering Department, Middle East Technical University** by,

Prof. Dr. Canan Özgen _____
Dean, Graduate School of **Natural and Applied Sciences**

Prof. Dr. Ozan Tekinalp _____
Head of Department, **Aerospace Engineering**

Assoc. Prof. Dr. İlkay Yavrucuk _____
Supervisor, **Aerospace Engineering Department, METU**

**Examining Committee Members:**

Prof. Dr. Ozan Tekinalp
Aerospace Engineering Department, METU _____

Assoc. Prof. Dr. İlkay Yavrucuk
Aerospace Engineering Department, METU _____

Prof. Dr. M. Kemal Leblebicioğlu
Electrical and Electronics Engineering, METU _____

Assoc. Prof. Dr. Tayfun Çimen
System Design and Control Engineer, ROKETSAN _____

Assist. Prof. Dr. Ali Türker Kutay
Aerospace Engineering Department, METU _____

**Date:** _____

**I hereby declare that all information in this document has been obtained and presented in accordance with academic rules and ethical conduct. I also declare that, as required by these rules and conduct, I have fully cited and referenced all material and results that are not original to this work.**

Name, Last Name: MERVE OKATAN

Signature :

# ABSTRACT

KALMAN FILTER BASED APPLICATIONS FOR HELICOPTERS

Okatan, Merve
M.S., Department of Aerospace Engineering
Supervisor : Assoc. Prof. Dr. İlkay Yavrucuk

September 2014, 99 pages

The study in this thesis comprises Kalman Filter based applications for helicopters. In the first part of this thesis, a Kalman filter for a helicopter is designed to integrate micro-electromechanical sensors with the Global Navigation Satellite Systems to achieve desired accuracy levels. It is implemented to a non-linear helicopter model and its performance is shown through simulations. In the second part of this thesis, Kalman Filter approach is adopted to neural network based adaptive controllers as a modification term in the update law. In order to control the attitude of the helicopter, a linear model inversion based controller with a neural network adaptive element is implemented, and its modification term is designed using a Kalman Filter approach. The approach is compared with other existing modification terms in the literature through simulations.

Keywords: helicopter, Kalman filter, navigation, adaptive control

# ÖZ

HELİKOPTERLERDE KALMAN FİLTRE UYGULAMALARI

Okatan, Merve
Yüksek Lisans, Havacılık ve Uzay Mühendisliği Bölümü
Tez Yöneticisi : Doç. Dr. İlkay Yavrucuk

Eylül 2014 , 99 sayfa

Bu tez, helikopterler için Kalman Filtre tabanlı uygulamaları içermektedir. Bu tezin ilk kısmında, bir Kalman Filtresi, hedeflenen doğruluk hassasiyetini sağlamak amacıyla mikro-elektromekanik sensörleri ve Küresel Konumlama Sistemlerini tümleştirmek için tasarlanmıştır. Bu tümleşim algoritması doğrusal olmayan bir helikopter modeline entegre edilmiş ve performansı simülasyon ortamında gösterilmiştir. Bu tezin ikinci kısmında ise Kalman filtresi yaklaşımı, yapay sinir ağı tabanlı bir adaptif kontrolcünün güncelleme kuralında, modifikasyon terimi olarak kullanılmıştır. Helikopterin yönelimini kontrol edecek doğrusal model çevrimi tabanlı bir kontrolcü, yapay sinir ağı tabanlı adaptif eleman ile birlikte uygulanmış ve modifikasyon terimi Kalman filtresi yaklaşımı ile tasarlanmıştır. Bu yaklaşım literatürde bulunan modifikasyon terimleri ile simülasyon ortamında karşılaştırılmıştır.

Anahtar Kelimeler: helikopter, Kalman filtresi, navigasyon, adaptif kontrol

*to my family*

# ACKNOWLEDGMENTS

I would like to express the deepest appreciation to my supervisor Dr. İlkay Yavrucuk for guiding me to the right direction and encouraging me throughout the thesis study. Without his enthusiasm, energy and support, this thesis would not have been possible.

I want to emphasize my special thanks to Gönenç Gürsoy who guided and assisted me. I would never progressed and finished my thesis without him. I also wish to state my thanks to Onur Tarımcı for sharing his knowledge with me and helping me throughout the thesis.

I would like to thank my colleague in Roketsan, Ongun Kurt for sharing his time, energy and knowledge whenever I needed. He always helped me with useful discussions. I would also like to thank Celâl Ada for the discussions and support.

I would like to express my thanks to Ahmet Emre Topbaş for his endless support, trust and encouragement. He always believed and supported me while I was struggled with my work.

Last but not least, I would like to thank my family for their love and support throughout my life. They have always had faith in me.

# TABLE OF CONTENTS

# LIST OF TABLES

TABLES

# LIST OF FIGURES

FIGURES

# LIST OF ABBREVIATIONS

| | |
|---|---|
| $A$ | Full System Matrix |
| $A_1$ | System Matrix Containing the Effects of Rotationals States on Themselves |
| $A_2$ | System Matrix Containing the Effects of Translational States on Rotational States |
| $B$ | Full Control Matrix |
| $B_1$ | Control Matrix Containing the Effects of Longitudinal, Lateral and Pedal Controls on Rotational States |
| $b$ | Bias Error |
| $b_1$ | Neural Network Bias Term |
| $C$ | Measurement Innovation Covariance |
| $C_b^n$ | Transformation Matrix from Body Frame to Navigation Frame |
| $F$ | System Matrix of Error Propagation |
| $f_{ib}$ | Specific Force |
| $G$ | Matrix Containing the Effects of Noise on System States |
| $g$ | Gravitational Acceleration |
| $h$ | Altitude |
| $H$ | Measurement Matrix |
| $K$ | Controller Feedback Gain, Kalman Gain |
| $L$ | Latitude |
| $m$ | Misalignment Error |
| $M$ | Matrix Containing Scale-Factor and Misalignment Errors |
| $P$ | Error Covariance Matrix |
| $Q$ | System Noise Qovariance Matrix |
| $R$ | Measurement Noise Covariance Matrix |
| $R_0$ | Equatorial Radius of Earth |
| $p$ | Body Roll Rate |
| $q$ | Body Pitch Rate |
| $r$ | Body Yaw Rate |

| | |
|---|---|
| $s$ | Scale-Factor Error |
| $u$ | Full Control Input Vector |
| $u_1$ | Control Input Vector Containing Longitudinal, Lateral and Pedal Controls |
| $U_\phi, U_\theta, U_\psi$ | Pseudo Controls |
| $U_{PD}$ | Output of the PD Controller |
| $U_{NN}$ | Output of the NN Controller |
| $u$ | Body Velocity in x-axis |
| $v$ | Body Velocity in y-axis |
| $w$ | Body Velocity in z-axis |
| $V$ | Velocity Vector |
| $W, V$ | Neural Network Weights |
| $x$ | Full State Vector |
| $x_1$ | Rotational States |
| $x_2$ | Translational States |
| $x_k$ | Kalman Filter State Vector |
| $z$ | Measurement Vector |
| $\Delta(x, \dot{x}, u)$ | Modelling Error, Uncertainty |
| $\delta_{long}$ | Longitudinal Control |
| $\delta_{lat}$ | Lateral Control |
| $\delta_{coll}$ | Collective Control |
| $\delta_{ped}$ | Pedal Control |
| $\Delta$ | Difference From Trim |
| $\beta$ | Neuron Activation Function |
| $\gamma, \Gamma_w, \Gamma_v$ | Neural Network Learning Rates |
| $\sigma$ | Neural Network Modification Gain |
| $\lambda$ | Longitude |
| $\Phi$ | State Transition Matrix |
| $\phi$ | Roll Angle |
| $\theta$ | Pitch Angle |
| $\psi$ | Yaw Angle |
| $\Psi$ | Attitude |
| $\omega$ | Random Noise |
| $\omega_{ib}$ | Angular rate |

**Subscripst and Superscripts**

| | |
|---|---|
| $()_{acc}$ | Accelerometer |
| $()_{gyr}$ | Gyroscope |
| $()_D$ | Desired |
| $()_{com}$ | Output of the Command Filter |
| $()_{sys}$ | Output of the System |
| $()_m$ | Reference Model |
| $()_N$ | North |
| $()_E$ | East |
| $()_D$ | Down |
| $()^T$ | Transpose of a Matrix |
| $()_k$ | Before Time Update |
| $()_{k+1}$ | After Time Update |
| $()^-$ | Before Measurement Update |
| $()^+$ | After Measurement Update |
| $\dot{()}$ | First Derivative with respect to Time |
| $\ddot{()}$ | Second Derivative with respect to Time |
| $\hat{()}$ | Estimation |

**Acronyms**

| | |
|---|---|
| $DGPS$ | Differential Global Positioning System |
| $DOF$ | Degree-of-Freedom |
| $ECEF$ | Earth Centered Earth Frame |
| $GPS$ | Global Positioning System |
| $GNSS$ | Global Navigation Satellite System |
| $INS$ | Inertial Navigation System |
| $IMU$ | Inertial Measurement Unit |
| $KF$ | Kalman Filter |
| $LPNN$ | Linear-in-the-Parameter Neural Network |
| $MEMS$ | Micro-Electro Mechanical Sensors |
| $MRAC$ | Model Reference Adaptive Control |
| $NN$ | Neural Networks |
| $PD$ | Proportional-Derivative |
| $PID$ | Proportional-Integral-Derivative |
| $SHLNN$ | Single Hidden Layer Neural Network |

| | |
|---|---|
| $UAV$ | Unmanned Aerial Vehicle |
| $VTOL$ | Vertical Take-off Landing |
| $WGS84$ | World Geodetic System |

# CHAPTER 1

# INTRODUCTION

Control systems together with navigation systems of airborne vehicles are of primary interest of research in aviation. Many improvements are being presented throughout the literature. In navigation systems, some improvements are on inertial sensors and on the navigation algorithms to enhance the precision. In control systems, recent research has focused on the control of nonlinear systems, to deal with uncertainties of nonlinear systems and to achieve autonomous flights.

A development achieved in recent years on sensors are the Micro-Electromechanical Sensors (MEMS) which replace big, heavy and expensive systems. However, these advantages come with a drawback: Accuracy of MEMS is less compared to its counterparts. Thus, to use MEMS, additional work is needed in software, and this is a challenging task when the system is nonlinear and the uncertainties exist in the system and noise in measurements.

In control systems, various techniques are developed to deal with nonlinearities and uncertainties. Some well-known popular techniques are Robust Control and Adaptive Control. Adaptive control is an efficient method dealing with uncertainties. Often it does not require prior information about the bounds of uncertainties. Recently, performance enhancements in adaptive control have been achieved by developing different neural network structures and augmenting the baseline adaptation law with modification terms. The ultimate goal of the modifications in adaptive control is to enhance the baseline adaptive law to achieve an optimum modeling error compensation.

In this thesis work, a high-fidelity helicopter is used to develop navigation and con-

trol system by using Kalman Filter optimization algorithm. Each application is a challenging task due to helicopter's nonlinear nature and the uncertainties present in the system.

Firstly, a navigation system for a helicopter is developed. Sensor models are constructed by considering the error characteristics and their contribution to the error budget. The navigation algorithms are developed to obtain attitude, velocity and position of the helicopter from the sensor outputs, namely specific forces and angular rotations. The main objective of the study is to obtain an accurate navigation solution with low cost inertial sensors. Therefore, a Kalman Filter is designed to integrate the Inertial Navigation System solution with the Global Navigation Satellite System.

Another objective of this thesis is the use of Kalman Filter approach in neural network based adaptive control. For this purpose, a controller is designed for the helicopter's attitude control. The helicopter control inputs are obtained by implementing the linear model inversion method. However, due to linearization and modelling errors, uncertainties arise in the system. To compensate for those uncertainties, the controller is augmented with neural networks. Kalman Filter approach is implemented to the modification term of the adaptive weight update law of neural networks. The purpose is to demonstrate the improvement of the Kalman Filter approach in the system response and in control input compared to its alternatives.

All algorithms are tested in simulations. The model used in simulations is a high-fidelity helicopter model. Component build-up is used to generate a nonlinear 6 degree-of-freedom (DOF) simulation model. Models for each helicopter component, such as the main rotor, tail rotor, fuselage, landing gear, etc. are formed by using geometric, inertial and aerodynamic parameters of that component. Main rotor model was modeled using Peters- He Finite State Dynamic Wake model with second order flapping dynamics. Tail rotor was constructed using Blade Element Momentum Theory. The model combines the external forces and moments of each component at the center of gravity of the aircraft. From the non-linear model, trim conditions can be found and the model can be linearized around the equilibrium points [1].

## 1.1 Literature Survey

Use of Kalman Filter to integrate different sensors have been studied and implemented for several applications in the past decades. In 1999, Jun et al. [2] studied Kalman Filtering to combine inertial sensors, inclinometers and Global Positioning Systems (GPS) to estimate the accurate navigation solution of a robot helicopter. Two Kalman Filters were used in this study which avoids dynamic modeling of the system. In 2004, Choukroun et al. [3] presented a novel Kalman Filter to estimate attitude errors and gyroscope drifts for spacecraft applications by constructing the error equations with quaternions. The study results showed that the proposed filter is efficient when the initial estimation errors are high, where typical extended Kalman Filter fails. Godha and Cannon [4] used Differential Global Positioning System (DGPS) to aid the MEMS-based navigation solution and to estimate the errors for a land vehicle application. In this study [4], performance of MEMS type sensors in integrated navigation were compared with tactical grade sensors and it was shown that sub-meter level performance can be achieved also with low cost sensors when there is no signal outage. Another study was carried out for the attitude determination of hovering and vertical take-off, landing systems (VTOL) [5]. In this paper [5], Gao et al. combined accelerometer and gyroscope outputs based on extended Kalman Filter. Another study including the integration of only the inertial sensors based on Kalman Filter was conducted for Unmanned Aerial Vehicle (UAV) applications [6]. YongLiang et al. [7], used Kalman Filter to combine inertial sensors with magnetometers for accurate estimation of attitude of a VTOL UAV. By Lau et al. [8], Kalman Filter based GPS/INS integration method was applied to unmanned miniature helicopter in 2010. In this study [8], new method was proposed against GNSS signal outages. Seung-Min Oh [9] proposed a new method for multisensor fusion by using unscented Kalman Filter. The new approach was analyzed with a 6-DOF UAV simulations and seen to be efficient in terms of accuracy and the ease of combining different types of sensors. In 2011, Pan et al. [10], proposed an unscented Kalman Filter for attitude estimation of a Miniature Unmanned Helicopter. Electronic compass was used with MEMS accelerometer and gyroscopes and it was shown that the proposed method is computationally efficient. Hieu et al. [11] applied loosely coupled GPS/INS integration for land vehicles in 2012. The results showed

that integrated navigation provides meter-level precision even if signal outages occur in short intervals. Another study concerning the GPS signal outage was carried out by Nakanishi et al. [12] for autonumous unmanned helicopter. In this paper, Kalman Filter was proposed for integration of INS, GPS and barometric altimeter to improve the reliability of the system on vertical channel and in case of signal outages.

In neural network based adaptive control the fundamental approach was established by Narendra et al. [13, 14] in 1970s. In 1984, Ioannou and Kokotovic [15] proposed a modification term called $\sigma$-modification. In this paper, $\sigma$-modification was shown to improve the damping of the baseline adaptive law to compensate for the weight drift when the neural network inputs are not persistently exciting. However, when the tracking error gets small, performance of this modification degrades. Narendra and Annaswamy [16] proposed a new term called e-modification to overcome this problem in 1987. With this modification term, norm of the tracking error is used to scale the damping of $\sigma$-modification. $Q$-modification was developed to use the integral of the tracking error over a finite time window by K. Y. Volyanskyy [17] and shown to be computationally intensive. An optimal control modification was introduced in 2010 by Nguyen et al. [18]. In this paper, it was shown that fast adaptation can be achieved without resulting in high gain control when the minimization of the squares of the tracking error is formulated as an optimal control problem [18]. Around the same times, $K$-modification was proposed by Kim et al.. In this study, stiffness term was added to the baseline adaptation law which can also be combined with damping terms like $\sigma$- and e-modification. This modification improves the transient performance. Moreover, in cases like control input delays, robustness of the adaptation is increased. In another study reported by the same authors, $K$-modification was combined with $H_2$ approach which provides an optimal variable gain [19, 20].

Another recent update to the method is proposed by Chowdhary et al. [21, 22]. It uses both recorded and instantaneous data in the update law. This approach is called concurrent learning. The method guarantees bounded weights around the optimal values for linearly parameterized uncertainty, even if the states are not persistently excited. Least square modification was used for concurrent learning. With this modification, an optimal estimate of the ideal weights can be achieved with smooth convergence.

Recently, it is shown that the modification terms that are summarized above can be expressed by taking the gradient of a norm of the constraint violation [23]. In this study, a new approach which forms an alternative method to the well-known existing modifications was proposed. In the method, a Kalman Filter optimization was used to reduce the violation of a linear constraint. This approach provides required tracking performance with less control effort especially for the case of high learning gain adaptation and existing sensor noise.

Recent research has focused on the control of the rotorcraft due to its nonlinearities and uncertainties. The controls and states are cross-coupled, hence, it is a challenging control problem. It is well known that the cross-coupled states in a helicopter can be controlled with model inversion and neural networks [24, 25, 26, 27]. These control strategies were applied to F/A-18 airplane [28], an AH-64 helicopter [29] and a tiltrotor aircraft [26].

## 1.2 Contribution of this Thesis

A comprehensive application of the Kalman Filter is applied to a high fidelity helicopter simulation. A Kalman Filter is designed to integrate MEMS inertial sensors and GNSS. Its performance is tested using a high-fidelity helicopter simulation to achieve accurate states. Similar work has been carried out in literature for small, unmanned helicopters. Moreover, attitude control system is developed for a full size helicopter. Adaptive control is applied by using neural networks to compensate for the uncertainties existing in the system. Kalman Filter approach is implemented as a modification term to the adaptation law as an original contribution, which is a novel technique in literature and has not been implemented to a helicopter yet.

## 1.3 Thesis Structure

The organization of the thesis is as follows. The INS/GNSS integration algorithm is presented in Chapter 2. MEMS and GNSS sensor models, inertial navigation algorithm and Kalman Filter algorithm are explained in detail. Simulation results of

the navigation system are also provided in this chapter. Kalman Filter approach in adaptive control as modification term is described in detail in Chapter 3. Structure of the controller and neural networks are detailed and e-modification is derived with Kalman Filter approach for two neural network structures. The simulation results of the KF-based e-modification are presented and compared with baseline adaptive law and standard e-modification for different maneuvers in this chapter. Finally, conclusions are summarized in Chapter 4 and future works are stated.

# CHAPTER 2

# KALMAN FILTER FOR HELICOPTER NAVIGATION

Inertial Measurement Units (IMU) have been one of the frequently used sensors in navigation applications. Various IMU sensors with different grades of accuracy are available for aviation, naval and land applications. The emerging technology in the area of IMUs is Micro-Electromechanical Systems (MEMS). MEMS sensors meet the demand for small, light sensors with low power consumption and low costs. These parameters make the inertial sensors suitable for a wide range of applications with limited space, payload capacity or budget.

The accuracy of the MEMS sensors are less compared to other traditional sensors. However, it is expected that the accuracy of the MEMS sensors will improve and will have a similar performance to its counterparts in future. Since inertial navigation is a dead-reckoning system, even the most accurate sensors will diverge from the real solution in time.

Other widely used technology in the navigation systems in recent years is Global Navigation Satellite Systems (GNSS). GNSS has global coverage and it provides high accuracy. Moreover, GNSS receiver prices are low compared to IMU sensors which have equivalent precision. The main drawback of the GNSS; however, is its dependency to external sources. The stand-alone use of GNSS generally does not meet the requirements of reliability for many applications due to signal outages or jamming conditions especially for military applications.

The drawbacks of these two navigation systems are overcome by combining the Inertial Navigation System (INS) and GNSS. By integrating these systems, drifting of

the INS solution and discontinuity in GNSS solution in case of signal outages are prevented. Thus, continuous solution is obtained while high accuracy is maintained.

Due to its convenience in terms of size and cost, MEMS inertial sensors are preferred in helicopters; therefore, GNSS aiding is necessary to improve the performance. In this chapter, INS/GNSS integration applied to a non-linear helicopter model is presented. First, detailed explanation over the Inertial Navigation System of the helicopter model is given. Second, the main concept of Global Navigation Satellite Systems is described. Finally, integration of these two systems is explained with detailed mathematical models of the systems.

## 2.1 Navigation Systems Preliminaries

### 2.1.1 Coordinate Systems

This section provides the coordinate systems that are used in the context of this thesis. Four different coordinate systems are used to define and represent the attitude, velocity and the position of the helicopter.

*Earth-Centered Inertial Frame*

This frame is a non-accelerating and non-rotating frame with respect to the fixed stars, which has its origin at the center of the Earth. The z-axis points through the North Pole, while the x- and y-axis lies in the equatorial plane. The inertial frame is denoted by ‘i’.

*Earth-Centered Earth-Fixed Frame*

The origin of this frame is at the center of the Earth and it rotates with the Earth. Z-axis points through the North Pole, x-axis lies in the equatorial plane and points the reference zero (Greenwich) meridian and the y-axis completes the frame according to the right-hand rule. The Earth frame is denoted by ‘e’.

*Body Frame*

The body frame is centered at the center of gravity of the helicopter. It moves and

rotates with the helicopter. X-axis points through the nose of the aircraft and z-axis points through the center of the Earth. Y-axis points to the right to form an orthogonal frame. The body frame is denoted by 'b'.

*Navigation Frame*

Navigation frame moves with the helicopter but it does not rotate with the helicopter. X-axis points through north, y-axis points through east and z-axis points through down direction. The navigation frame is denoted by 'n'.

**Notation:** For describing position and velocity, following notation is used throughout this work.

$$x^{\gamma}_{\alpha\beta}$$

Here, $x$ is the kinematic property of frame $\beta$ with respect to frame $\alpha$, expressed in the frame $\gamma$.

### 2.1.2 Inertial Navigation System

Inertial Navigation System (INS) consists of 3 accelerometers and 3 gyroscopes (IMU) and a navigation processor. Accelerometers measure specific force ($f_{ib}$) which can be defined as non-gravitational acceleration and gyroscopes measure angular rate ($\omega_{ib}$) of the body frame with respect to the inertial frame. Navigation processor computes the position, velocity and attitude of the vehicle (P, V, $\Psi$) by using the IMU sensor measurements, on the basis of an integration-based algorithm. Figure 2.1 shows the schematic of the Inertial Navigation System.

Navigation algorithm comprises of three main stages; namely attitude update, velocity update and position update. In addition, gravity model is necessary to obtain the total acceleration from the specific force. Attitude update is performed basically by integrating the angular rate measurements, velocity update is performed by integrating the total acceleration while position update is obtained by integrating the velocity. Navigation algorithm is an iterative process; therefore, initialization of the parameters is necessary.

Since the navigation solutions are obtained by integrating the sensor measurements,

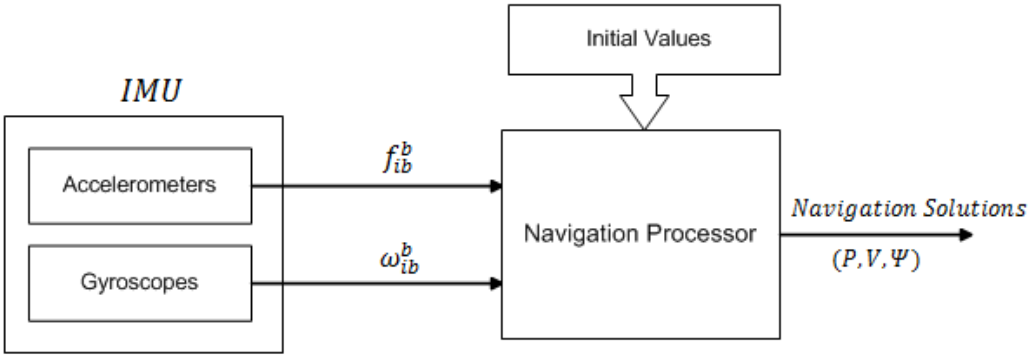


Figure 2.1: Schematic of INS

errors exhibited in sensors grow within time and this phenomenon causes drift in time from the true solution. Therefore, for long term applications, usage of solitary INS will result in incorrect navigation solution.

Below, advantages and disadvantages of the INS are summarized [30].

Advantages:

- It operates continuously,
- It provides high-bandwidth and high rate output,
- It operates everywhere without any need for external sources.

Disadvantages:

- Accuracy degrades with time,
- Initialization is necessary, (initial values of attitude, velocity and position)
- High accuracy systems are expensive and bulky.

### 2.1.3 Global Navigation Satellite System

Global Navigation Satellite Systems (GNSS) refer to navigation systems which provide the user three dimensional position and velocity solution by measuring ranges from satellite to user. Satellites and user receivers have accurate clocks which are

synchronized to transmit and receive the time-tagged signals, respectively. With the help of the difference between transmitted time and received time of the signals, range between the satellites and the user receiver can be calculated.

GNSS consists of three main segments which are space segment, control and ground segment and the user segment. Space segment consists of satellites which broadcast signals. Control segment monitor and control the satellites to synchronize and calibrate the clocks and to perform satellite maneuvers whenever necessary. User segment is the unit consisting of receivers and antennas which receives the signals and processes them to obtain navigation solution [30]. Figure 2.2 shows the architecture of the GNSS.

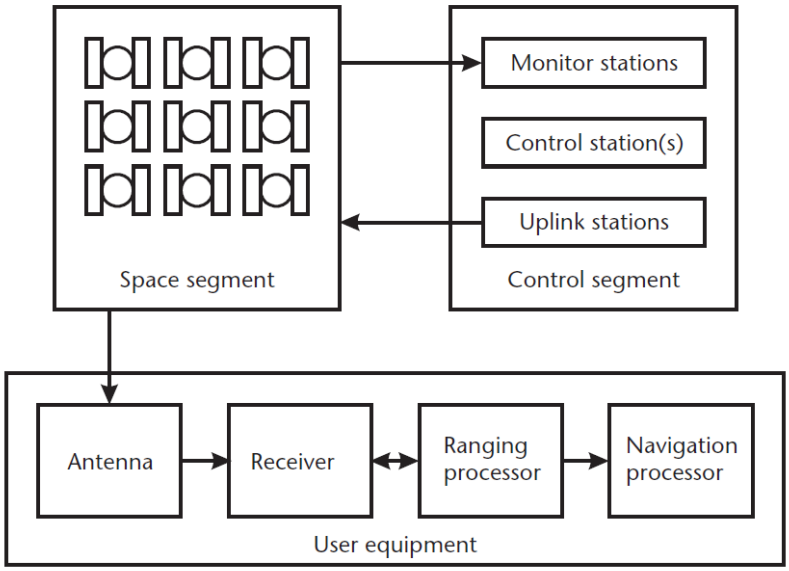


Figure 2.2: GNSS System Architecture

In order to calculate three-dimensional position and the clock error of the receiver, at least four satellites should be tracked by the GNSS receiver. The navigation solutions provided by GNSS are expressed in Earth Centered Earth Frame (ECEF). GNSS solutions are vulnerable to intentional or unintentional signal losses and jamming. Advantages and drawbacks of the usage of GNSS are given below [30].

Advantages:

- It provides global coverage,
- It provides high long term accuracy (a few meters),

- Accuracy does not degrade with time,
- Receiver prices are relatively low.

Disadvantages:

- It depends on external signals to operate,
- Output rate is low,
- It does not provide attitude solution,
- Signal outages may occur easily.

### 2.1.4 INS/GNSS Integration

Advantages and drawbacks of the INS and GNSS stated in previous sections are complementary; therefore, integrating their solution provides continuous and accurate solution in short and long term with high output rate. GNSS prevents the INS solution diverging from the true solution and INS provides continuous output in case of signal outages. This integration also makes possible to use low cost inertial sensors such as MEMS which cannot provide acceptable accuracy levels when used alone.

Multi-sensor fusion is generally performed by using Kalman filter. Kalman filter is a complementary filter used in order to separate the error from the signal by using more than one measurements of the same signal. It gives optimal estimations for linear Gaussian systems. Figure 2.3 demonstrates the basic principle of the Kalman filter.

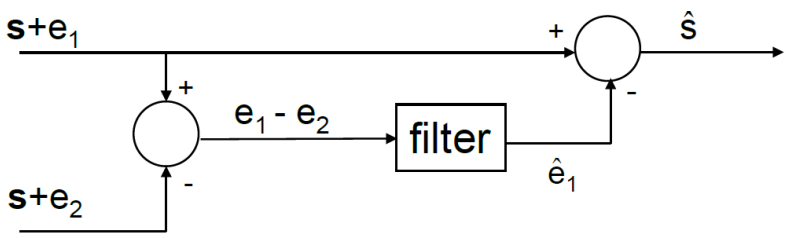


Figure 2.3: Complementary Filtering

In complementary filtering, it is important to identify the characteristics of the parameters that are desired to be separated. Since the errors in the signals are demanded to be eliminated in INS/GNSS integration, error characteristics of the signals should be defined to the filter properly. By the filter, errors are estimated based on the defined characteristics and they are eliminated from the original signal.

### 2.1.5 Helicopter Simulation Application

As an example application, Kalman Filter is implemented to a helicopter model which is a non-linear 6 degree-of-freedom (DOF) simulation model. Model is constructed by using component build-up method and the main components are such as main rotor, tail rotor, fuselage and landing gear [27]. For this work, the model is linearized around the 60 knots forward flight equilibrium point and the Kalman Filter is integrated to this model to analyze the performance.

In the helicopter model, a Flat Earth assumption is used, which means that the gravitational acceleration is constant regardless of the position of the vehicle. Moreover, the rotation of Earth is also neglected and therefore the earth frame becomes the inertial frame. Navigation and Kalman Filter algorithms are modeled, accordingly.

The overall system is illustrated with a block diagram in Figure 2.4.

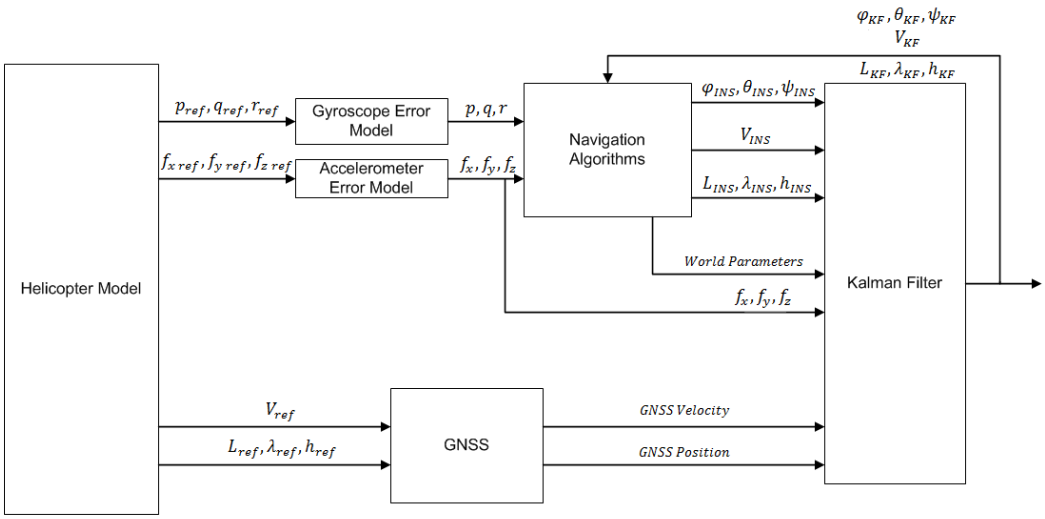


Figure 2.4: Block Diagram of the System

## 2.2 Theory

Integrated navigation system consists of IMU sensor model, algorithms to obtain navigation solutions and Kalman filter algorithm to perform INS/GNSS integration. In this section, methods and formulations used to form the integrated navigation system of the helicopter model are given in detail.

### 2.2.1 Sensor Model

Accelerometers and gyroscopes contain characteristic errors which can be constant or random. All types of sensors exhibit those errors, even the most accurate ones. However, order of the errors differs according to the type of the sensor. The most effective errors which contribute to the error budget are bias, scale-factor, axis misalignment and random noise. In this subsection, error types are explained and their contribution to the total error is investigated.

#### 2.2.1.1 Bias Error

Bias error is a constant error independent of the output of the sensors. In most cases, it is the dominant error type.

$$b_{acc} = \begin{bmatrix} b_{acc,x} & b_{acc,y} & b_{acc,z} \end{bmatrix} \tag{2.1}$$

$$b_{gyr} = \begin{bmatrix} b_{gyr,x} & b_{gyr,y} & b_{gyr,z} \end{bmatrix} \tag{2.2}$$

Bias drift is assumed to be zero ($ie, \dot{b} = 0$). Bias error may change turn-on to turn-on; however, it remains constant during the run.

Errors are represented in body-axis frame and subscripts ‘acc’ and ‘gyr’ refer to accelerometer and gyroscope, respectively.

#### 2.2.1.2 Scale-Factor and Misalignment Errors

Scale-factor error is the deviation of the sensor input-output gradient from the unity. It is represented with ‘*parts per million (ppm)*’. For instance, a sensor having 1 ppm

scale factor error gives the output 1.000001 times the actual measurement.

Misalignment errors occur due to the deterioration of the orthogonality of the sensitive axis due to manufacturing limitations. Scale-factor and misalignment errors can be expressed as the below matrices.

$$M_{acc} = \begin{bmatrix} s_{acc,x} & m_{acc,xy} & m_{acc,xz} \\ m_{acc,yx} & s_{acc,y} & m_{acc,yz} \\ m_{acc,zx} & m_{acc,zy} & s_{acc,z} \end{bmatrix} \tag{2.3a}$$

$$M_{gyr} = \begin{bmatrix} s_{gyr,x} & m_{gyr,xy} & m_{gyr,xz} \\ m_{gyr,yx} & s_{gyr,y} & m_{gyr,yz} \\ m_{gyr,zx} & m_{gyr,zy} & s_{gyr,z} \end{bmatrix} \tag{2.3b}$$

#### 2.2.1.3 Random Noise

All inertial sensors exhibit random noise due to various sources like electrical or mechanical instabilities.

The contribution of the aforementioned error sources is modeled by Groves [30] as given in equations 2.4 and 2.5 for accelerometers and gyroscopes, respectively.

$$\tilde{f}^b_{ib} = b_{acc} + (I_3 + M_{acc}) f^b_{ib} + w_{acc} \tag{2.4}$$

$$\tilde{\omega}^b_{ib} = b_{gyr} + (I_3 + M_{gyr}) \omega^b_{ib} + w_{gyr} \tag{2.5}$$

$f^b_{ib}$ and $\omega^b_{ib}$ represent the true counterparts of the measurements, while $\tilde{f}^b_{ib}$ and $\tilde{\omega}^b_{ib}$ represent the actual outputs. Superscripts represent the resolving axis system which is the body frame.

Inertial sensors are chosen as MEMS for helicopter model due to its advantages in size, weight and budget. In Table 2.1, specifications of the sensors are given.

Inertial sensors' output rate is 100 Hz.

Accelerometer and gyroscope outputs of the helicopter model having above characteristics are illustrated in figure 2.5(a) and 2.5(b).

Table 2.1: Inertial Sensor Error Characteristics

| **Error Characteristics** | **Gyroscopes** | **Accelerometers** |
|---|---|---|
| **Bias** | 200 deg/hr | 50 mg |
| **Scale Factor** | 1400 ppm | 1500 ppm |
| **Misalignment** | 0.5 mrad | 0.5 mrad |
| **Random Walk** | 7 deg/hr/$\sqrt{Hz}$ | 1000 $\mu$g/$\sqrt{Hz}$ |

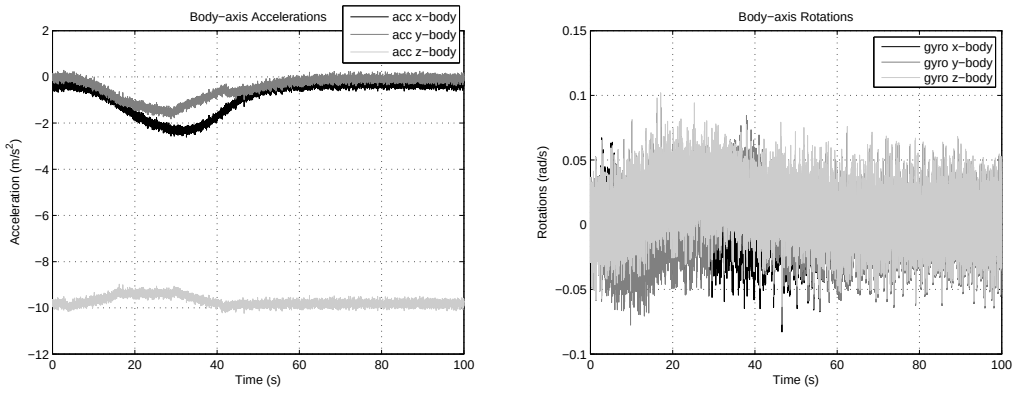


(a) Accelerometer Output

(b) Gyroscope Output

Figure 2.5: Helicopter Accelerometer and Gyroscope Outputs

### 2.2.2 GNSS Model

GNSS provides navigation solution in the order of a few meters which does not deteriorate with time. With this point of view, GNSS model is constructed by adding zero mean Gaussian noise to the true navigation solution for simulation purposes. Besides, GNSS provides the position and velocity solutions in ECEF frame; therefore, coordinate transformation should be performed before using them in the algorithms, if necessary.

$$P_{GNSS} = P_{true} + \varepsilon_P \tag{2.6}$$

$$V_{GNSS} = V_{true} + \varepsilon_V \tag{2.7}$$

For the helicopter model, GNSS accuracies are taken as in Table 2.2. GNSS receiver's output rate is 1 Hz.

Table 2.2: GNSS Accuracy Characteristics

| | **Position** | **Velocity** |
|---|---|---|
| **Horizontal** | 5 m | 0.1 m/s |
| **Vertical** | 10 m | 0.1 m/s |

### 2.2.3 INS Frame Mechanizations

Navigation solutions (position, velocity and orientation of the vehicle) are computed from the specific force and angular rate measurements coming from the inertial sensors through algorithms. These algorithms can be formed by using different coordinate frame mechanizations. They differ only in the means of simplicity and desired resolving coordinate frame of the navigation solution. In the context of this thesis, Navigation-frame Mechanization is implemented to obtain navigation solution. This form is preferred because position and velocity resolved in navigation frame are widely used in applications. Thus, need for additional coordinate frame transformations are prevented.

Navigation solutions are obtained from the inertial sensor outputs in three stages, namely attitude update, velocity update and position update. Flow chart of the navigation frame mechanization is illustrated in Figure 2.6. Detailed explanations and mathematical formulations of navigation algorithms are given in the following subsections (Section 2.2.3.1, Section2.2.3.2 and Section 2.2.3.3).

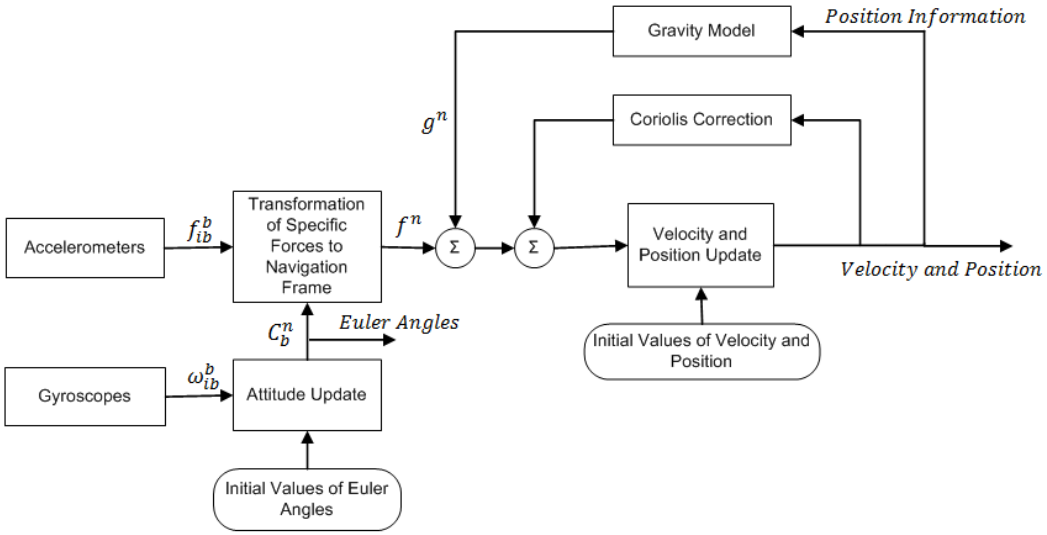


Figure 2.6: Navigation Frame Mechanization

#### 2.2.3.1 Attitude Update

Attitude update can be performed by updating Direction Cosine Matrix (DCM) from body-axis frame to the navigation-axis frame ($C_b^n$) given in equation 2.8 [30].

$$\dot{C}_b^n = C_b^n(\omega_{nb}^b\times) = C_b^n(\omega_{ib}^b\times) - (\omega_{in}^n\times)C_b^n \tag{2.8}$$

where $(\omega_{nb}^b\times)$ is the skew-symmetric matrix of the rotation rate of the body frame according to the navigation frame and $C_b^n$ can be obtained from Euler angles as;

$$C_b^n = \begin{bmatrix} \cos\theta\cos\psi & -\cos\phi\sin\psi+\sin\phi\sin\theta\cos\psi & \sin\phi\sin\psi+\cos\phi\sin\theta\cos\psi \\ \cos\theta\sin\psi & \cos\phi\cos\psi+\sin\phi\sin\theta\sin\psi & -\sin\phi\cos\psi+\cos\phi\sin\theta\sin\psi \\ -\sin\theta & \sin\phi\cos\theta & \cos\phi\cos\theta \end{bmatrix} \tag{2.9}$$

$\phi$, $\theta$ and $\psi$ are the roll, pitch and yaw angles of the helicopter, respectively.

By integrating above formula in discrete time, attitude update equation can be found as;

$$C_b^n(+) = C_b^n(-)C_{b+}^{b-} - [\omega_{in}^n\times](-)C_b^n(-)dt \tag{2.10}$$

where $\omega_{in}^n$ is the rotation rate of navigation frame according to the inertial frame and defined as in Equation 2.11.

$$\omega_{in}^n = \begin{bmatrix} \frac{V_{ib,E}}{R_0+h} \\ -\frac{V_{ib,N}}{R_0+h} \\ -\frac{V_{ib,E}\tan L}{R_0+h} \end{bmatrix} \tag{2.11}$$

$C_{b+}^{b-}$ defines the attitude update matrix in terms of the attitude increment, $\alpha_{ib}^b \approx \omega_{ib}^b dt$, and it is given in the below form [30]. (Equation 2.12)

$$C_{b+}^{b-} = I_3 + \frac{\sin|\alpha_{ib}^b|}{|\alpha_{ib}^b|}(\alpha_{ib}^b\times) + \frac{1-\cos|\alpha_{ib}^b|}{|\alpha_{ib}^b|^2}(\alpha_{ib}^b\times)^2 \tag{2.12}$$

#### 2.2.3.2 Velocity Update

Velocity update is performed by adding acceleration components which are specific forces measured by accelerometers and gravitational acceleration as well as accelerations due to transport rates between axis frames like Coriolis acceleration. Then, integrating the total acceleration, velocity is obtained. Detailed formulation of velocity update is given below.

According to Coriolis acceleration, variation of the position in inertial frame in terms of navigation frame can be expressed as,

$$\frac{d^2r}{dt^2}|_i = \frac{dV}{dt}|_i = \frac{dV}{dt}|_n + \omega_{in} \times V \tag{2.13}$$

Total acceleration in the inertial frame is the sum of the specific force and the gravitational acceleration.

$$\frac{d^2r}{dt^2}|_i = f + g \tag{2.14}$$

Finally, substituting equation 2.14 into equation 2.13, total acceleration of the helicopter in navigation frame is found to be:

$$\frac{dV}{dt}|_n = f + g - \omega_{in} \times V \tag{2.15}$$

Specific acceleration is measured in the body axis frame; therefore, it is needed to be transformed to the navigation frame. Finally, velocity update equation takes the following form.

$$\dot{V}_n = C_b^n f^b + g^n - \omega_{in}^n \times V^n \tag{2.16}$$

#### 2.2.3.3 Position Update

Position in navigation frame is represented as latitude, longitude and altitude $(L, \lambda, h)$. Time derivative of curvilinear positions are given below.

$$\dot{L} = \frac{V_{ib,N}^n}{R_0 + h} \tag{2.17a}$$

$$\dot{\lambda} = \frac{V^n_{ib,E}}{R_0 + h\cos L} \tag{2.17b}$$

$$\dot{h} = -V^n_{ib,D} \tag{2.17c}$$

Where $R_0$ is the equatorial radius of the Earth defined by WGS84 (World Geodetic System).

By integrating time derivative of the positions in discrete time, updated positions are obtained as,

$$L(+) = L(-) + (\frac{V^n_{ib,N}(-)}{R_0 + h(-)} + \frac{V^n_{ib,N}(+)}{R_0 + h(+)})\frac{dt}{2} \tag{2.18a}$$

$$\lambda(+) = \lambda(-) + (\frac{V^n_{ib,E}(-)}{R_0 + h(-)\cos L(-)} + \frac{V^n_{ib,E}(+)}{R_0 + h(+)\cos L(+)})\frac{dt}{2} \tag{2.18b}$$

$$h(+) = h(-) - (V^n_{ib,D}(-) + V^n_{ib,D}(+))\frac{dt}{2} \tag{2.18c}$$

### 2.2.4 INS/GNSS Integration

Integration of INS and GNSS is performed by Kalman Filter (KF). KF is an optimal estimation algorithm. It estimates the states, in agreement with the defined system dynamics and error characteristics of the systems. States are determined by the designer according to the requirements of the application. The estimation is performed by KF mainly in two stages. First stage is the time update of the states. Here, the mean and the covariance of the states are propagated in time. In second stage, measurement update is performed by using the auxiliary measurements, in this case; GNSS measurements. By using the difference between new measurements and the estimated ones by KF according to the system dynamics, errors are estimated in this stage.

Kalman filter can be a total-state or an error-state whether the estimated medium is state itself or only the errors of the states. In this work, error-state Kalman filter is implemented. Errors are estimated in KF and used to correct the primary means of navigation which is the INS solution.

In the following subsection (Section 2.2.4.1) the INS/GNSS integration algorithm (Kalman Filter algorithm) is explained in detail.

#### 2.2.4.1 Kalman Filter Algorithm

A 15-state Kalman filter is designed for the helicopter application.

States are determined to be;

- 9 navigation error states
  - 3 Euler Angle errors,
  - 3 Velocity errors in navigation frame,
  - 3 Position errors in navigation frame,
- Sensor bias errors
  - 3 accelerometer bias errors
  - 3 gyroscopes bias errors

Nine navigation error states are fed back to the INS solutions to correct them. Estimation of the bias errors is significant not only for their contribution to sensor error budget but also the estimation of the attitude errors; therefore, their estimation improves the performance of the Kalman filter considerably. The state vector is as given below in equation 2.19.

$$x = [\delta\phi \ \delta\theta \ \delta\psi \ \delta V_n \ \delta V_e \ \delta V_d \ \delta L \ \delta\lambda \ \delta h \ \delta b_{acc,x} \ \delta b_{acc,y} \ \delta b_{acc,z} \ \delta b_{gyr,x} \ \delta b_{gyr,y} \ \delta b_{gyr,z}]^T \tag{2.19}$$

In order to define the system dynamics, error propagation of the states should be modeled properly. The formulation of the error equations are obtained in detail for this purpose.

**Attitude Error Equations**

Time derivative of attitude angle error can be represented with the time derivative of its corresponding direction cosine matrix, $C_b^n$.

$$[\delta\dot{\Psi}\times] \approx \delta\dot{C}_b^n \tag{2.20}$$

where $[\delta\dot{\Psi}\times]$ represents the skew-symmetric matrix of the Euler angle errors. Error in the $C_b^n$ can be defined as in equation 2.21.

$$\delta C_b^n = I - C_b^n \tilde{C}_b^{nT} \tag{2.21}$$

$\tilde{C}_b^n$ defines the navigation solution, while $C_b^n$ represents its true counterpart. When its time derivative is taken,

$$\delta \dot{C}_b^n = -\dot{C}_b^n \tilde{C}_b^{nT} - C_b^n \dot{\tilde{C}}_b^{nT} \tag{2.22}$$

$\dot{C}_b^n$ can be expressed as the following equation.

$$\dot{C}_b^n = C_b^n [\omega_{ib}^b \times] - [\omega_{in}^n \times] C_b^n \tag{2.23}$$

When $\dot{C}_b^n$ and $\dot{\tilde{C}}_b^n$ are substituted into equation 2.22 and rearranged, Euler angle error propagation equation is given in the form of equation 2.24 [30].

$$\delta\dot{\Psi} = \hat{C}_b^n \delta\omega_{ib}^b - [\omega_{in}^n \times]\delta\Psi - (\tilde{\omega}_{in}^n - \omega_{in}^n) \tag{2.24}$$

$\hat{C}_b^n$ refers to Kalman estimate of the DCM and $\omega_{in}^n$ is the rotation of the navigation frame with respect to the inertial frame and it is expressed in navigation frame.

$(\tilde{\omega}_{in}^n - \omega_{in}^n)$ can be obtained as below (Equation 2.25) when some trigonometric formulation is applied and the small angle theory is assumed [30].

$$\tilde{\omega}_{in}^n - \omega_{in}^n = \begin{bmatrix} \frac{\delta V_{ib,E}^n}{R_0+h} \\ -\frac{\delta V_{ib,N}^n}{R_0+h} \\ -\frac{\delta V_{ib,E}^n \tan L}{R_0+h} \end{bmatrix} - \begin{bmatrix} 0 \\ 0 \\ \frac{V_{ib,E}^n}{R_0+h} \cos^2 L \end{bmatrix} \delta L + \begin{bmatrix} \frac{-\delta V_{ib,E}^n}{(R_0+h)^2} \\ \frac{\delta V_{ib,N}^n}{(R_0+h)^2} \\ \frac{\delta V_{ib,E}^n \tan L}{(R_0+h)^2} \end{bmatrix} \delta h \tag{2.25}$$

**Velocity Error Equations**

Time derivative of velocity error is expressed as in equation 2.26.

$$\begin{aligned} \delta\dot{V}^n &= \dot{\tilde{V}}^n - \dot{V}^n \\ &= \tilde{C}_b^n \tilde{f}^b + \tilde{g}^n - \tilde{\omega}_{in} \times \tilde{V}^n - [C_b^n f^b + g^n - \omega_{in} \times V^n] \end{aligned} \tag{2.26}$$

When the necessary substitutions and the arrangements are made, velocity error propagation can be found from equation 2.26 as below.

$$\delta\dot{V}^n = -[\tilde{C}_b^n \tilde{f}^b]\delta\Psi - \omega_{in} \times \delta V^n + [V^n \times](\tilde{\omega}_{in}^n - \omega_{in}^n) - \frac{2g}{R_0}\delta h + C_b^n \delta f^b \tag{2.27}$$

**Position Error Equations**

Position error propagation equations are obtained by neglecting small terms by Groves [30] as in equations 2.28a, 2.28b and 2.28c.

$$\delta \dot{L} = \frac{\delta V^n_{ib,N}}{R_0 + h} - \frac{\delta V^n_{ib,N} \delta h}{(R_0 + h)^2} \tag{2.28a}$$

$$\delta \dot{\lambda} = \frac{\delta V^n_{ib,E}}{(R_0 + h)\cos L} + \frac{V^n_{ib,E} \sin L \delta L}{(R_0 + h)\cos^2 L} - \frac{V^n_{ib,E} \delta h}{(R_0 + h)^2 \cos L} \tag{2.28b}$$

$$\delta \dot{h} = -\delta V^n_{ib,D} \tag{2.28c}$$

**Accelerometer and Gyroscope Error Equations**

Accelerometer and gyroscope instrument error terms can be defined respectively as,

$$\delta f^b = \Delta \tilde{f}^b - \Delta f^b \tag{2.29}$$

$$\delta \omega^b = \Delta \tilde{\omega}^b - \Delta \omega^b \tag{2.30}$$

Instrument errors and its estimation are modeled in Ref. [31] as,

$$\Delta f^b = F_{vacc} b_{acc} + v_{acc} \qquad \Delta \omega^b = F_{\Psi gyr} b_{gyr} + v_{gyr} \tag{2.31}$$

$$\Delta \tilde{f}^b = F_{vacc} \tilde{b}_{acc} \qquad \Delta \tilde{\omega}^b = F_{\Psi gyr} \tilde{b}_{gyr} \tag{2.32}$$

Finally, instrument errors were obtained as below.

$$\delta f^b = F_{vacc} \delta b_{acc} + v_{acc} \qquad \delta \omega^b = F_{\Psi gyr} \delta b_{gyr} + v_{gyr} \tag{2.33}$$

$$\delta f^n = C^n_b F_{vacc} \delta b_{acc} + C^n_b v_{acc} \qquad \delta \omega^n = F_{\Psi gyr} \delta b_{gyr} + C^n_b v_{gyr} \tag{2.34}$$

Here $v_{acc}$ and $v_{gyr}$ represent the measurement noise error, while $F_{vacc}$ and $F_{\Psi gyr}$ which are the submatrices of the system matrix, are identity matrices for bias errors [31].

Furthermore, bias error time derivatives are modeled as [31],

$$\delta \dot{b}_{acc} = F_{accacc} \delta b_{acc} + \omega_{acc} \tag{2.35}$$

$$\delta \dot{b}_{gyr} = F_{gyrgyr} \delta b_{gyr} + \omega_{gyr} \tag{2.36}$$

Sensor errors are assumed to be random walk, therefore; $F_{accacc}$ and $F_{gyrgyr}$ are taken as zero matrices and $\omega_{acc}$ and $\omega_{gyr}$ are random noises.

When the error equations are arranged, general state-space model is obtained for error propagation of the states.

$$\dot{x} = Fx + Gw \tag{2.37}$$

System matrix F is formed in continuous time and needs to be converted in discrete time. This can be performed by Taylor series expansion but another method is applied which is believed to be more stable, stated by Farrell [31].

$$\Sigma = \begin{bmatrix} -F & GQG^T \\ 0 & F^T \end{bmatrix} dt \tag{2.38}$$

The Q matrix is the system noise covariance matrix in continuous form; it defines the system noise to the Kalman filter which are mainly accelerometer and gyroscope random walks. Q is a diagonal matrix and diagonal elements are; velocity random walk, angular random walk, accelerometer bias random walk and gyroscope random walk.

By taking the exponential of the matrix in equation 2.38, discrete system noise matrix $(Q_d)$ and state transition matrix $(\Phi)$ are obtained as in equations 2.40 and 2.41, [31].

$$e^{\Sigma} = \begin{bmatrix} -X & \Phi^{-1}Q_d \\ 0 & \Phi^T \end{bmatrix} dt \tag{2.39}$$

$$\Phi = e^{\Sigma}[(n+1):2n, (n+1):2n]^T \tag{2.40}$$

$$Q_d = \Phi e^{\Sigma}[1:n, (n+1):2n]^T \tag{2.41}$$

Where n is the number of the states.

After obtaining the state transition matrix and system noise matrix in discrete time, time update of Kalman filter is performed.

Time update of states:

$$x_{k+1}^{-} = \Phi_k x_k^{+} \tag{2.42}$$

Time update of covariance matrix:

$$P_{k+1}^{-} = \Phi_k P_k^{+} \Phi_k^T + Q_d \tag{2.43}$$

Subscripts $k$ and $k+1$ indicate the time indices, while superscripts $(+)$ and $(-)$ means after and before the measurement update, respectively. State estimates are initialized from zero and error covariances are initialized according to the state uncertainties in the application.

Time update is performed at 100 Hz which is the output rate of the inertial sensors. On the other hand, measurement update is performed at 1 Hz when the GNSS data is available.

At times when the GNSS data is available, firstly Kalman gain is computed. Kalman gain is a measure of whether GNSS solution or INS solution will be weighted for the estimation of states and it is computed as,

$$K_{k+1} = P_{k+1}^{-} H_{k+1}^{T} (H_{k+1} P_{k+1}^{-} H_{k+1}^{T} + R_{k+1})^{-1} \tag{2.44}$$

Kalman gain being large means that states are estimated towards the new measurements, while Kalman gain being small means that states are estimated towards the previous estimations.

H is the measurement matrix. It defines how the measurement vector relates with the state vector. In this application, position and velocity of GNSS are used as auxiliary measurement; therefore, measurement matrix is chosen to be;

$$H = \begin{bmatrix} 0_3 & 0_3 & -I_3 & \dots & 0_3 \\ 0_3 & -I_3 & 0_3 & \dots & 0_3 \\ 0_3 & 0_3 & 0_3 & \dots & 0_3 \end{bmatrix} \tag{2.45}$$

Minus signs are due to sign convention.

R is the measurement noise covariance matrix. It defines the error characteristics of the GNSS measurements to the Kalman Filter. R is a diagonal matrix having the diagonal elements as; GNSS horizontal position accuracy, GNSS vertical positon accuracy, GNSS horizontal velocity accuracy and GNSS vertical velocity accuracy.

Measurements are modeled as,

$$z = \begin{bmatrix} P_{GNSS} - P_{INS} \\ V_{GNSS} - V_{INS} \end{bmatrix} \tag{2.46}$$

Measurement update of states:

$$x_{k+1}^{+} = x_{k+1}^{-} + K_{k+1}(z - H_{k+1}x_{k+1}^{-}) \tag{2.47}$$

Measurement update of the covariance matrix:

$$P_{k+1}^{+} = (I - K_{k+1}H_{k+1})P_{k+1}^{-} \tag{2.48}$$

This algorithm can be summarized with a flowchart as in Figure 2.7.

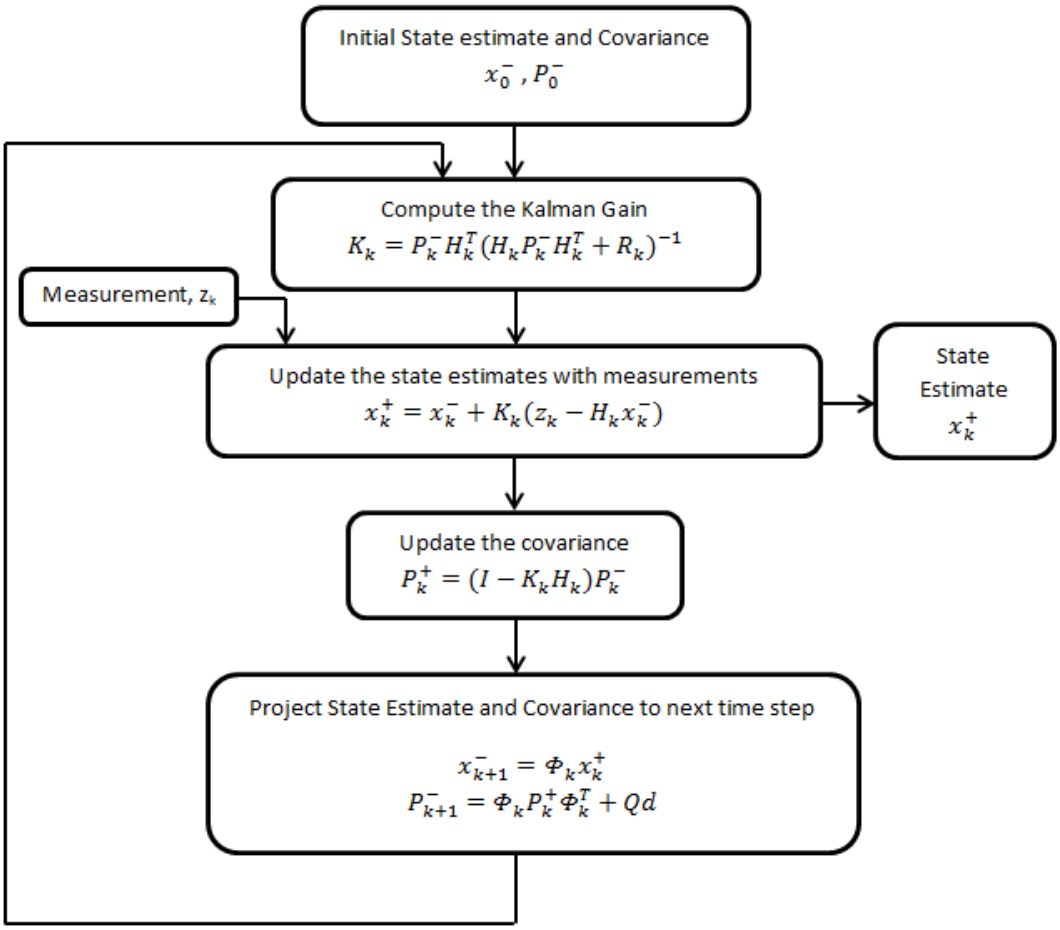


Figure 2.7: Flowchart of Kalman Filter Algorithm

After estimating the errors of the states, they are fed back to the INS solution to obtain the integrated navigation solution. Kalman filter is designed as closed loop which means corrected INS solutions are fed back to the navigation algorithms. With this way, navigation algorithm errors are kept small. This is necessary for low accuracy inertial sensors since small angle approximation is assumed in the propagation of

the errors. With this configuration, raw INS solution cannot be obtained with the integrated navigation solution.

#### 2.2.4.2 Kalman Filter Performance

While illustrating the performance of the Kalman filter in the simulation, true values of the navigation solutions are used to compare the KF and INS results, and drifts and errors are calculated accordingly. However, in real time applications, it is difficult to verify KF's estimated states since true navigation solutions are not available. In real time, KF performance can be verified by using the measurement innovations. The measurement innovations of a Kalman filter is the difference between the actual observation and the predicted observation. It gives an indication of whether the measurements and state estimates are consistent. The measurement innovation is defined as [32],

$$\delta z_k^- = z_k - H_k x_k^- \tag{2.49}$$

The measurement innovation covariance is,

$$C_k^- = H_k P_k^- H_k^T + R_k \tag{2.50}$$

If the innovation sequence has a zero mean white noise characteristic within the covariance given, then the Kalman filter is working properly.

## 2.3 Simulation Results

In this section, the performance of the INS/GNSS integration is shown via simulations. Algorithms derived in previous sections are modeled in Matlab/Simulink. Stability and performance of the Kalman filter is shown using a maneuvering helicopter. Moreover, analyses are done when GNSS signal outage exists.

The control inputs of the helicopter are decided such that helicopter performs both longitudinal and lateral maneuvers during the flight simulation. Flight duration is taken as 300 seconds. In Figure 2.8 control inputs commanded to helicopter are given. In Figures 2.9, 2.10 and 2.11, Kalman Filter performance illustrated for the attitude,

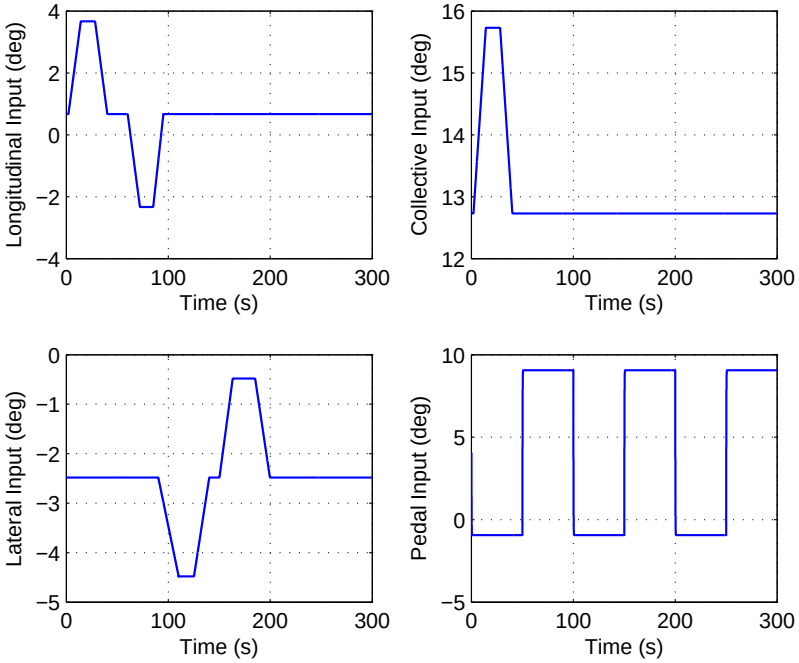


Figure 2.8: Helicopter Control Inputs

velocity and position of the helicopter, respectively. Kalman filter is formed as closed loop and pure INS solution is not available since the corrected navigation solution is fed back to the INS in this form. However, pure INS solution is also obtained separately to compare the solutions and illustrate the effectiveness of Kalman filter. The results of the pure INS are given in the same figures.

It can be seen from the figures (Figures 2.9, 2.10 and 2.11) that INS solution deviates

from the actual solution due to the integration of the MEMS sensor errors in time. In such a short time (300 s), INS solution accumulates large errors which makes impossible the use of MEMS as the only navigational source.

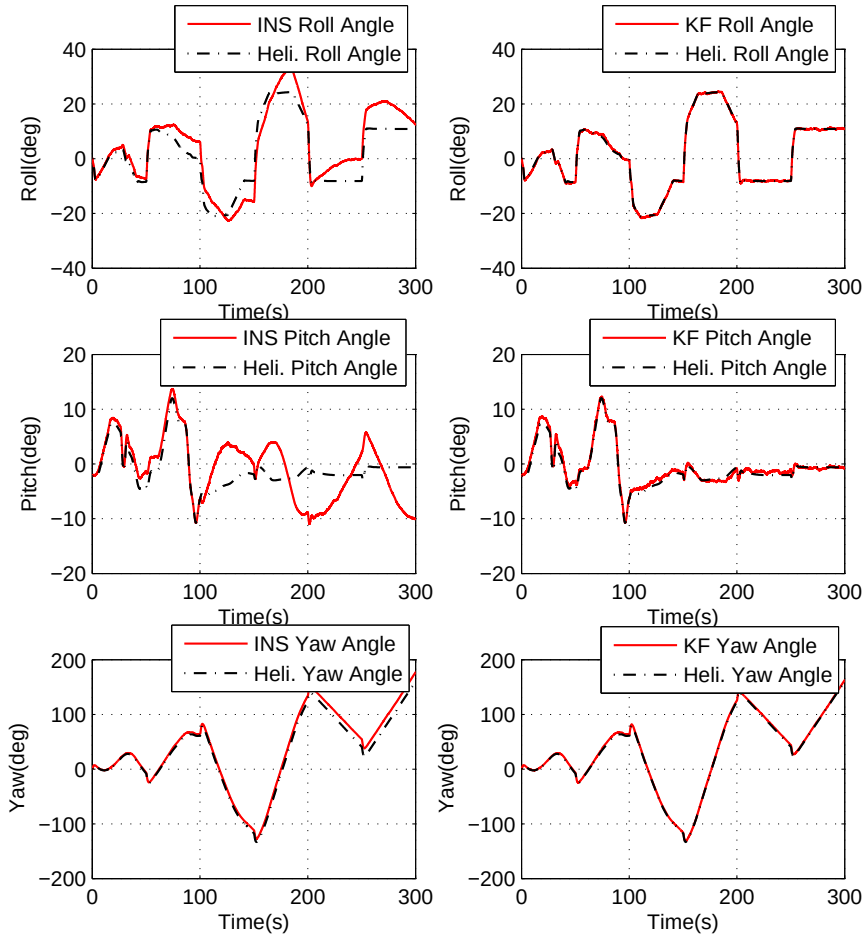


Figure 2.9: Comparison of INS and KF Attitude Solutions

However; its integration with the GNSS improves the solution significantly. The errors are estimated at 1 Hz and kept small by correcting the inertial solution but they are propagated in time at 100 Hz which is the inertial sensor output rate. This phenomenon can be observed from 2.12 which shows the difference between actual velocity of the helicopter and KF solution more clearly. From this figure, it can be seen that errors grow until the new GNSS measurement is available. When the new measurement is taken, errors are estimated and compansated from the system forming this sawtooth view.

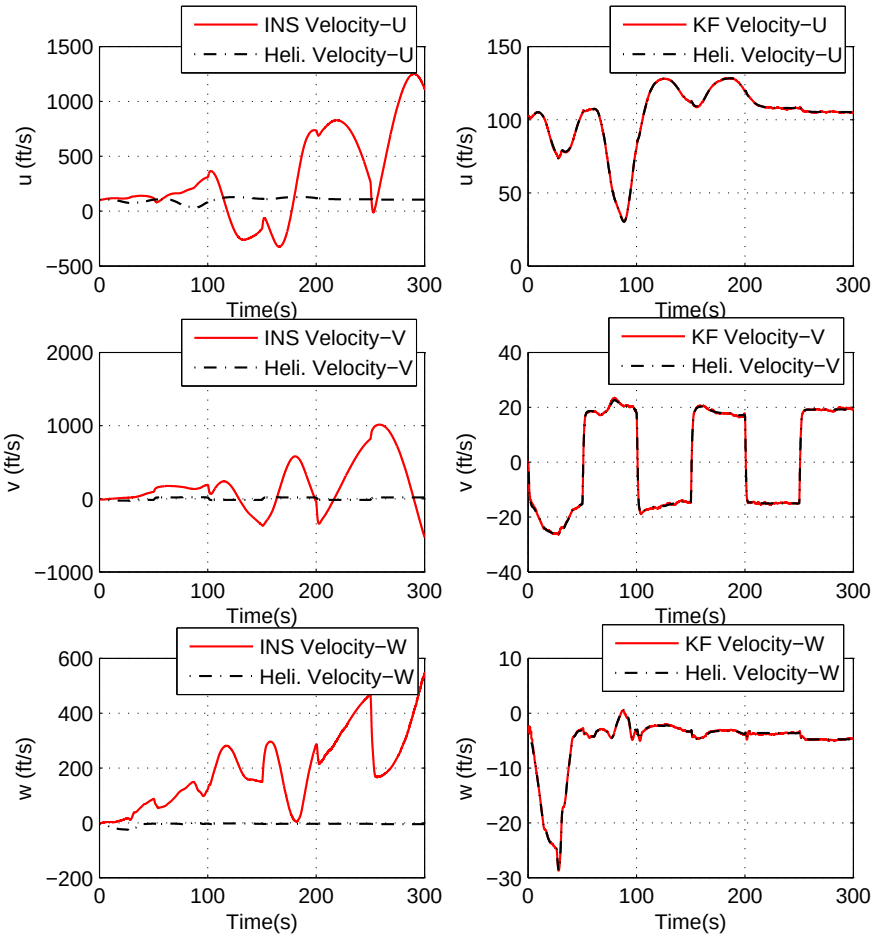


Figure 2.10: Comparison of INS and KF Velocity Solutions

Errors between the actual values and the integrated navigation solution are shown in Figures 2.13, 2.14 and 2.15 for attitude, velocity and position, respectively with red solid lines. The black dotted lines represent the corresponding covariances.

As it can be seen from the covariances, the errors are zero mean and less than 1.5 deg for roll and pitch channel and less than 4 deg for yaw channel which is more difficult to observe. On the other hand, velocity errors are less than 2 ft/s while position errors are less than 15 ft. Moreover, errors are in the covariances during the flight as expected. From Figure 2.14 which shows the error covariances of velocity, trend of the covariance propagation can be seen more closely. it can be observed that error covariances are tend to grow like errors when measurements are not available. When the new measurement is taken, errors and error covariances are estimated. Thus,

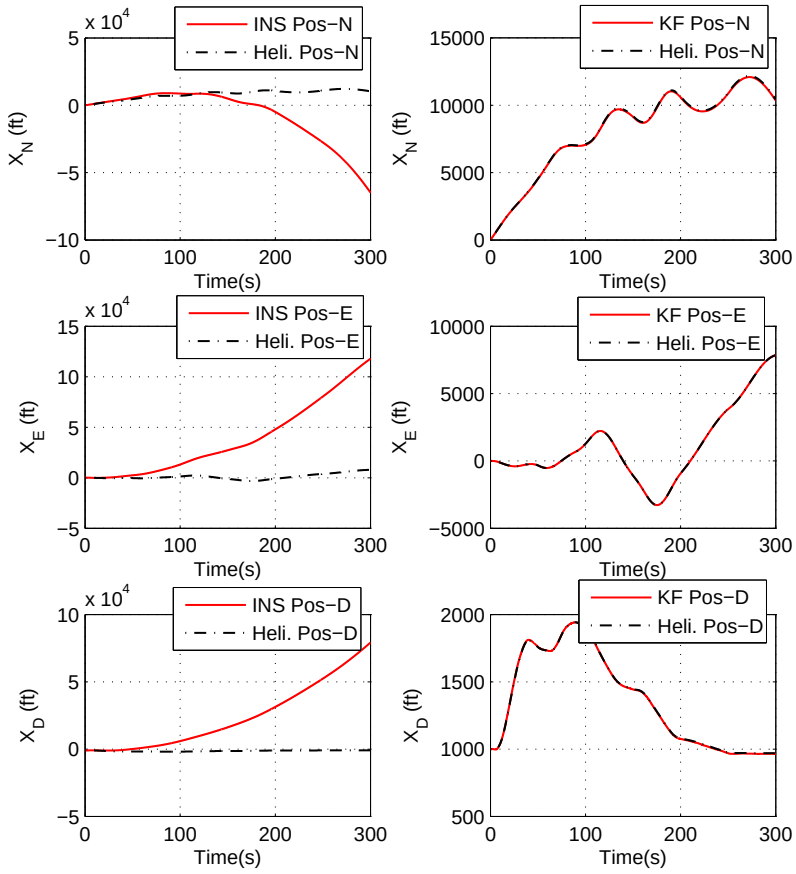


Figure 2.11: Comparison of INS and KF Position Solutions

uncertainty of the system is decreasing with every new measurement.

Since the analysis are performed in simulation environment, actual attitude, velocity and position values are available. However; in real-life applications, actual values are not known. Therefore; performance and stability analysis of Kalman filter is verified through the measurement innovations (Section 2.2.4.2). Therefore; measurement innovations are also examined for the stability in this study. Figure 2.16(a) and Figure 2.16(b) show the measurement innovations of the KF with the covariances for position and velocity measurements, respectively.

As it can be seen from the figures, measurement innovations are zero-mean Gaussian and their deviations are within the covariances for both position (Figure 2.16(a)) and velocity (Figure 2.16(b)). As a result, this indicates that Kalman filter is working properly.

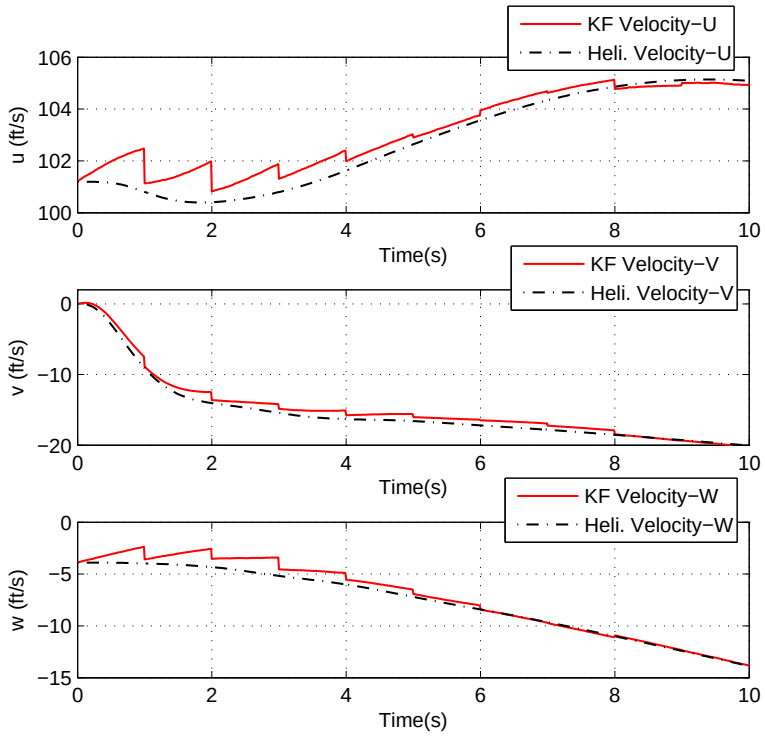


Figure 2.12: Appearance of Kalman Filter Velocity Solution

Beside of attitude, velocity and position of the helicopter, accelerometer and gyroscope bias errors are also estimated by Kalman filter. Bias estimations are not fed back to the sensor inputs; however, their effects are taken into consideration by the filter when estimating the errors from system dynamics. The accelerometer bias and gyroscope bias errors are 50 mg and 200 deg/hr, respectively as given before in Table 2.1. The estimations are given in Figure 2.17(a) and 2.17(b) with black lines.

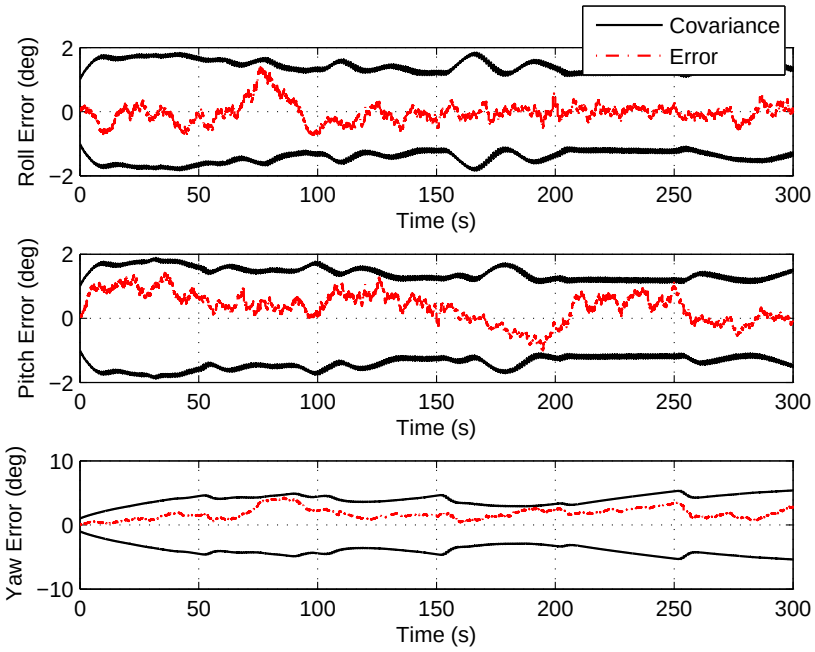


Figure 2.13: Attitude Errors and Error Covariances

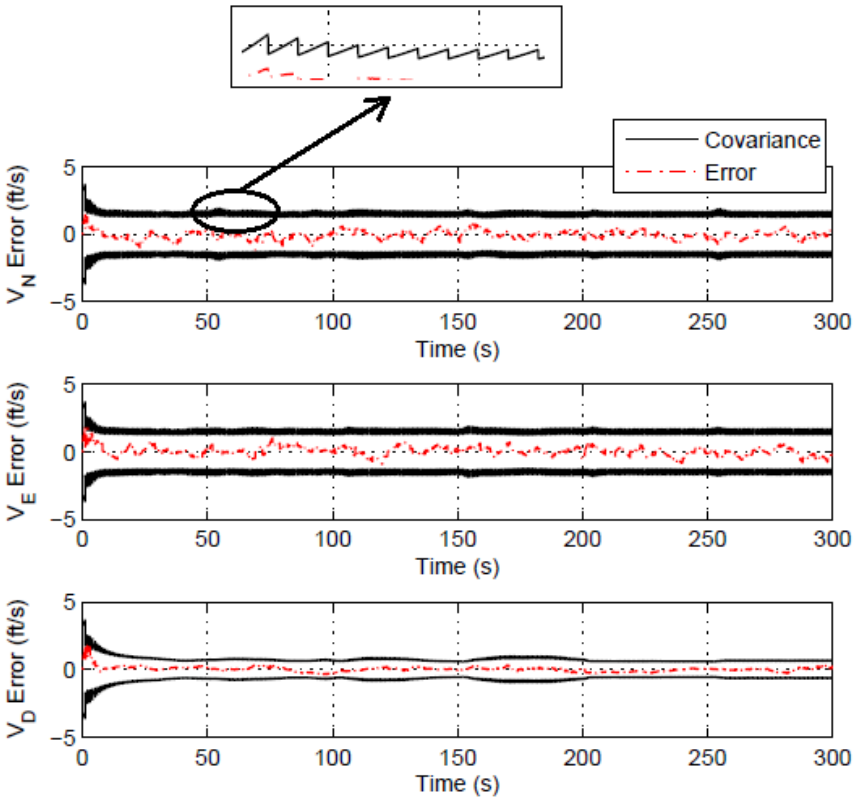


Figure 2.14: Velocity Errors and Error Covariances

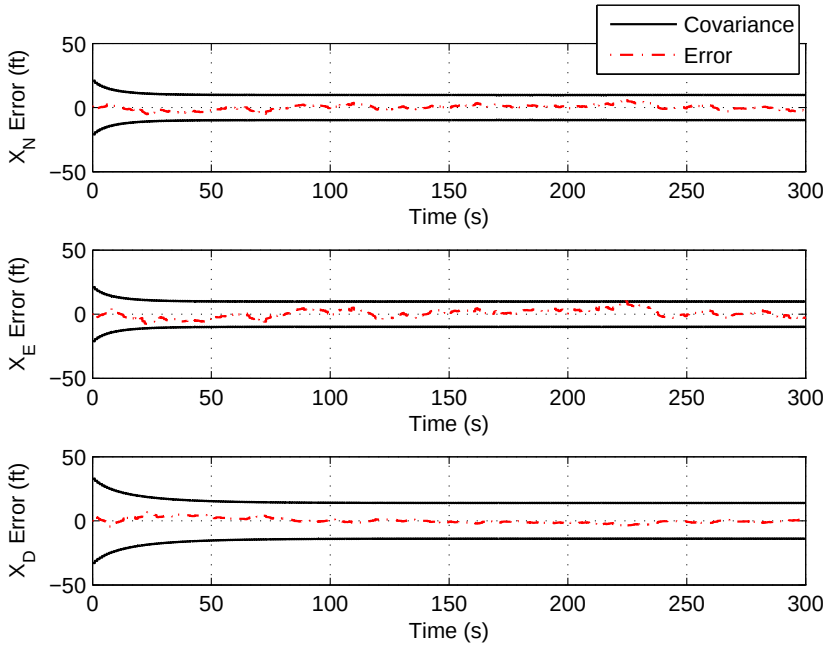


Figure 2.15: Position Errors and Error Covariances

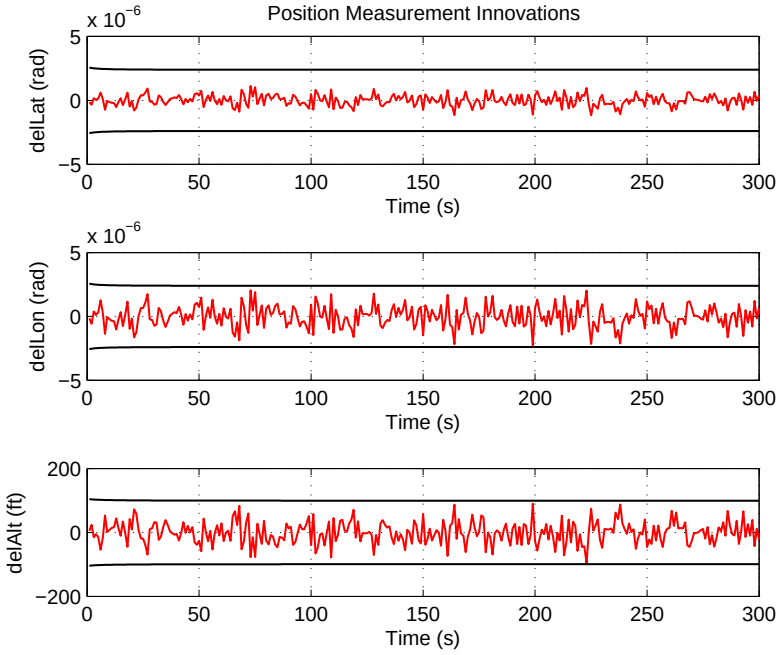


(a) Position Innovations

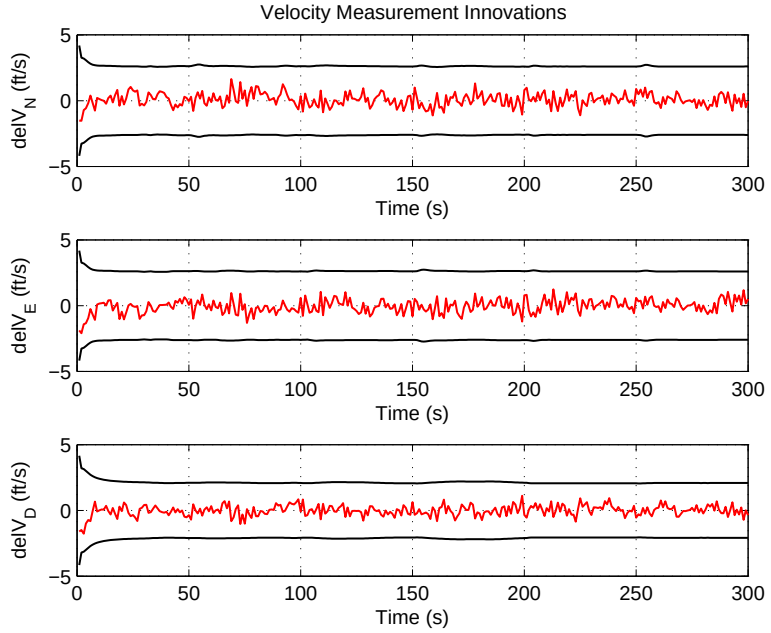


(b) Velocity Innovations

Figure 2.16: Measurement Innovations and Innovation Covariances

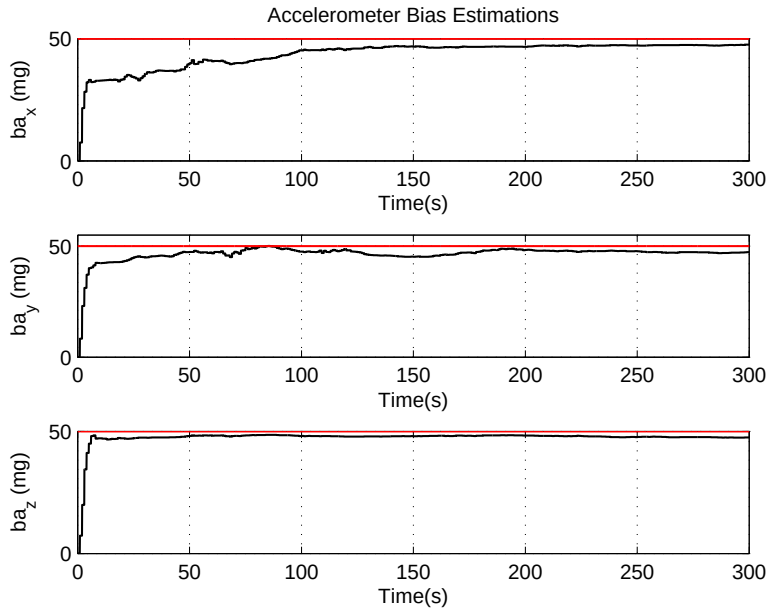


(a) Accelerometer Bias Estimations

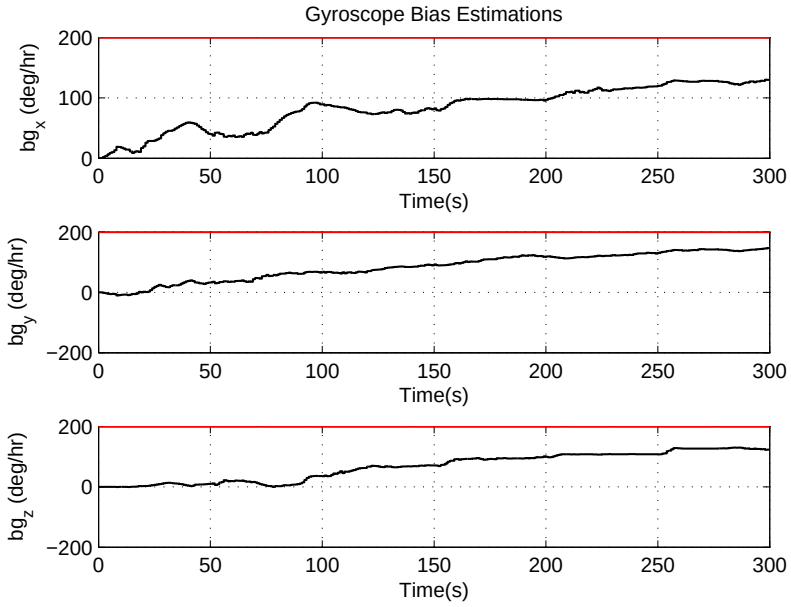


(b) Gyroscope Bias Estimations

Figure 2.17: Inertial Sensor Bias Estimations

One of the most critical disadvantages of GNSS is its dependency on external signals. Signal outage may occur due to several reasons and INS/GNSS integration bridges those outages. In the simulation, GNSS signal is cut off between the $50^{th}$ and $150^{th}$ seconds to analyze the performance of the Kalman filter when signal outage occurs during the flight.

Integrated navigation solution and the actual values are given in Figures 2.18, 2.19 and 2.20 for the case of signal outage. From the figures, it can be seen that errors grow when there is no signal available from the GNSS. However, when the signal is reacquired Kalman filter estimates the accumulated error and compansates them from the system.

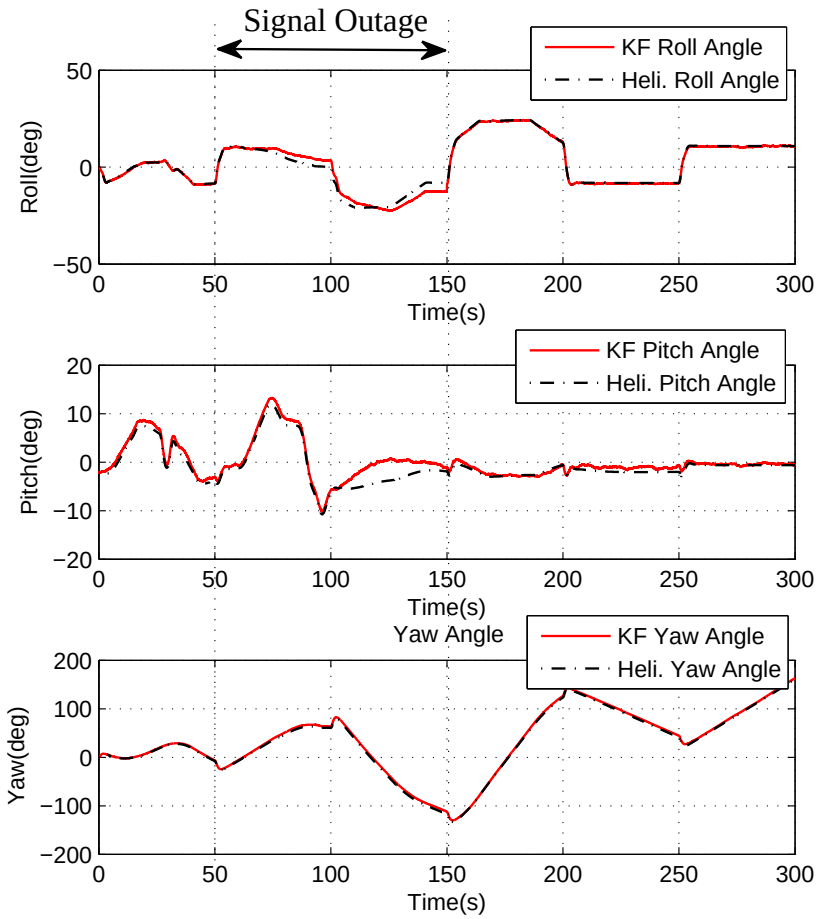


Figure 2.18: Attitude of the Helicopter when Signal Outage Occurs

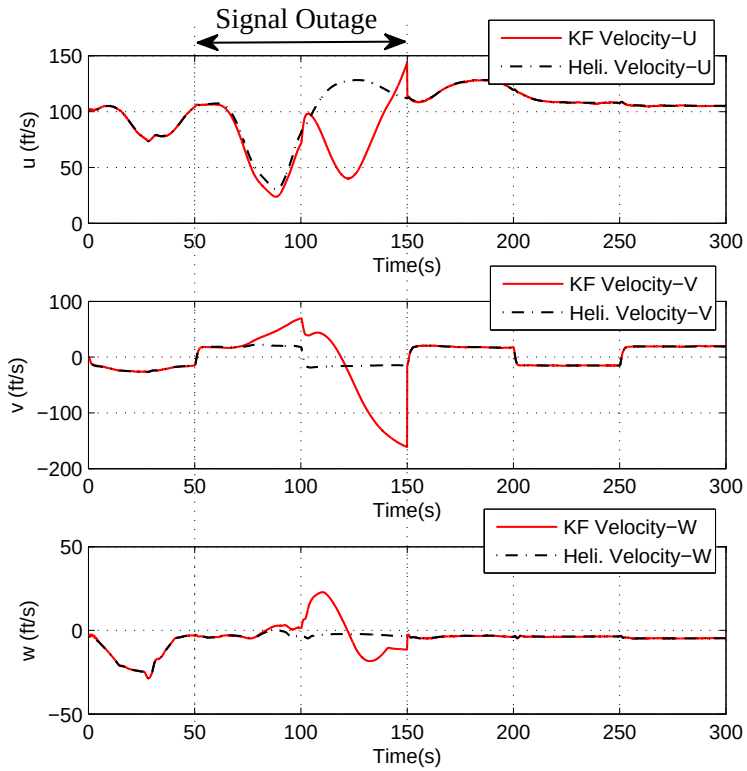


Figure 2.19: Velocity of the Helicopter when Signal Outage Occurs

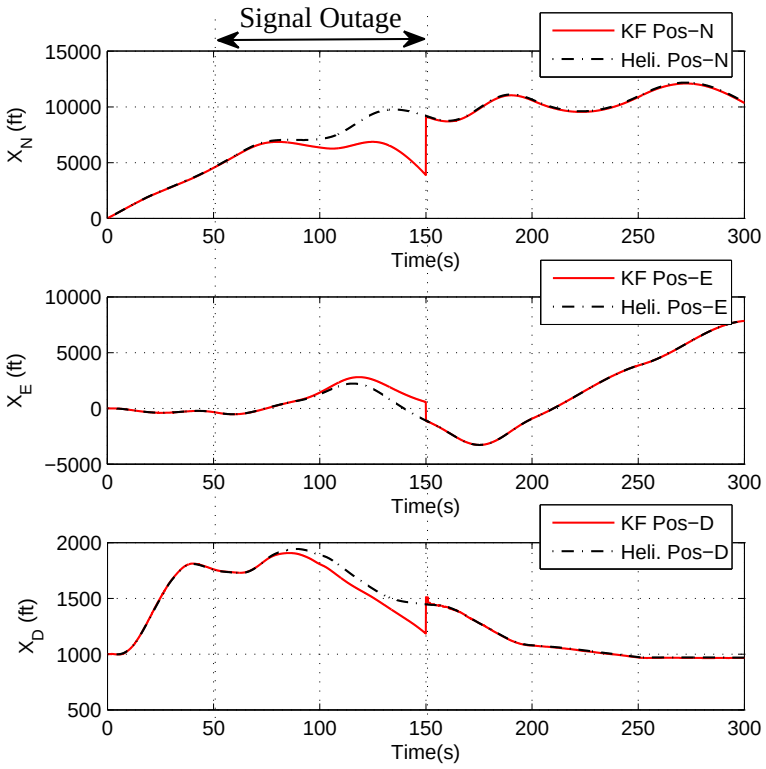


Figure 2.20: Position of the Helicopter when Signal Outage Occurs

For illustration, covariances of attitude and velocities are given in Figures 2.21 and 2.22 for the case of signal outage. As expected, covariances are expanding during the signal outage and errors are always in the covariance limits which indicates that Kalman filter works properly.

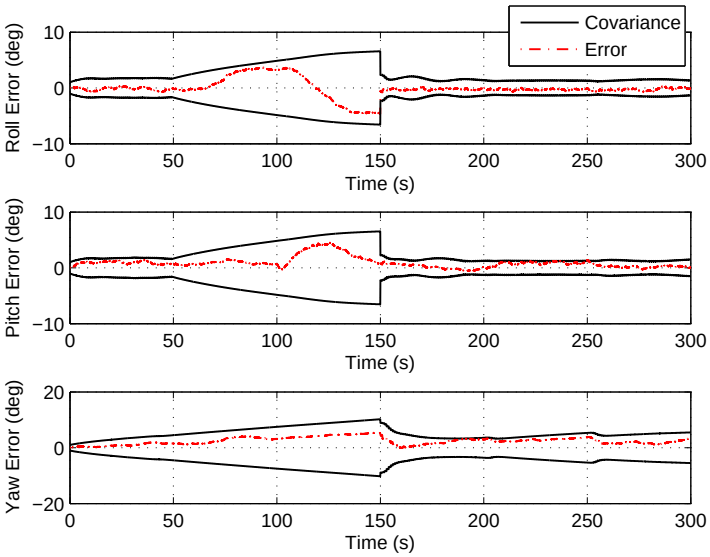


Figure 2.21: Attitude Errors and Covariances when Signal Outage Occurs

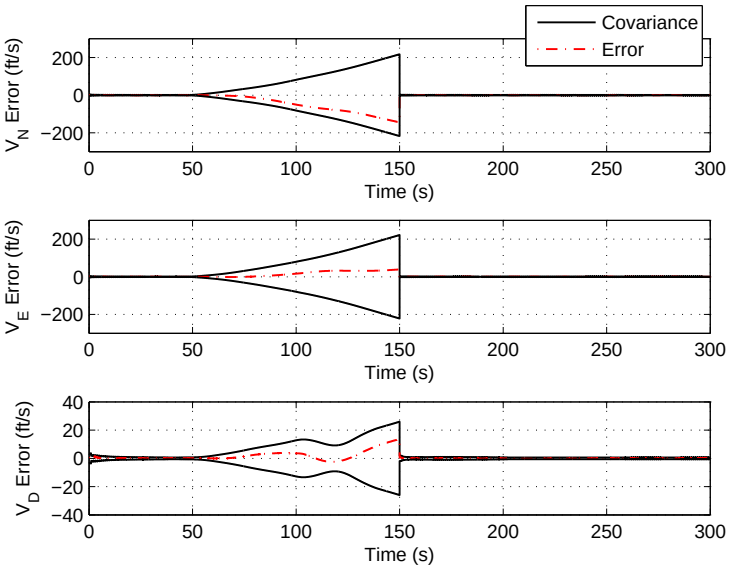


Figure 2.22: Velocity Errors and Covariances when Signal Outage Occurs

# CHAPTER 3

# KALMAN FILTER BASED APPROACH IN ADAPTIVE CONTROL

Adaptive control is an approach to accommodate for uncertainties. In many applications, uncertainties exist due to linearization errors, modeling errors, assumptions or external disturbances, etc. Research focuses on the performance improvement of adaptive control.

Adaptive control using neural networks is an approach used for many aerospace applications. In this method, typically a linear model is inverted for the design of a model inversion controller. A neural network is used to compensate for the model uncertainty. A linear controller is wrapped around the inverted model for stability. The update law of the neural network is derived using Lyapunov Theory [26, 33].

The neural network update law is later updated with modification terms for various reasons, mainly to improve boundedness [15, 16, 17, 19, 23]. Yucelen et al. state in their study [23] that in general, these modification terms are found by taking the gradient of a norm of the constraint violation and proposed a new approach which forms an alternative method to the well-known existing modifications. It is reported that Kalman Filter optimization can be used to reduce the violation of a linear constraint.

In this thesis work, proportional-derivative (PD) controller is used to control the rotational states of a helicopter which are roll, pitch and yaw channels, and Linear Model Inversion is used to obtain helicopter control inputs [21, 26]. Both Linear-in-Parameter Neural Network and Single Hidden Layer Neural Network adaptation laws are implemented to take the uncertainties into consideration and Kalman Filter

approach as a modification term is adopted in neural networks. In this chapter, controller structure is explained, theory of the Kalman Filter approach is discussed and this approach is applied as the well-known e-modification term.

## 3.1 Adaptive Control Preliminaries

Many applications present model uncertainties and controllers of air vehicles are expected to operate reliably under these conditions. As mentioned earlier, adaptive control is an effective way to fulfill the requirements in the presence of uncertainties. To improve the performance of the baseline adaptation law and ensure the boundedness, modification terms have been used. Some of these widely used modification terms are illustrated below with their contribution.

Adaptive control can be formed by using neural networks. Linear in Parameter Neural Network (LPNN) is a simple kind of neural network which consists of a single layer. Single layer means that the inputs are connected directly to the outputs through weights. In this form, adaptive control input is obtained as the linear combination of the selected inputs.

LPNN baseline weight update law is a gradient based parameter update law. It can be obtained by taking the negative gradient of a cost function chosen as the enforcing constraint on the weight estimates. It is defined in the following well-known form as in equation 3.1 [34].

$$\dot{\hat{W}}(t) = \gamma\beta(x(t))e^T(t)PB \tag{3.1}$$

where $\gamma$ is called the positive learning rate,

$\beta(.)$ is a known vector of basis functions,

$x(t)$ is the input vector,

$e(t)$ is the tracking error vector and

$P$ is a positive-definite matrix which is the solution of the following Lyapunov equation.

$$A_m^T P + PA_m + Q = 0 \tag{3.2}$$

for any $Q > 0$, ensures that $\hat{W}$ remains bounded and that $e(t) \to 0$ as $t \to \infty$.

Adaptive control element is obtained as linear combinations of the estimated weights. Gradient based methods have been widely used to solve linearly parameterized parameter identification problems [21].

$$u_{ad}(t) = \hat{W}^T \beta(x(t)) \tag{3.3}$$

Figure 3.1 illustrates the block diagram of the adaptive controller.

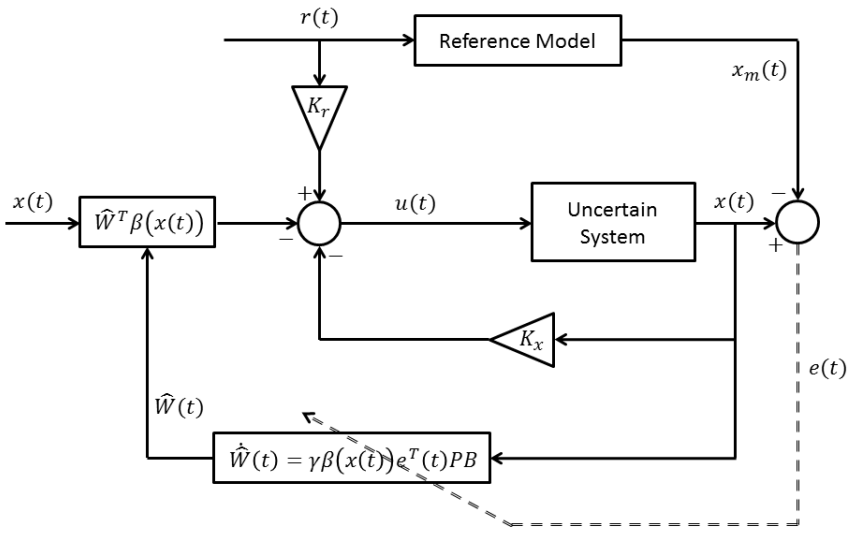


Figure 3.1: Block Diagram of LPNN based Adaptive Controller

To improve the boundedness of the weights for the performance and stability considerations, modification terms are added to the baseline adaptive law.

In 1984, Ioannou and Kokotovic [15] proposed a modification term called $\sigma$- modification. This term improves the damping of the ideal adaptive law by adding the weight itself to adaptation law by multiplying it with a gain called modification learning rate. $\sigma$-modification adaptive law is given in equation 3.4.

$$\dot{\hat{W}}(t) = \gamma(\beta(x(t))e^T(t)PB - \sigma\hat{W}(t)) \tag{3.4}$$

When the tracking error gets small, adaptive weight of $\sigma$-modification have a tendency to go back to zero which means that learnt adaptive gain is lost which is actually the cause of the small tracking error [35]. In 1987, Narendra and Annaswamy [16] proposed the e-modification to overcome this problem. E-modification adds a tracking error related term to the modification learning rate in $\sigma$-modification. The

adaptation law with e-modification is given in equation 3.5.

$$\dot{\hat{W}}(t) = \gamma(\beta(x(t))e^T(t)PB - \sigma|e(t)|\hat{W}(t)) \tag{3.5}$$

Since these systems are non-linear, the stability analysis depends on Lyapunov Stability Theory. Accordingly, system is stable if the states remain bounded in the response of a bounded reference command [35].

These modification terms ($\sigma$- and e-modification) ensure that the adaptive weights remain bounded. However; there is a tradeoff between damping and adaptation rate, meaning that additional damping slows down the rate of the tracking error becoming small.

## 3.2 Model Reference Adaptive Control

In Ref. [23], Yucelen et al. proposed a new method which forms an alternative to previously mentioned well-known modification terms. In this paper, Model Reference Adaptive Control (MRAC) is presented and LPNN adaptive law is applied to compensate for the linearization errors of the system. Furthermore, new KF optimization approach for modification terms is proposed for the LPNN adaptive law. In this section, this approach is investigated first.

Consider the following uncertain system where $\Delta(.)$ represents the unknown uncertainty,

$$\dot{x}(t) = Ax(t) + B[u(t) + \Delta(x(t))] \tag{3.6a}$$

$$y(t) = Cx(t) \tag{3.6b}$$

where $x(t)$ is the state vector, $u(t)$ is the control input and $y(t)$ is the output vector. In nonlinear systems, A, B and C matrices are usually found by linearizing the nonlinear system dynamics around certain equilibrium points. For the given system, uncertainty can be thought of as linearization error.

Baseline controller for the given system is defined in the form of equation 3.7.

$$u_n(t) = -K_x x(t) + K_r r(t) \tag{3.7}$$

Where $r(t)$ is the bounded reference command, $K_x$ and $K_r$ are the feedback gain matrices and $u_n(t)$ represents the nominal control input. These feedback gains adjust the states of the open-loop system to achieve the states of the reference model (Equations 3.8a and 3.8b).

$$\dot{x}_m(t) = A_m x_m(t) + B_m r(t) \tag{3.8a}$$

$$y_m(t) = C_m x_m(t) \tag{3.8b}$$

The uncertainty $\Delta(.)$ is assumed as structured uncertainty in the form of,

$$\Delta(x(t)) = W^T \beta(x(t)) \tag{3.9}$$

In order to compensate this uncertainty, baseline controller is augmented with the adaptive controller.

$$u(t) = u_n(t) - u_a(t) \tag{3.10}$$

$$u_a(t) = \hat{W}^T \beta(x(t)) \tag{3.11}$$

Where $\beta(.)$ is the basis function and $\hat{W}$ represents the estimation of the adaptive weights. Adaptation law is applied as linear-in-parameter neural network (LPNN) with the e-modification.

$$\dot{\hat{W}}(t) = \gamma(\beta(x(t))e^T(t)PB - \sigma|e(t)|\hat{W}(t)) \tag{3.12}$$

Block diagram of the system can be seen in previous section in Figure 3.1.

In the following section (Section 3.3), Kalman Filter approach presented in Refs. [23, 36] is detailed.

## 3.3 Kalman Filter Approach in Adaptive Control

It is reported that adaptive control modification terms can be obtained by taking the gradient of a norm of the constraint violation [23]. This constraint can be imposed to the system and can be re-formulated as an optimization problem. The idea behind this approach is that instead of defining a high modification learning rate to satisfy all

possible conditions, optimizing the gain with a variable gain can produce better results. Because, fixed modification learning rate can magnify the unmodeled dynamics and the effect of sensor noise.

An optimal estimation algorithm produces estimates of the states of the dynamic system on the basis of noisy measurements and an uncertain model of the system dynamics. To transform the weight update law into optimization problem, adaptive weight should be considered and defined as a stochastic process. Similar to auxiliary measurements that aid to estimate the states in navigational Kalman Filter, linear constraint on the weight estimation can be defined as measurement; thus, weight estimation can be performed on the basis of satisfying the constraint.

This approach is constructed with both linear-in-parameter neural networks and single hidden layer neural networks structure.

### 3.3.1 Linear-in-Parameter Neural Network

The linear constraint on the weight estimate is assumed in the following form.

$$\hat{W}^T(t)\phi(t, x(t), u(t)) = 0 \tag{3.13}$$

$\phi(.)$ is a known function determined by the designer according to the desired modification type. It can be expressed in the equivalent vector form,

$$vec(\hat{W}^T(t)\phi(t, x(t), u(t))) = \Phi^T(t, x(t), u(t))w = 0 \tag{3.14}$$

w is the vector containing the columns of the W matrix, while $\Phi$ is the Kronecker product of the $\phi$ function with the identity matrix, $I$. $(ie, \Phi = I_{mxm} \otimes \phi)$

Now, stochastic process can be defined as in equations 3.15 and 3.16. $q(t)$ and $r(t)$ are zero-mean Gaussian, white noise processes with covariances Q and R, respectively.

$$\dot{w}_m = q(t) \tag{3.15}$$

$$z(t) = \Phi^T(t, x(t), u(t))w + r(t) \tag{3.16}$$

Here, $z(t)$ is regarded as measurement and its estimation is given in equation 3.17.

$$\hat{z}(t) = \Phi^T(t, x(t), u(t))\hat{w} \tag{3.17}$$

After defining the stochastic system, Kalman Filter which is an optimal estimation algorithm, is applied to the optimization problem.

$$\dot{\hat{w}}_m(t) = \bar{S}(t)\Phi(t, x(t), u(t))\bar{R}^{-1}(z(t) - \hat{z}(t)), \qquad \hat{w}_m(0) = 0 \quad (3.18a)$$

$$\dot{\bar{S}}(t) = -\bar{S}\Phi(t, x(t), u(t))\bar{R}^{-1}\Phi^T(t, x(t), u(t))\bar{S}(t) + \bar{Q}, \quad \bar{S}(0) = S_0 \quad (3.18b)$$

$ie, \bar{R} = I_{lxl} \otimes R$

'$S$' is the so-called covariance of the weight estimation. Kalman gain is the expression given as $\bar{S}\Phi(t, x(t), u(t))\bar{R}^{-1}$ in equation 3.18b. Since our aim is to satisfy the constraint on the weight estimation, measurement is chosen as $z(t) = 0$. Substituting the measurement and the estimation of the measurement into equation 3.18a, final form of the Kalman Filter equation is obtained and reduced to the following form (Equations 3.19a and 3.19b). The proof of the reduction can be found in Ref. [23].

$$\dot{\hat{W}}_m(t) = -S(t)\phi(t, x(t), u(t))R^{-1}\phi^T(t, x(t), u(t)), \qquad \hat{W}_m(0) = 0 \quad (3.19a)$$

$$\dot{S}(t) = -S(t)\phi(t, x(t), u(t))R^{-1}\phi^T(t, x(t), u(t))S(t) + Q, \qquad S(0) = S_0 \quad (3.19b)$$

Augmenting with the KF modification term, the baseline adaptation law becomes

$$\dot{\hat{W}}(t) = \gamma(\beta(x(t))e^T(t)PB - \sigma_{kf}S(t)\phi(t, x(t), u(t))R^{-1}\phi^T(t, x(t), u(t))) \quad (3.20)$$

Here, $\sigma_{kf}$ is a positive modification gain and $\sigma_{kf}S(t)$ can be interpreted as variable gain. KF approach ensures the boundedness of the weights and the proof can be found in Ref. [23].

This method can be used to reformulate new or the existing modification terms to form a modification term with variable learning rate. Traditional e-modification in LPNN structure is given in Equation 3.21.

$$\dot{\hat{W}}(t) = \gamma(\beta(x(t))e^T(t)PB - \sigma_e|e(t)|\hat{W}(t)) \quad (3.21)$$

This modification term can be obtained with KF approach by selecting the constraint as follows, indicates that $\phi(.)$ is $|e(t)|^{1/2}I_s$ where $I_s$ is the identity matrix.

$$|e(t)|^{1/2}\hat{W} = 0 \quad (3.22)$$

By substituting the $\phi(.)$ into Equations 3.19a and 3.19b, e-modification with KF approach is obtained.

$$\dot{\hat{W}}(t) = \gamma(\beta(x(t))e^T(t)PB - \sigma_{kf}|e(t)|S(t)R^{-1}\hat{W}(t)) \tag{3.23}$$

$$\dot{S}(t) = -|e(t)|S(t)R^{-1}S(t) + Q \tag{3.24}$$

### 3.3.2 Single Hidden Layer Neural Network

There exist many types of neural networks, but the basic principles are similar. In this work, single hidden layer neural network (SHL-NN) is adopted instead of linear-in-parameter neural network (LPNN) discussed in Section 3.3.1. SHL-NN is preferred to LPNN since even one hidden layer improves the approximation of nonlinear function, significantly [37].

In multi-layer neural networks, first layer is the inputs, last layer is the outputs and the layers between them are called the hidden layers which are not connected directly to the system. These layers are connected through weight coefficients which represent the degree of importance of the given connection in the neural network. Structure of the SHL neural network is illustrated in Figure 3.32.

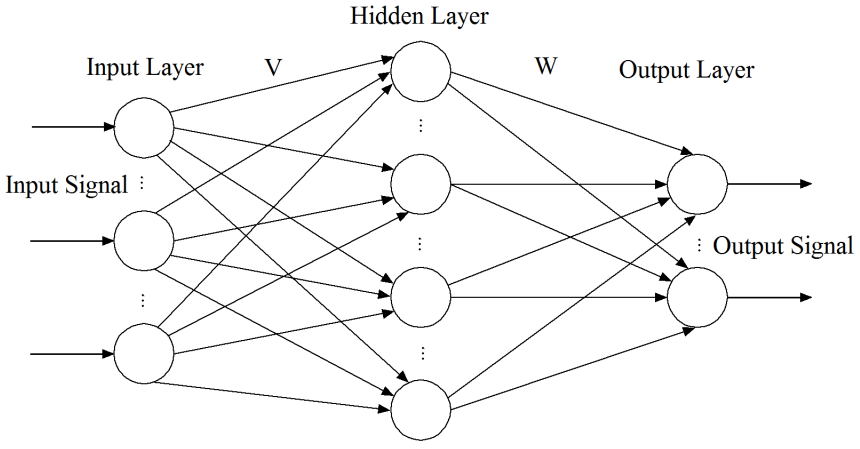


Figure 3.2: Structure of Single Hidden Layer Neural Network

The output of SHL neural network can be defined as:

$$U_{NN} = \hat{W}(t)^T\beta(V^T(t)(x(t))) \tag{3.25}$$

Kalman Filter approach as an alternative to e-modification is adapted to neural network controller. Similar to Section 3.3.1 linear constraint is assumed on the weight estimations of the SHL neural network weights [36].

$$\hat{W}^T\phi_1(t, x(t), u(t)) = 0 \tag{3.26}$$

$$\hat{V}^T\phi_2(t, x(t), u(t)) = 0 \tag{3.27}$$

The problem of estimating W and V can be formulated as an optimization problem.

$$\dot{\hat{w}}_m = q_1(t) \tag{3.28}$$

$$z_1(t) = \Phi_1^T(t, x(t), u(t))w + r_1(t) \tag{3.29}$$

$$\dot{\hat{v}}_m = q_2(t) \tag{3.30}$$

$$z_2(t) = \Phi_2^T(t, x(t), u(t))v + r_2(t) \tag{3.31}$$

Here, $z_1(t)$ and $z_2(t)$ are regarded as measurements. The estimates of $z_1(t)$ and $z_2(t)$ are given by equations 3.32 and 3.33

$$\hat{z}_1(t) = \Phi_1^T(t, x(t), u(t))\hat{w} \tag{3.32}$$

$$\hat{z}_2(t) = \Phi_2^T(t, x(t), u(t))\hat{v} \tag{3.33}$$

And measurements are taken as $z_1(t) = 0$ and $z_2(t) = 0$ to satisfy the constraints. When the measurements and the estimation of the measurements are substituted into Kalman Filter algorithm in continuous time given in equation 3.18a in Section 3.3.1, Kalman filter associated with this problem is obtained as follows.

$$\dot{\hat{W}}_m(t) = -S_1(t)\phi_1(t, x(t), u(t))R_1^{-1}\phi_1^T(t, x(t), u(t)) \tag{3.34a}$$

$$\dot{S}_1(t) = -S_1\phi_1(t, x(t), u(t))R_1^{-1}\phi_1^T(t, x(t), u(t))S_1(t) + Q_1 \tag{3.34b}$$

$$\dot{\hat{V}}_m(t) = -S_2(t)\phi_2(t, x(t), u(t))R_2^{-1}\phi_2^T(t, x(t), u(t)) \tag{3.35a}$$

$$\dot{S}_2(t) = -S_2\phi_2(t, x(t), u(t))R_2^{-1}\phi_2^T(t, x(t), u(t))S_2(t) + Q_2 \tag{3.35b}$$

Baseline adaptive law using single hidden layer neural network is given below.

$$\dot{\hat{W}}(t) = -(\beta(t) - \beta'(t)\hat{V}^T(t)(x(t))e^T(t)Pb)\Gamma_w - \dot{\hat{W}}_m \tag{3.36}$$

$$\dot{\hat{V}}(t) = -\Gamma_v(x(t)e^T(t)Pb\hat{W}^T(t)\beta'(t)) - \dot{\hat{V}}_m \tag{3.37}$$

Traditional e-modification in SHL structure can be formed as:

$$\dot{\hat{W}}(t) = -(\beta(t) - \beta'(t)\hat{V}^T(t)(x(t))e^T(t)Pb)\Gamma_w - \sigma_{we}\|e^TPb\|\hat{W} \tag{3.38}$$

$$\dot{\hat{V}}(t) = -\Gamma_v(x(t)e^T(t)Pb\hat{W}^T(t)\beta'(t)) - \sigma_{ve}\|e^TPb\|\hat{V} \tag{3.39}$$

Well-known e-modification with Kalman Filter approach can be achieved by enforcing a linear constraint on the weights as in equations 3.40 and 3.41[36].

$$\hat{W}^T\|e^TPb\|^{1/2} = 0 \tag{3.40}$$

$$\hat{V}^T\|e^TPb\|^{1/2} = 0 \tag{3.41}$$

Such that $\phi(.)$ is selected as $\|e^TPb\|^{1/2}I_s$ which is the Frobenius norm of the tracking error related term. By substituting $\phi(.)$ into Kalman filter formulation (equations 3.34a,3.34b and 3.35a, 3.35b) KF-based e-modification is obtained as given in equation 3.42a, 3.42b and 3.43a, 3.43b.

$$\dot{\hat{W}}_m(t) = -S_1\|e^TPb\|^{1/2}R_1^{-1}\|e^TPb\|^{1/2}\hat{W}, \qquad \hat{W}(0) = 0 \tag{3.42a}$$

$$\dot{S}_1(t) = -S_1(t)\|e^TPb\|^{1/2}R_1^{-1}\|e^TPb\|^{1/2}S_1(t) + Q_1, \qquad S_1(0) = S_{10} \tag{3.42b}$$

$$\dot{\hat{V}}_m(t) = -S_2\|e^TPb\|R_2^{-1}\hat{V}, \qquad \hat{V}(0) = 0 \tag{3.43a}$$

$$\dot{S}_2(t) = -S_2(t)\|e^TPb\|R_2^{-1}S_2(t) + Q_2, \qquad S_2(0) = S_{20} \tag{3.43b}$$

## 3.4 Application of Kalman Filter Modification

A Kalman Filter approach as modification term in adaptive control is applied to a helicopter model. PD controller is implemented to control the rotational states of the helicopter, which are roll, pitch and yaw channels. In addition, command filter is used to slow down the reference signal so that helicopter can follow the given command. Linear model inversion is applied to obtain the helicopter control inputs and this controller is augmented with neural networks to take into consideration of the errors arise from model inversion and linearization.

### 3.4.1 Command Filter

Command filter is a second order low pass filter used in order to transform the reference input into desired aircraft response [27]. Command filters are implemented to all channels to slow down the reference input to the frequency range that helicopter can follow. Figure 3.3 illustrates the output of the command filter for given step input for roll channel.

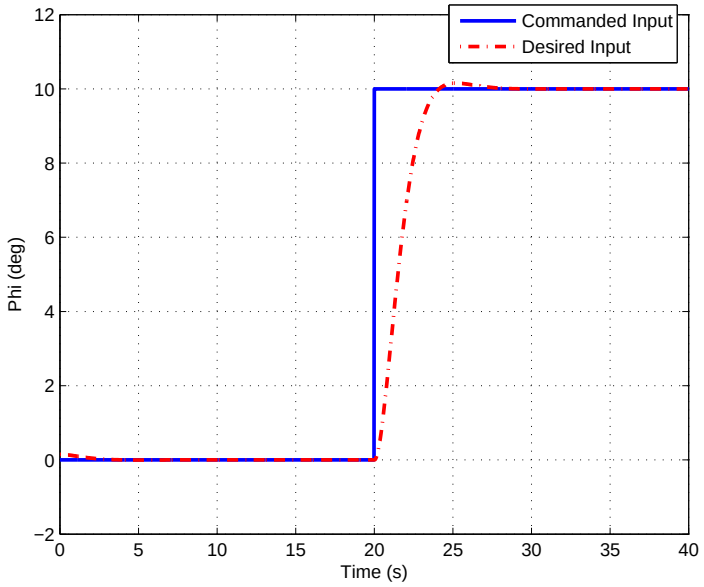


Figure 3.3: Response of Command Filter

The natural frequency and damping ratio of the command filter are chosen as 1 rad/s and 0.8, respectively. Command filter also provides the first and second derivative of that channel which are used to obtain derivative error and used as command accelerator, respectively.

### 3.4.2 Controller

As stated before, PD controller is applied to control the roll, pitch and yaw channels of the helicopter. The output of the PD controller is augmented with the neural network (Section 3.3). In equation 3.44, dynamics of the PD controller for roll channel is

given.

$$U_{PD,\phi} = K_P(\phi_{com} - \phi_{sys}) + K_D(\dot{\phi}_{com} - \dot{\phi}_{sys}) \tag{3.44}$$

$U_{PD,\phi}$ is the output of PD control, $\phi_{com}$ represents the desired roll input reference coming from command filter, $\phi_{sys}$ represents the system response and $K_P$ and $K_D$ are the feedback gains. The output of the PD controller together with the Euler angle accelerations and neural network control inputs (Section 3.3) form the pseudo controls. Pseudo controls of other two channels, pitch and yaw, are formed in the same way as the roll channel.

$$U_\phi = \ddot{\phi}_{com} + U_{PD,\phi} - U_{NN,\phi} \tag{3.45}$$

Linear model inversion is used to generate the helicopter control inputs [26, 21]. Consider the nonlinear system representing the dynamics of the helicopter.

$$\ddot{x} = f(x, \dot{x}, u) \tag{3.46}$$

The dynamics can be approximated as in Equation 3.47, which is assumed to be invertible. $\nu$ represents the pseudo control inputs.

$$\nu = \hat{f}(x, \dot{x}, u) \tag{3.47}$$

In order to obtain the control inputs, approximate model is inverted.

$$u = \hat{f}^{-1}(x, \dot{x}, \nu) \tag{3.48}$$

However, approximating the actual dynamics results in a modeling error which is defined as;

$$\Delta(x, \dot{x}, u) = f(x, \dot{x}, u) - \hat{f}(x, \dot{x}, u) \tag{3.49}$$

Model tracking error can be defined in the form of;

$$e = \begin{bmatrix} x_m - x \\ \dot{x}_m - \dot{x} \end{bmatrix} \tag{3.50}$$

Taking the derivative of Equation 3.50 and using a proportional-derivative controller, the following error dynamics can be constructed [21, 38].

$$\dot{e} = A_m e + B[\nu_{ad} - \Delta] \tag{3.51}$$

where $\nu_{ad}$ is the output of the adaptive control. In order to cancel the modeling uncertainty, $\nu_{ad} - \Delta = 0$ should be satisfied. In other words, modeling error is compansated with the adaptive element. $\nu_{ad}$ is named throughout this work as $U_{NN}$.

Model inversion is performed for the linearized dynamics at 60 knots forward flight. However; in order to invert the model, control matrix $B$ should be invertible. In our case, system consists of 8 states while there exists 4 controls which means that $B$ matrix is not a square matrix, in other words $B$ matrix is not invertible. In order to obtain the inversion of the model system is reduced such that $B$ matrix is invertible. This can be performed without generating significant loss of dynamic characteristics of the system by decoupling the rotational and translational dynamics. Since the rotational states are fast while the translational dynamics are slow in dynamics, errors that occur due to cross coupling of the dynamics can be neglected.

Full linear state-space system is given in equation 3.52.

$$\dot{x} = Ax + Bu \tag{3.52}$$

If the dynamics of rotational and translational states are decoupled, full system matrix can be separated as in equation 3.53,[26, 27].

$$\dot{x}_1 = A_1 x_1 + A' x' + B_1 u_1 \tag{3.53}$$

In equation 3.53, $x_1$ vector consists of rotational states $p, q$ and $r$, $A_1$ matrix contains the relation of the rotational states with themselves, $x'$ is the vector which consists of translational states $u, v$ and $w$ and $A'$ matrix contains the relation of translational matrix with the rotational states. Control inputs are chosen as $\delta_{long}, \delta_{lat}$ and $\delta_{ped}$, which are longitudinal, lateral and pedal inputs, respectively. $B_1$ matrix contains the relation between the controls with the rotational states. Collective control is also added to the $x'$ vector since its effect on rotational states is slower than other control inputs. Finally, decoupled system equations take the following form.

$$\begin{bmatrix} \dot{p}_D \\ \dot{q}_D \\ \dot{r}_D \end{bmatrix} = A_1 \begin{bmatrix} \Delta p \\ \Delta q \\ \Delta r \end{bmatrix} + A_2 \begin{bmatrix} \Delta u \\ \Delta v \\ \Delta w \\ \Delta \delta_{coll} \end{bmatrix} + B_1 \begin{bmatrix} \Delta \delta_{long} \\ \Delta \delta_{lat} \\ \Delta \delta_{ped} \end{bmatrix} \tag{3.54}$$

When the control input ($u_1$) matrix is left alone from the decoupled system dynamics, linear model inversion is obtained.

$$\begin{bmatrix} \Delta\delta_{long} \\ \Delta\delta_{lat} \\ \Delta\delta_{ped} \end{bmatrix} = B_1^{-1}\{ \begin{bmatrix} \dot{p}_D \\ \dot{q}_D \\ \dot{r}_D \end{bmatrix} - A_1 \begin{bmatrix} \Delta p \\ \Delta q \\ \Delta r \end{bmatrix} - A_2 \begin{bmatrix} \Delta u \\ \Delta v \\ \Delta w \\ \Delta\delta_{coll} \end{bmatrix} \} \tag{3.55}$$

$\dot{p}_D, \dot{q}_D$ and $\dot{r}_D$ can be obtained from the pseudo controls. Transformation equations are given as equations 3.56a, 3.56b and 3.56c, [26].

$$\dot{p}_D = U_\phi - U_\psi \sin\theta - \dot{\psi}\dot{\theta}\cos\theta \tag{3.56a}$$

$$\dot{q}_D = U_\theta \cos\phi - \dot{\theta}\dot{\phi}\sin\phi + U_\psi \sin\phi\cos\theta + \dot{\psi}\dot{\phi}\cos\phi\cos\theta - \dot{\psi}\dot{\theta}\sin\phi\sin\theta \tag{3.56b}$$

$$\dot{r}_D = -U_\theta \sin\phi - \dot{\theta}\dot{\phi}\cos\phi - U_\psi \cos\phi\cos\theta - \dot{\psi}\dot{\phi}\sin\phi\cos\theta - \dot{\psi}\dot{\theta}\cos\phi\sin\theta \tag{3.56c}$$

Adaptive element is augmented with the system by using neural networks detailed in Section 3.3.

The block diagram of the whole system is given in Figure 3.4.

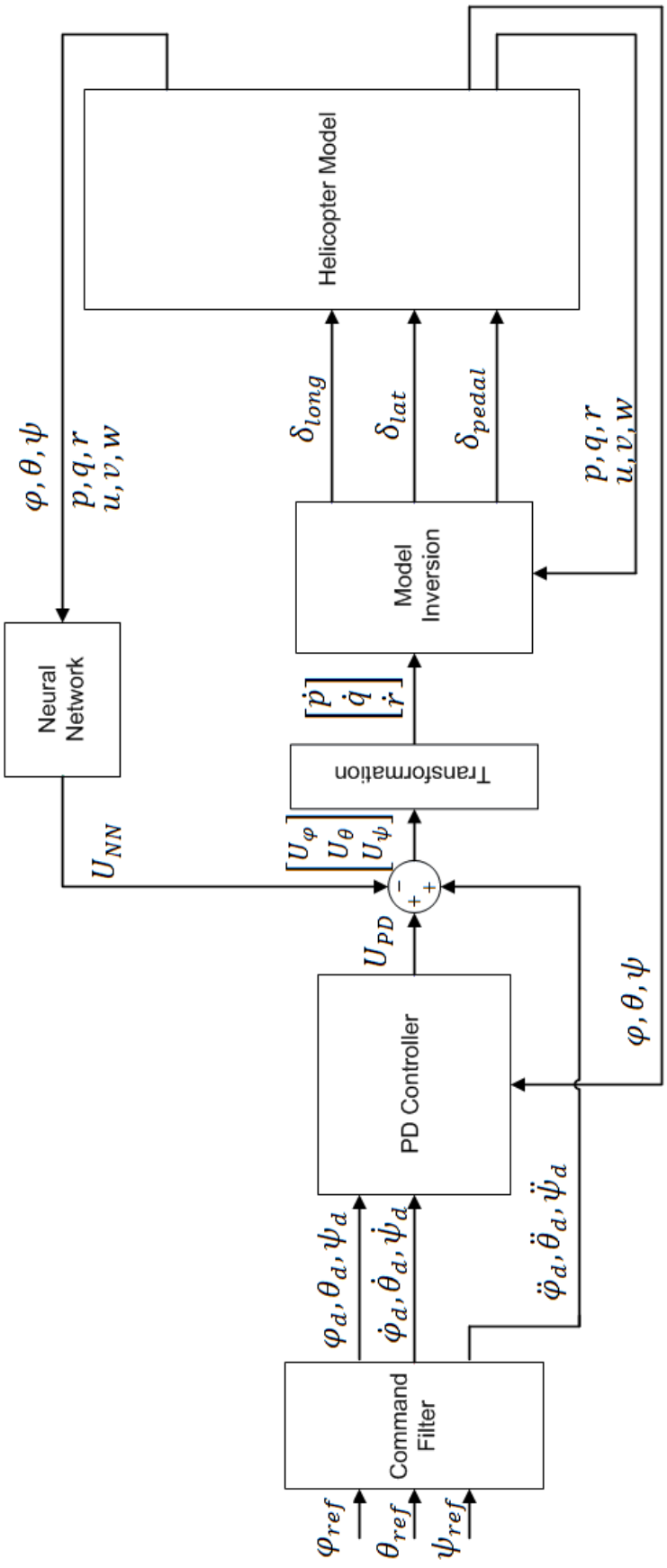


Figure 3.4: Block Diagram of the System

## 3.5 Simulation Results

The Kalman Filter approach in adaptive control as a modification term is demonstrated using a simplified aircraft model and a high fidelity helicopter simulation. The attitude controller and e-modification term derived as given in Section 3.3 by using KF optimization algorithm is modeled in Simulink/Matlab. Firstly, KF-based e-modification is implemented on the rolling motion of an aircraft to stabilize this motion, then it is implemented to the helicopter to control the rotational states.

Rolling motion which is called as Wing Rock dynamics is used in Ref. [23] to illustrate the performance of the KF approach. This sample dynamics is also used in this work with different reference model and uncertainty characteristics to fully understand the effect of the KF approach.

Helicopter model is used as the original work and the actual application. KF based e-modification is implemented by using both LPNN and SHL-NN structure to the helicopter. Performance of the KF based e-modification when the helicopter is under longitudinal and lateral maneuver is examined independently.

Neural network parameters which are common in every simulation are given below. P matrix which is the solution of a Lyapunov function is used as in 3.57 [33].

$$P = \begin{bmatrix} \frac{K_D}{K_P} + \frac{1}{2K_D} & \frac{1}{2K_P} \\ \frac{1}{2K_P} & \frac{1+K_P}{2K_PK_D} \end{bmatrix} \tag{3.57}$$

And vector b is given as;

$$b = \begin{bmatrix} 0 \\ 1 \end{bmatrix} \tag{3.58}$$

Moreover, basis function is selected to be sigmoidal basis function for both LPNN and SHL-NN which is in the given form (Equation 3.59) where $\bar{x}$ is the neural network input vector and $a$ is the activation potentials. Activation potentials are the design parameters.

$$\beta(\bar{x}) = \frac{1}{1 + e^{-a\bar{x}}} \tag{3.59}$$

In the following sections, simulation results of the mentioned applications are pro-

vided for various scenarios.

### 3.5.1 Wing Rock Dynamics

Wing Rock dynamics is the rolling motion of a aircraft. This motion occurs in aircrafts with highly swept wings at high angle of attack and side-slip angles. If it is not be controlled the oscillations can grow unboundedly. Similar to [21, 23], the dynamics can be simplified as follows:

$$\dot{\phi}(t) = p(t) \tag{3.60a}$$

$$\dot{p}(t) = u(t) + \Delta(\phi, p) \tag{3.60b}$$

where $\Delta(.)$ is the uncertainty and defined in this work as below.

$$\Delta(\phi, p) = 0.1278\phi(t) + 0.7579p(t) - 0.4245|\phi(t)|p(t) + 0.5195|p(t)|p(t)$$

Effect of the uncertainty on the system is given in Figure 3.5, it is clearly seen that uncertainty worsened the performance of the system significantly.

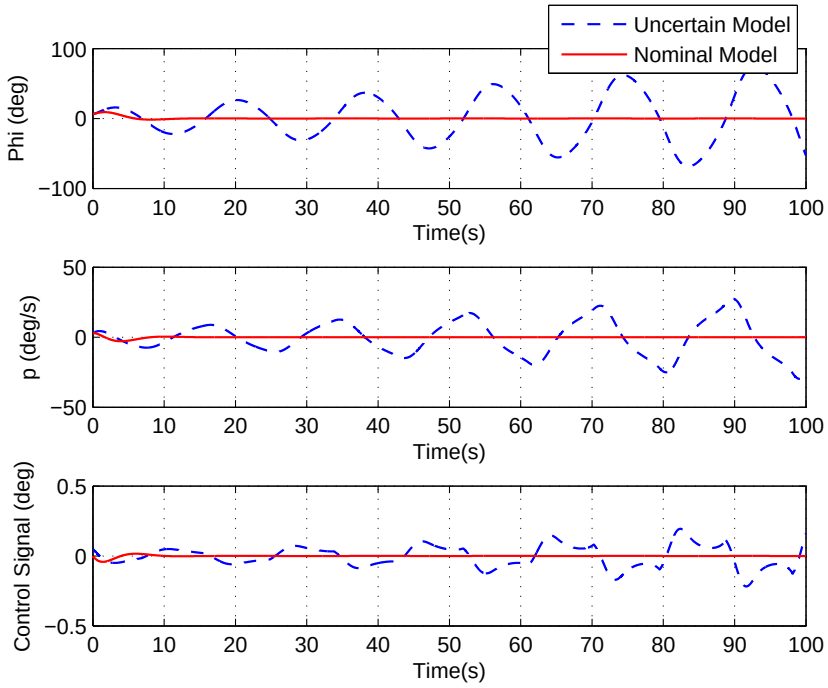


Figure 3.5: Nominal Control Performance with and without Uncertainty

The reference model mentioned in Section 3.2 is selected such that natural frequency and damping ratio of the desired model is 0.7 rad/s and 0.6, respectively. In this

application, Kalman Filter parameters are chosen to be $S_0 = I, R = 0.05I$ and $Q = I$ where $I$ is the identity matrix. Since the aim is to stabilize the rolling motion, reference inputs of the roll angle and roll rate are taken to be zero. System states and control input are obtained by using baseline adaptive law, standard e-modification and KF-based e-modification for different learning rates.

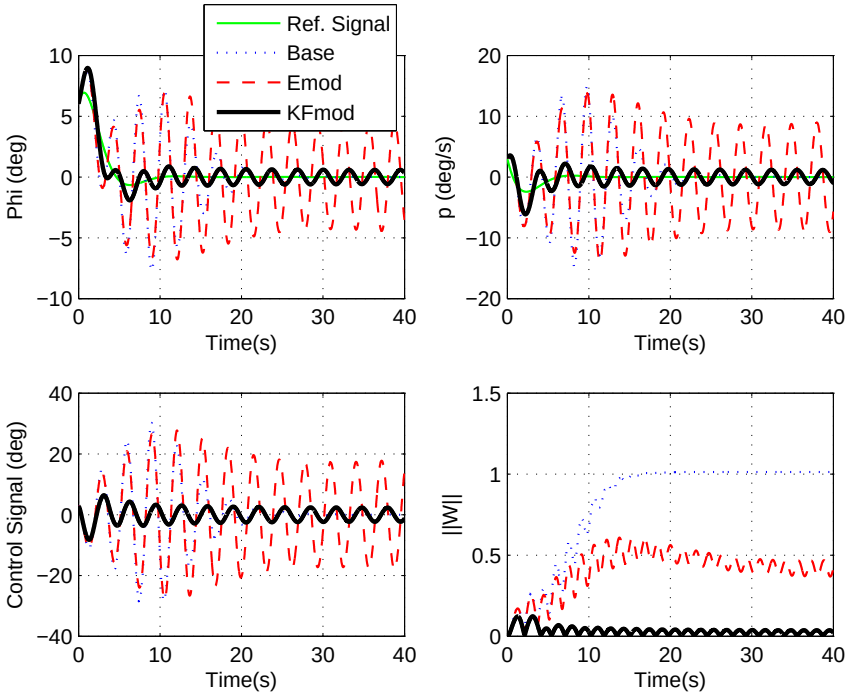


Figure 3.6: Performance Comparison of Adaptive Laws ($\gamma = \gamma\sigma_e = \gamma\sigma_{kf} = 1$)

In Figure 3.6, 3.7 and 3.8, KF approach in modification term improves the damping performance of the system significantly. Blue dash-dot lines represent the results of baseline adaptive law, red dashed lines represent the standard e-modification and black solid lines represent the KF-based e-modification in figures. Both baseline law and standard e-modification result in high oscillatory responses. Moreover, high control effort is necessary to achieve the tracking. On the other hand, due to its variable modification gain, control effort is optimal for KF approach. Modification gain is adjusted as the tracking error gets small and unnecessary control effort is eliminated with this approach. As a result of this adjustment, system produces smoother response in response to the small and unoscillatory control input.

This approach is effective especially when there are oscillations or noise in the system when its effects amplify with learning rates in baseline law and standard modification

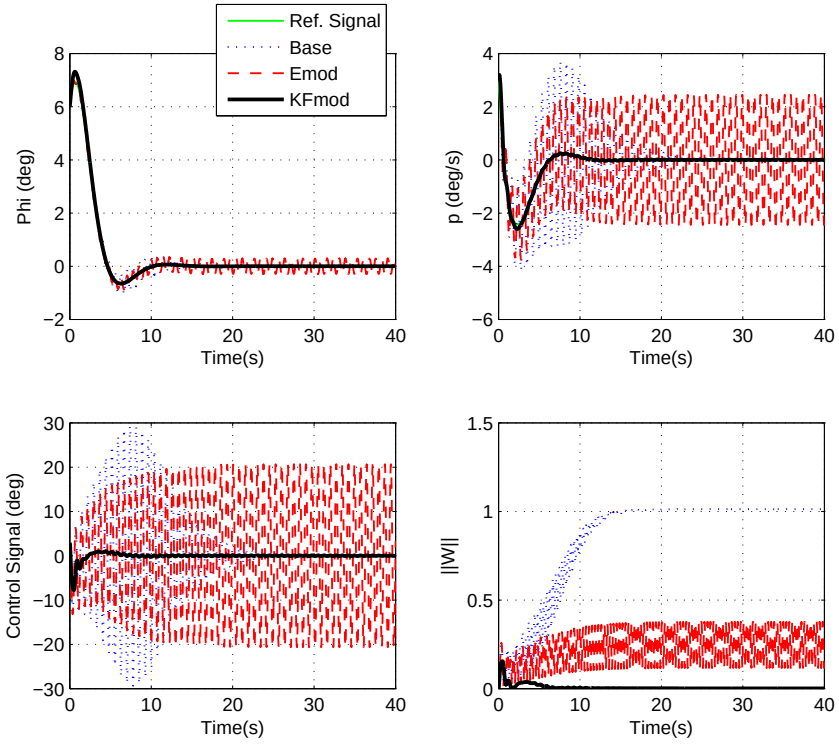


Figure 3.7: Performance Comparison of Adaptive Laws ($\gamma = \gamma\sigma_e = \gamma\sigma_{kf} = 20$)

terms. Therefore, performance is also investigated when the system is under sensor noise with learning rate 20. E-modification with Kalman approach also provides better results according to its alternatives in this case. The performance comparison is given in Figure 3.9 when the system is under sensor noise.

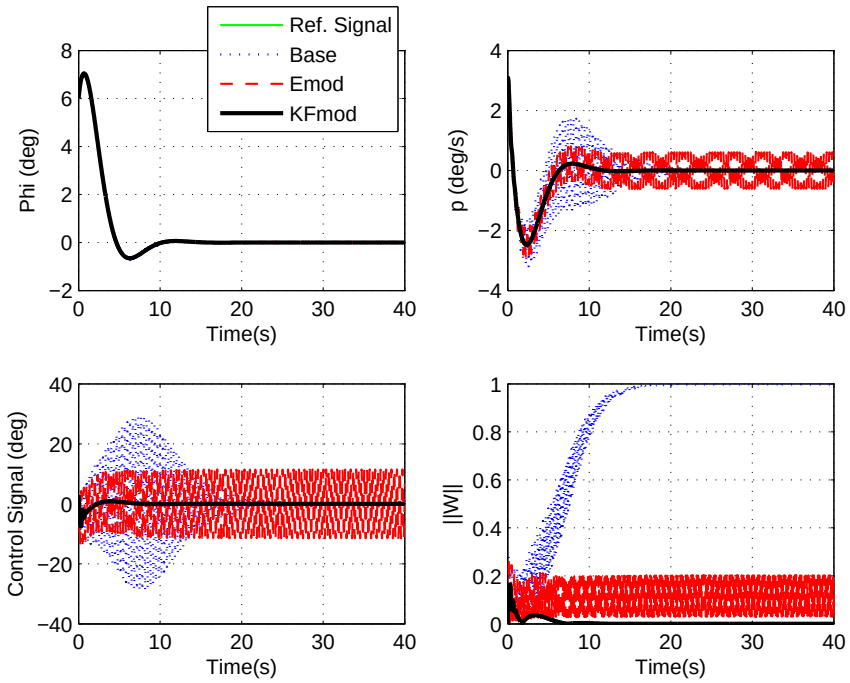


Figure 3.8: Performance Comparison of Adaptive Laws ($\gamma = \gamma\sigma_e = \gamma\sigma_{kf} = 100$)

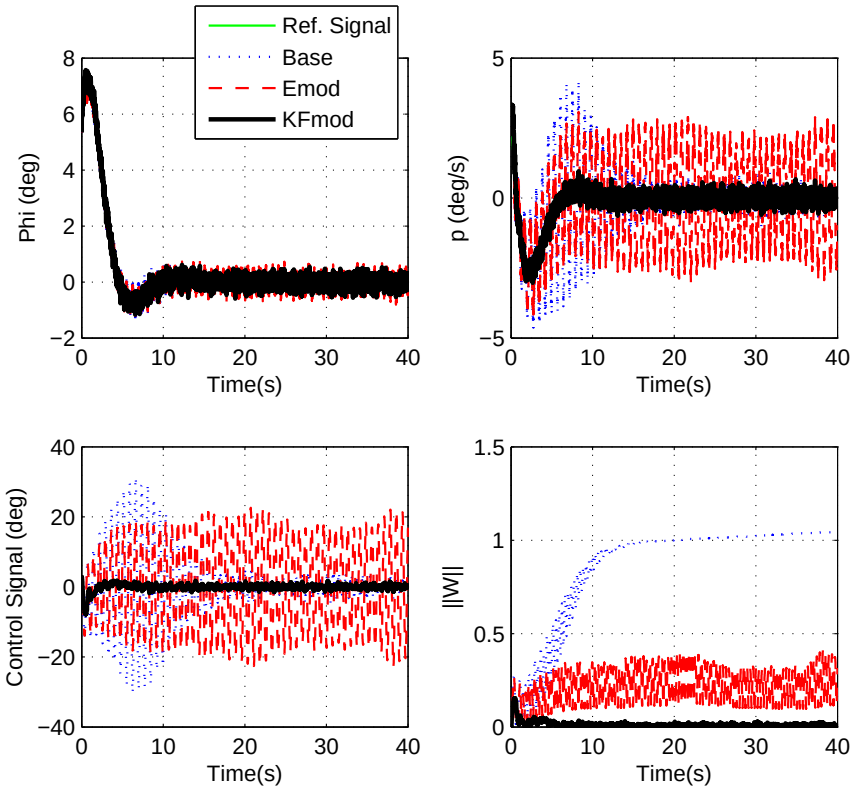


Figure 3.9: Performance Comparison of Adaptive Laws Under Sensor Noise ($\gamma = \gamma\sigma_e = \gamma\sigma_{kf} = 20$)

### 3.5.2 Helicopter Model Application

In this section, Kalman filter based e-modification is implemented to a high fidelity helicopter model. Helicopter application is the original work of this thesis. Neural network adaptive controller is constructed by using LPNN and SHL-NN structure and implemented to the helicopter model. Performance of the adaptive controller with baseline law and with e-modification terms are investigated.

LPNN adaptive controller is implemented to a single channel of the helicopter. The analyses are performed for both longitudinal and lateral channels while other channels are kept at zero reference with proportional-integral-derivative (PID) controller.

SHL-NN adaptive controller which is a multi-input multi-output neural network structure is implemented to all channels (roll, pitch and yaw). In other words, the output of the neural network is a vector containing the adaptive elements of the three channels.

#### 3.5.2.1 Results with LPNN

Adaptive controller constructed with LPNN is implemented to a single channel of the helicopter. Controller of the theta channel $(\theta)$ is augmented with LPNN in longitudinal channel while controller of the psi channel $(\psi)$ is augmented with LPNN in lateral channel. In both applications, other two channels are kept at zero reference with PID controller. The block diagram of the controller is given for longitudinal channel in Figure 3.10.

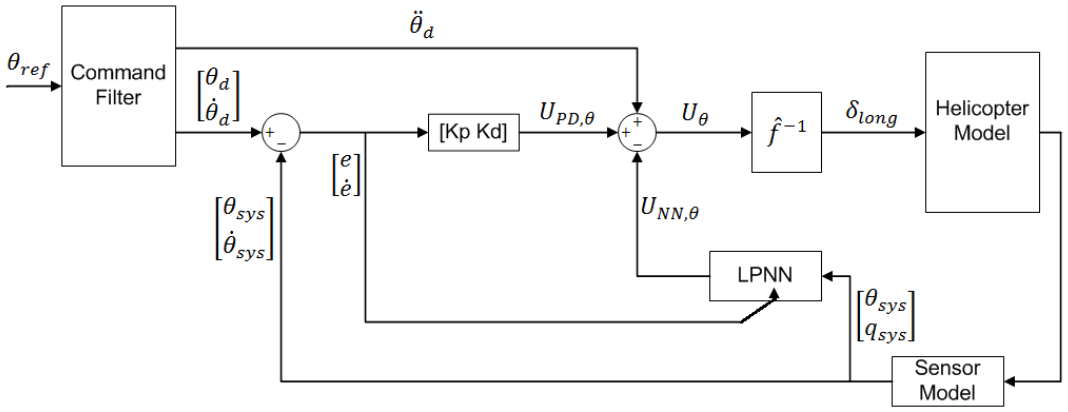


Figure 3.10: Block Diagram of the Longitudinal Controller Augmented with LPNN

Performance of the channels are analyzed for two different input references, which are step signal input and sine signal input.

**Step Input**

A step input is given as the reference input in simulations for both longitudinal and lateral channels.

**Longitudinal Channel**

15 degree step input is fed to the system meaning that helicopter performs pull-up push-down maneuver. Neural network inputs chosen for longitudinal channel are given below, where $b_1$ is the neural network bias term.

$$\bar{x}_{long} = [\theta \;\; q \;\; \theta q \;\; b_1]^T \tag{3.61}$$

Activation potentials of the neurons are selected to be:

$$a = [1 \;\; 1 \;\; 0.1]$$

Feedback gains of the PD controller are chosen such that natural frequency of the desired dynamics is 1 rad/s and its damping ratio is 0.8. Kalman Filter parameters for longitudinal channel are chosen to be $S_0 = I, R = 0.1I$ and $Q = 0.001I$ and for the case which sensor noise is taken into consideration, these parameters are tuned to be $S_0 = I, R = 0.1I$ and $Q = 0.01I$. $I$ is the identity matrix.

Simulations are performed for different learning rates and baseline law, standard e-modification and KF-based e-modification are compared in terms of tracking performance and control efficiency. Helicopter longitudinal input is the control signal of interest in this case. In Figure 3.11, response of the helicopter can be seen when the controller is not augmented with neural networks. The modelling error existing in the system degrades system performance significantly.

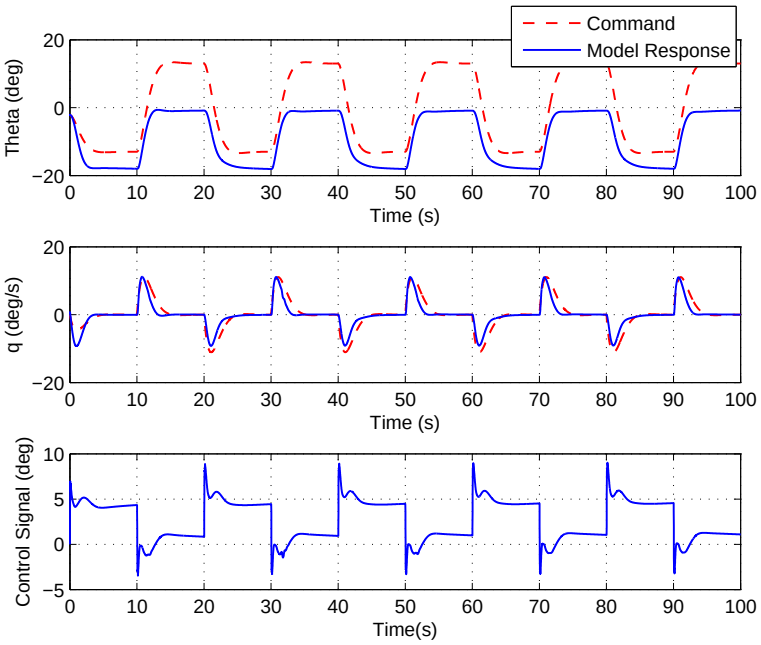


Figure 3.11: Controller Performance in Longitudinal Channel without Adaptive Control

Figures 3.12 and 3.13 show the performance comparison of the adaptive laws for learning rate 5 and 10, respectively. Kalman Filter approach gives smoother response among the adaptive laws. Moreover, it achieves the required tracking performance with less control effort. Its effectiveness is more obvious when the learning rate is higher (Figure 3.13) since higher gains cause the amplification of modelling errors and sensor noises. In addition, high control inputs are necessary to achieve the tracking in these cases. Kalman Filter approach optimizes the modification gain according to tracking error.

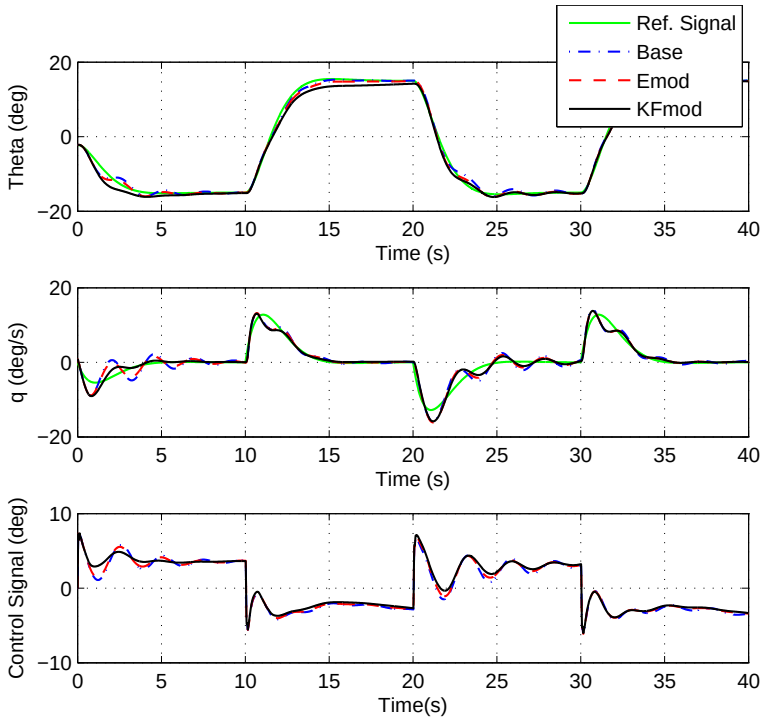


Figure 3.12: Longitudinal Performance Comparison of Adaptive Laws with LPNN

$(\gamma = \gamma\sigma_e = \gamma\sigma_{kf} = 5)$

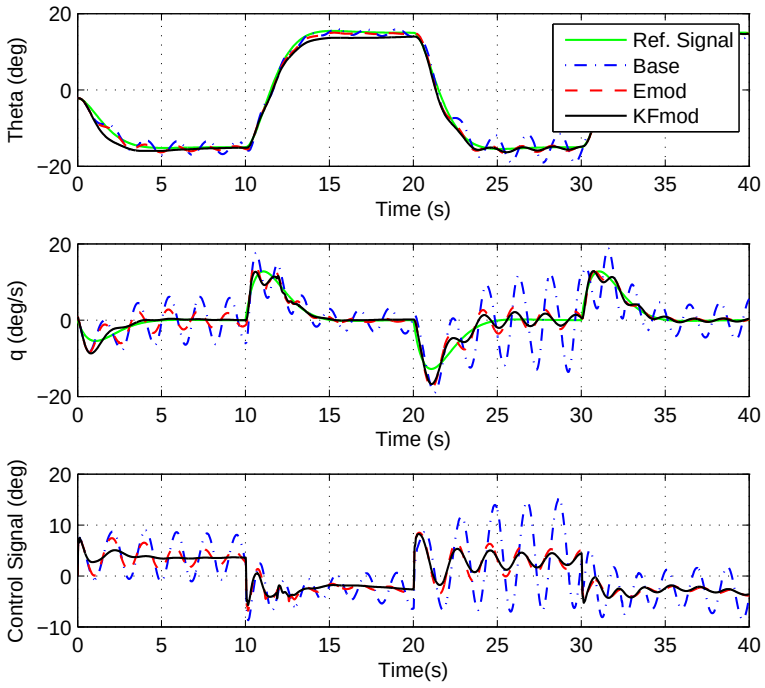


Figure 3.13: Longitudinal Performance Comparison of Adaptive Laws with LPNN

$(\gamma = \gamma\sigma_e = \gamma\sigma_{kf} = 10)$

Sensor noise is added to the system to evaluate the performance of the KF approach. Similar to previous results, KF approach provides less oscillatory system response with smaller control effort. The comparison of the adaptive laws when the system is under sensor noise is shown in Figure 3.14.

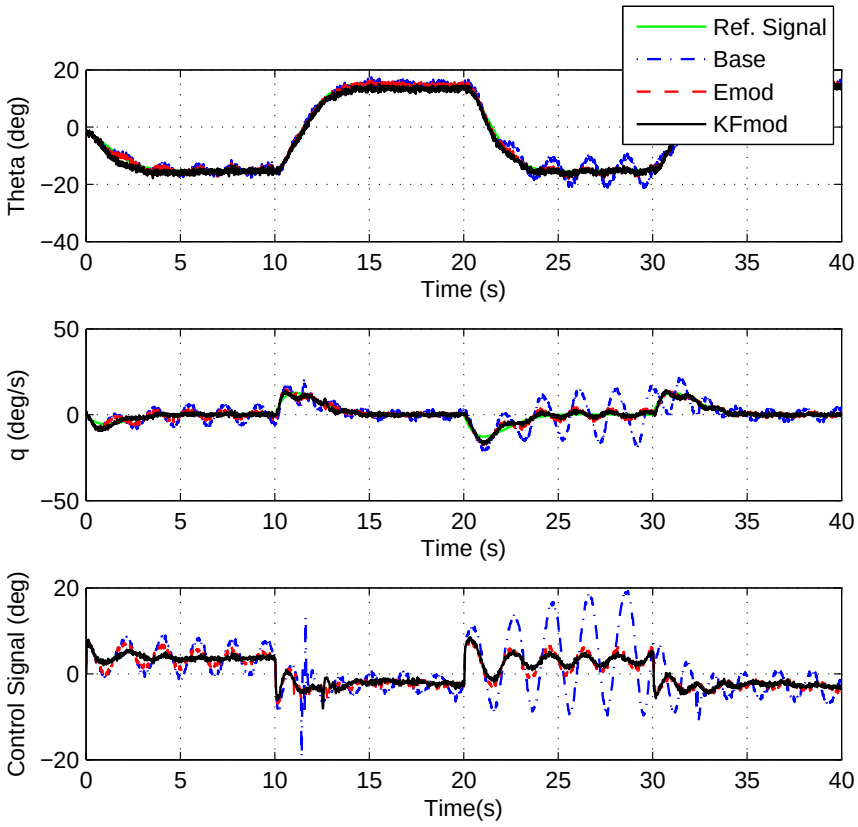


Figure 3.14: Longitudinal Performance Comparison of Adaptive Laws under Sensor Noise ($\gamma = \gamma\sigma_e = \gamma\sigma_{kf} = 10$)

Adaptive weight norms are also investigated for different adaptive laws. Figure 3.15 shows this comparison for system with and without sensor noise. It can be seen from the figure that weight norm is small for KF approach indicating that its control effort is minimum among the others.

The body velocities of the helicopter during pull-up push-down maneuver are given in Figure 3.16.

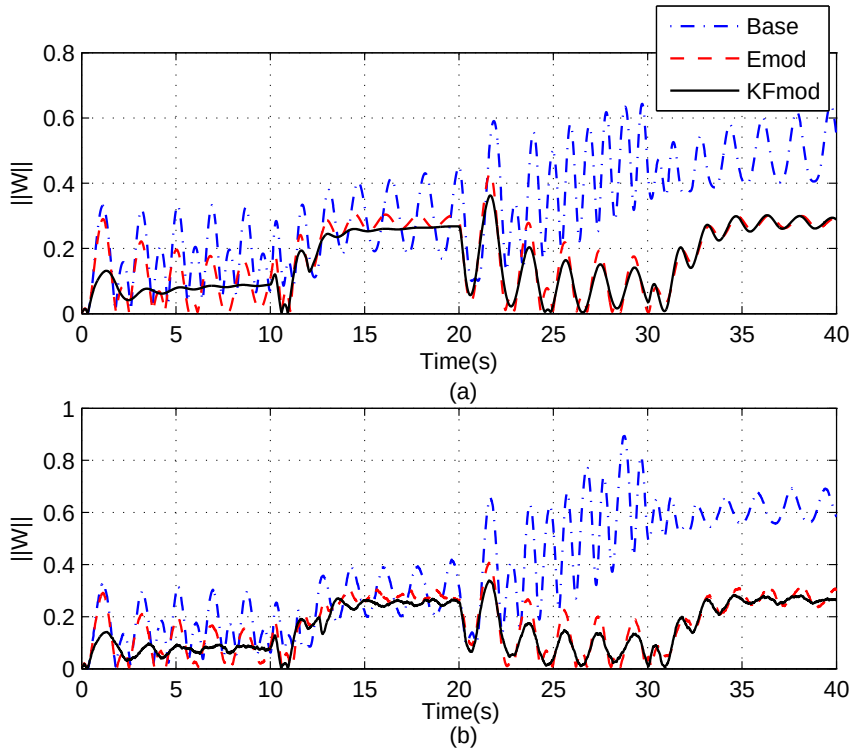


Figure 3.15: Comparison of Adaptive Weight Norms (a)Without Sensor Noise (b)With Sensor Noise

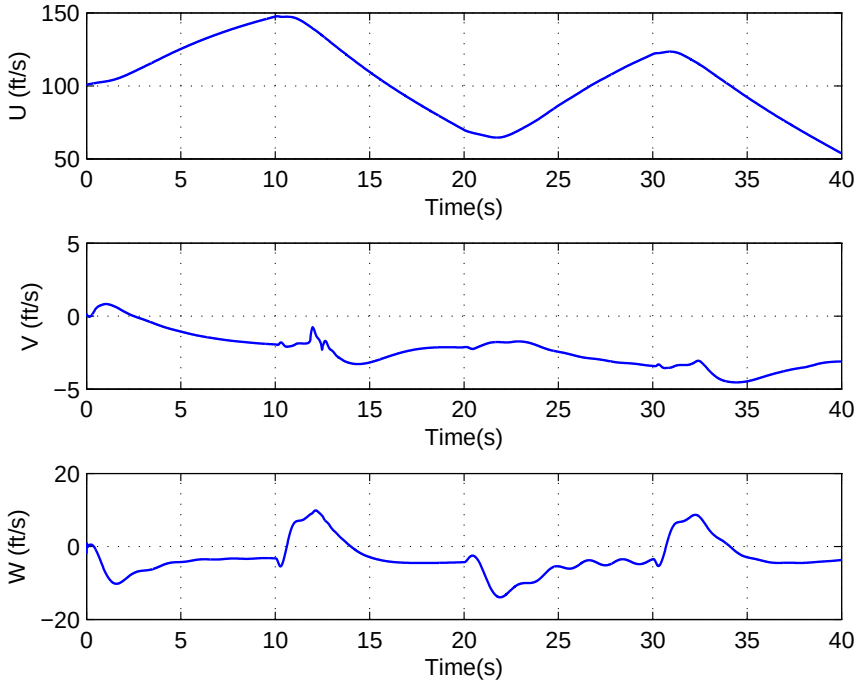


Figure 3.16: Body Velocities of the Helicopter During Longitudinal Maneuver

**Lateral Channel**

30 degree step input is given to the yaw angle ($\psi$) for lateral channel simulations. Neural network inputs chosen for lateral channel ($\psi$) are given below where $b_1$ is the neural network bias term.

$$\bar{x}_{lat} = [\psi \;\; r \;\; \psi r \;\; b_1]^T \tag{3.62}$$

Activation potentials of the neurons are chosen to be:

$$a = [1 \;\; 1 \;\; 1]$$

Feedback gains of the PD controller are chosen such that natural frequency of the desired dynamics is 1 rad/s and its damping ratio is 0.8. Kalman Filter parameters for lateral channel are chosen to be $S_0 = 10I$, $R = I$ and $Q = 0.1I$.

In Figure 3.17, system response without adaptive control is given. Control signal is the helicopter pedal input in this case.

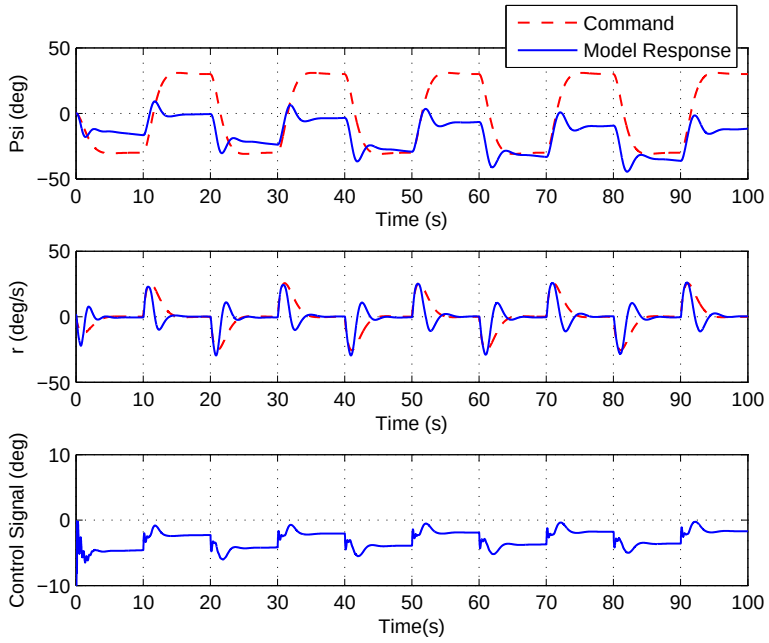


Figure 3.17: Controller Performance in Lateral Channel without Adaptive Control

In Figures 3.18 and 3.19 system response can be seen for adaptive control learning rates 10 and 20, respectively. Similar to longitudinal simulation results, KF approach provides the best results with less control effort. However, adding damping to the system is a compromise with tracking performance. Although KF approach tracking error is bigger than the alternatives, it satisfies the required level of tracking.

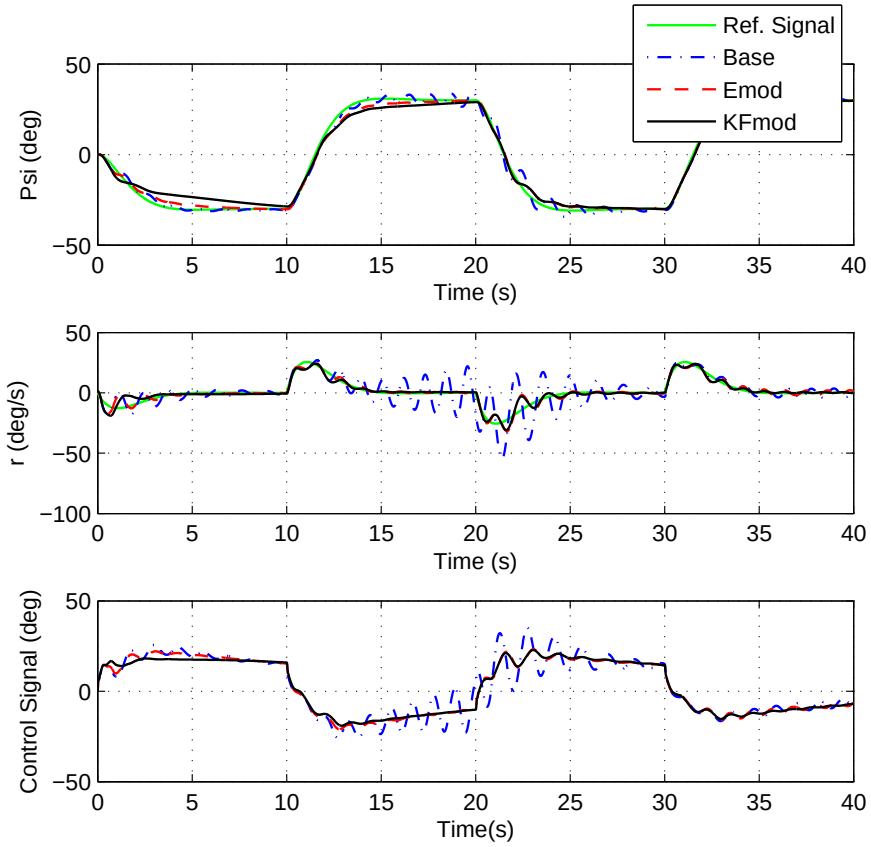


Figure 3.18: Lateral Performance Comparison of Adaptive Laws with LPNN ($\gamma = \gamma\sigma_e = \gamma\sigma_{kf} = 10$)

Simulation with sensor noise is performed for learning rate 20. As expected, e-modification with Kalman Filter approach provides less oscillatory response with less control input. Results are given in Figure 3.20.

Adaptive control effort is compared for different adaptive laws in terms of adaptive weight norms. From Figure 3.21, it can be seen that norm of the weights is the smallest for KF approach.

The body velocities of the helicopter during yaw maneuver are given in Figure 3.22.

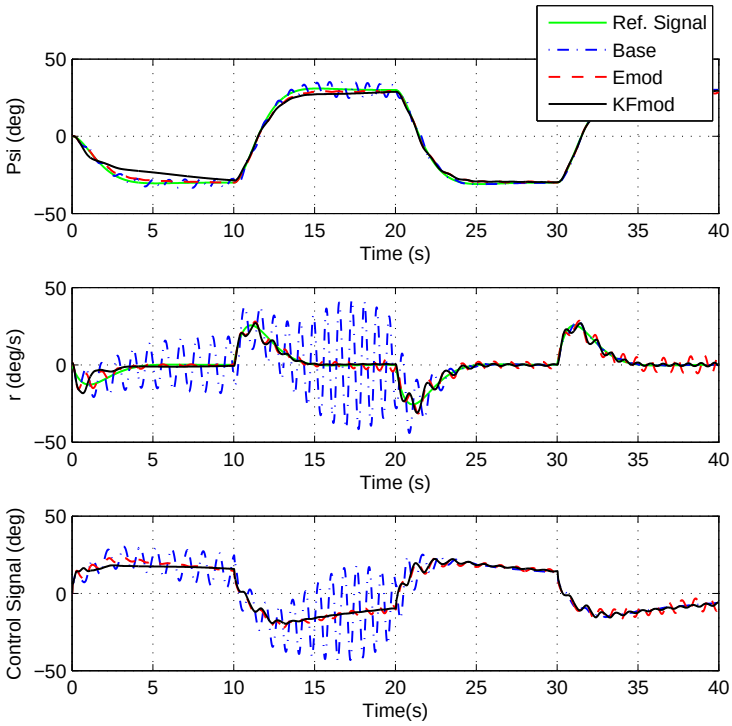


Figure 3.19: Lateral Performance Comparison of Adaptive Laws with LPNN ($\gamma = \gamma\sigma_e = \gamma\sigma_{kf} = 20$)

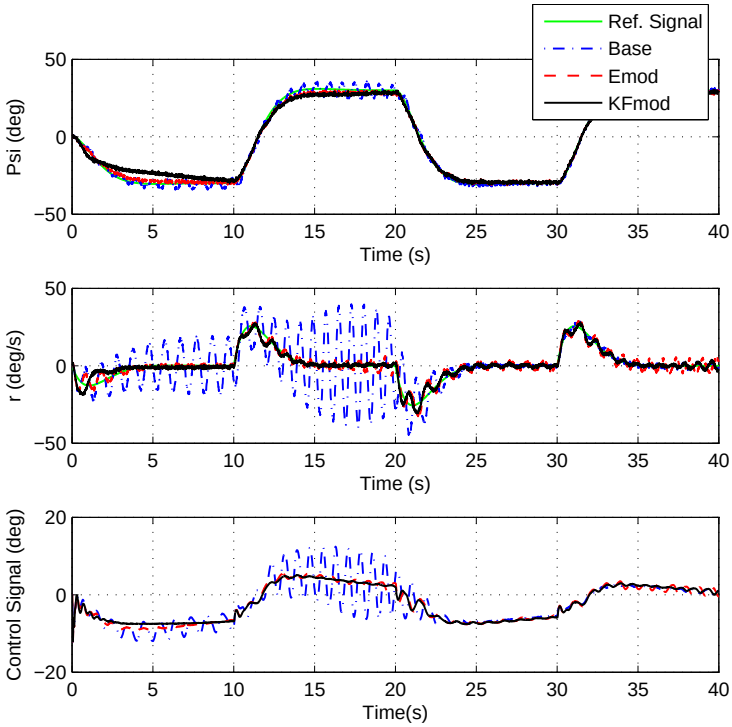


Figure 3.20: Lateral Performance Comparison of Adaptive Laws under Sensor Noise ($\gamma = \gamma\sigma_e = \gamma\sigma_{kf} = 20$)

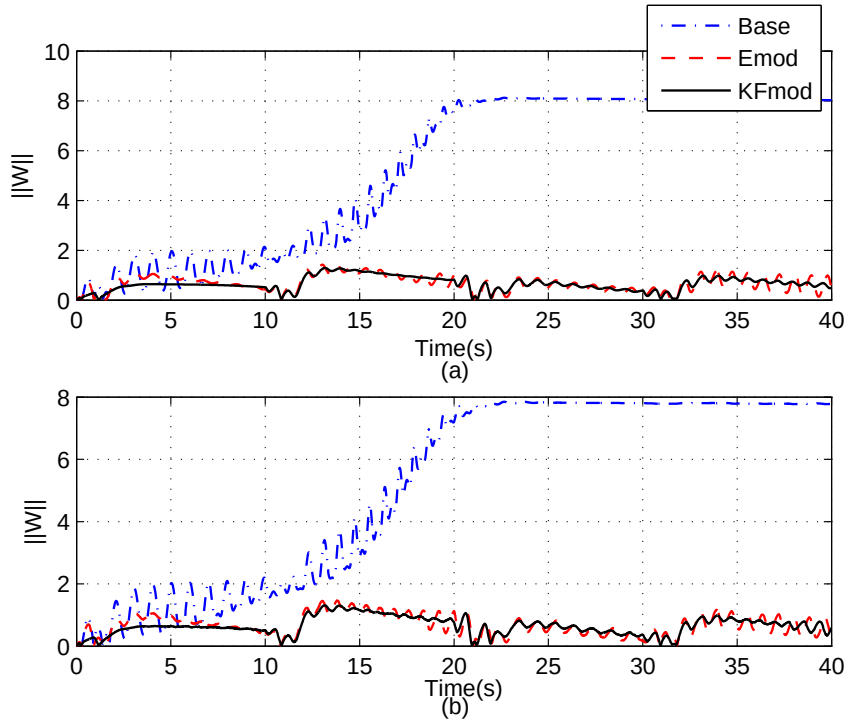


Figure 3.21: Comparison of Adaptive Weight Norms (a)Without Sensor Noise (b)With Sensor Noise

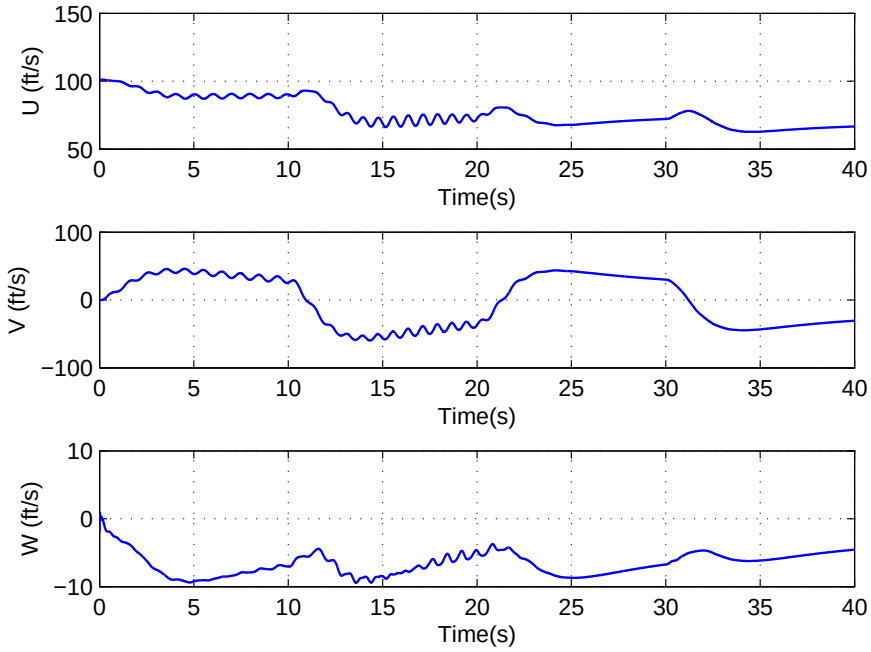


Figure 3.22: Body Velocities of the Helicopter During Lateral Maneuver

**Sine Signal Input**

In this part, sine signal input is given as the reference input in simulations for both longitudinal and lateral channels to investigate the system performance with different command inputs.

**Longitudinal Channel**

10 degree sine input is fed to the longitudinal channel ($\theta$) of the system in this case to analyze the performance of KF approach with a different command input. Kalman Filter parameters for sine input simulation are chosen to be $S_0 = 10I, R = 0.1I$ and $Q = 0.01I$.

In Figure 3.23 and 3.24 performance comparisons of the adaptive laws for learning rate 10 are given for the system with and without sensor noise. From the results, it is observed that KF approach performs better in terms of control effort relative to standard e-modification in the nominal case as well as when the system is under sensor noise. System response with KF-based e-modification requires less control input to achieve the required level of tracking while providing system response almost without oscillations.

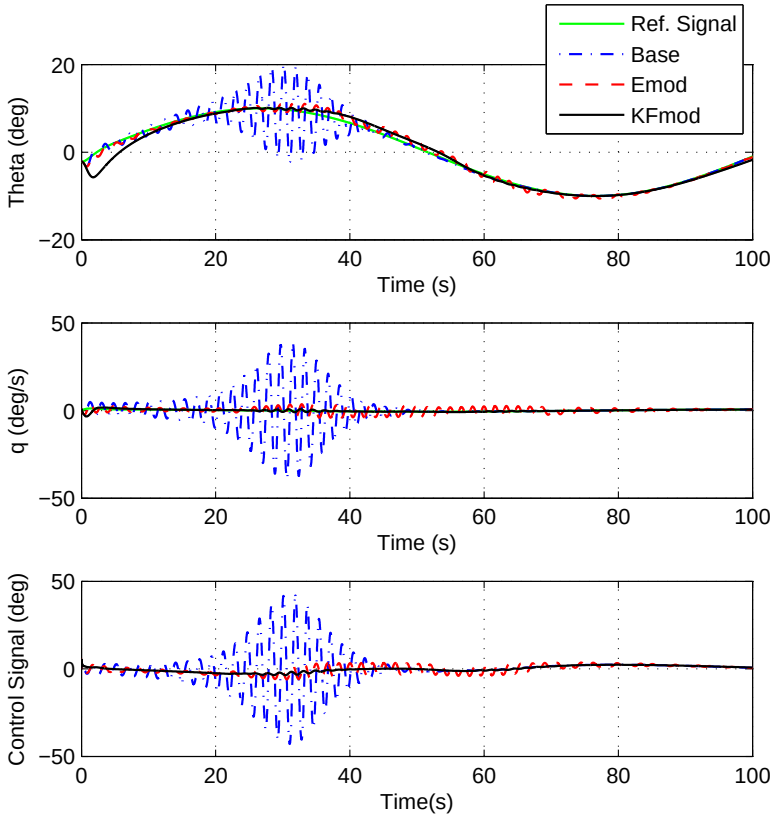


Figure 3.23: Performance Comparison of Adaptive Laws with Longitudinal Sine Input ($\gamma = \gamma\sigma_e = \gamma\sigma_{kf} = 10$)

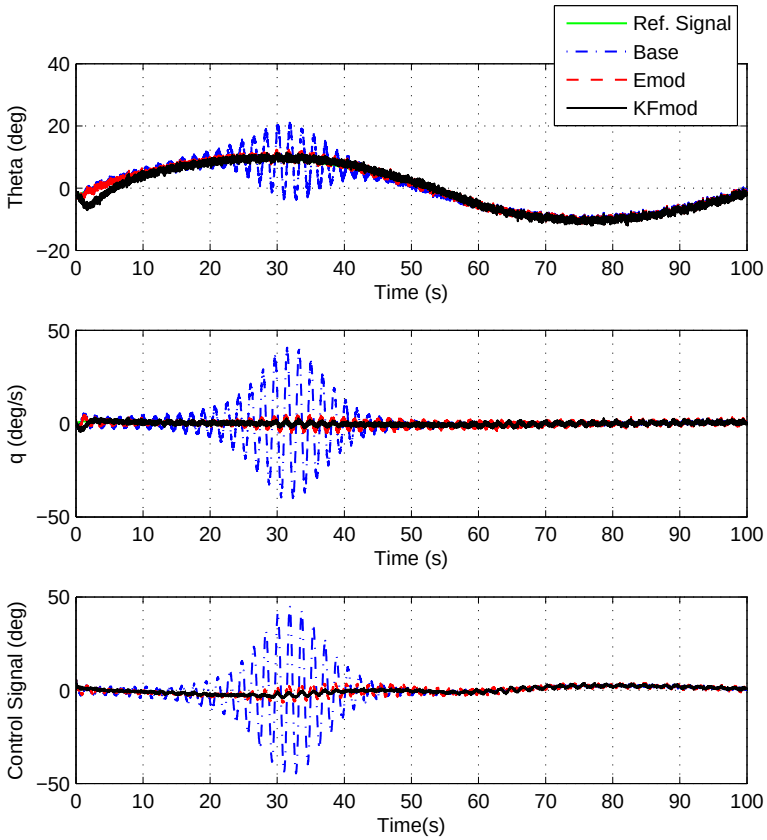


Figure 3.24: Performance Comparison of Adaptive Laws with Longitudinal Sine Input under Sensor Noise ($\gamma = \gamma\sigma_e = \gamma\sigma_{kf} = 10$)

Adaptive control efficiency is evaluated in terms of adaptive weight norms in Figure 3.25 for nominal system and for the system when the sensors are noisy. KF approach provides smooth control input with smaller magnitude for both case.

Body velocities of the helicopter are given in Figure 3.26.

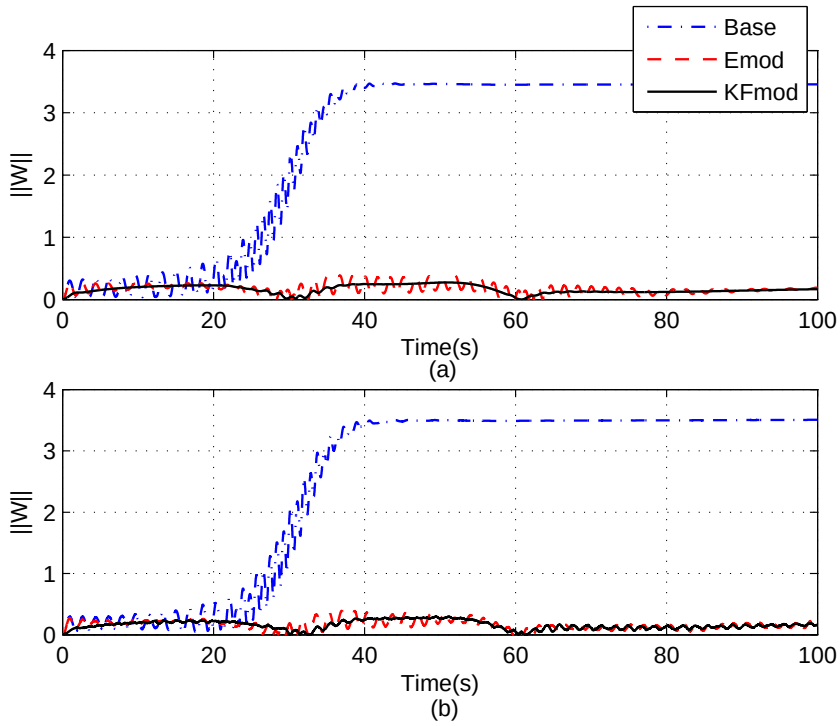


Figure 3.25: Comparison of Adaptive Weight Norms (a)Without Sensor Noise (b)With Sensor Noise

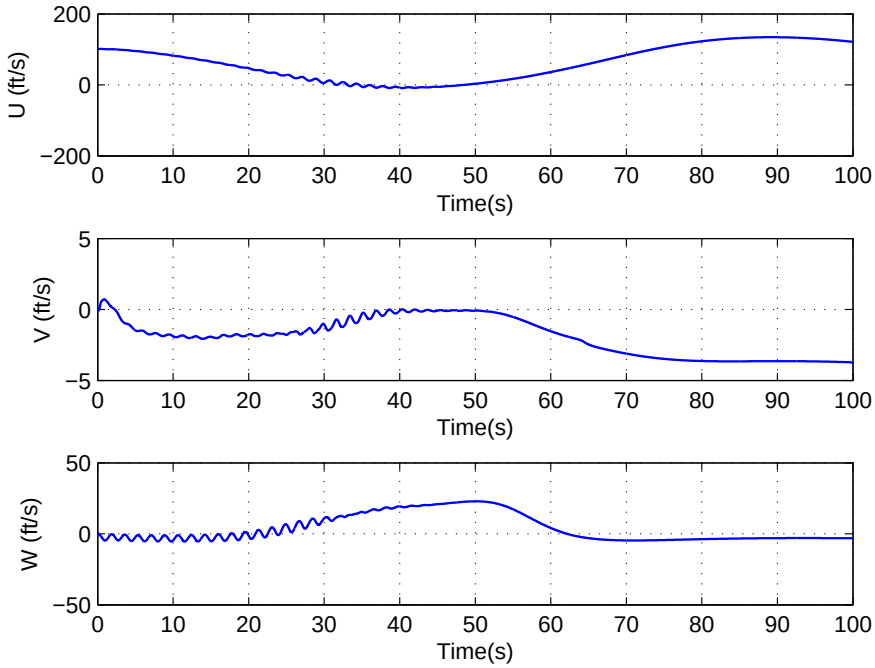


Figure 3.26: Body Velocities of the Helicopter with Longitudinal Sine Input

**Lateral Channel**

30 degree sine input is fed to the yaw channel ($\psi$) of the system in this case to analyze the performance of the KF approach with a different command input in lateral dynamics. Similar to previous case, Kalman Filter parameters for lateral channel simulations are chosen to be $S_0 = 10I$, $R = 0.1I$ and $Q = 0.01I$.

Comparison of adaptive laws for lateral channel is performed for learning rates 10 and 20. Tracking performance and the control effort of the helicopter can be seen in Figures 3.27 and 3.28 when the learning rates are 10 and 20, respectively. The baseline adaptive law and standard e-modifications result in high control input to satisfy the tracking, leading to an oscillatory system response. On the other hand, KF-based e-modification provides smooth system response and control input with little oscillations. Besides, with this approach tracking error is kept small during the flight simulation.

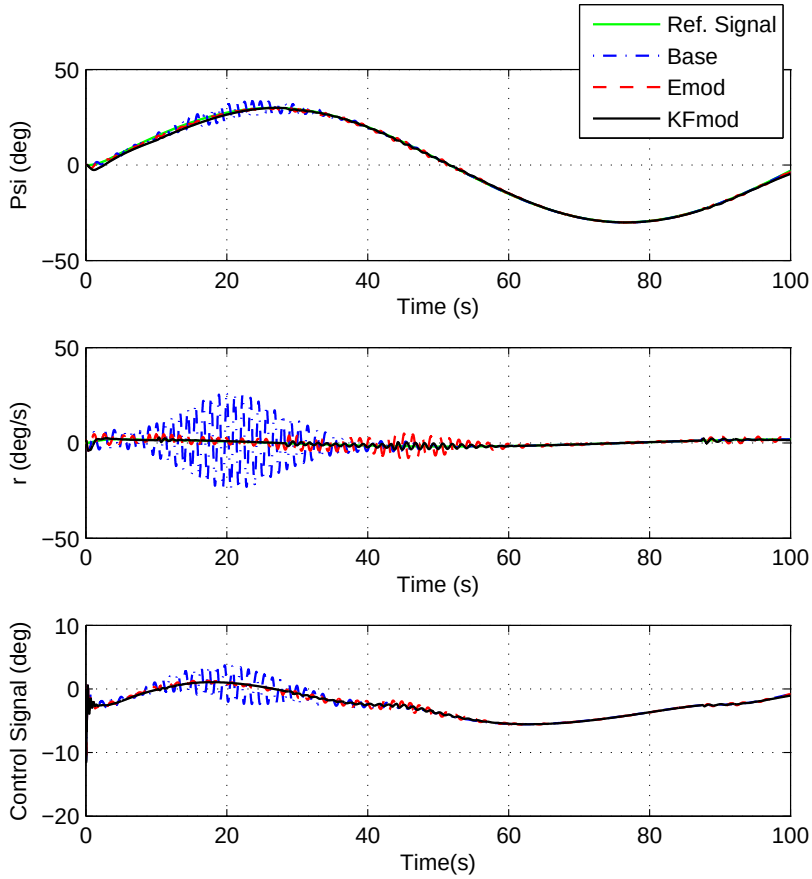


Figure 3.27: Performance Comparison of Adaptive Laws with Lateral Sine Input ($\gamma = \gamma\sigma_e = \gamma\sigma_{kf} = 10$)

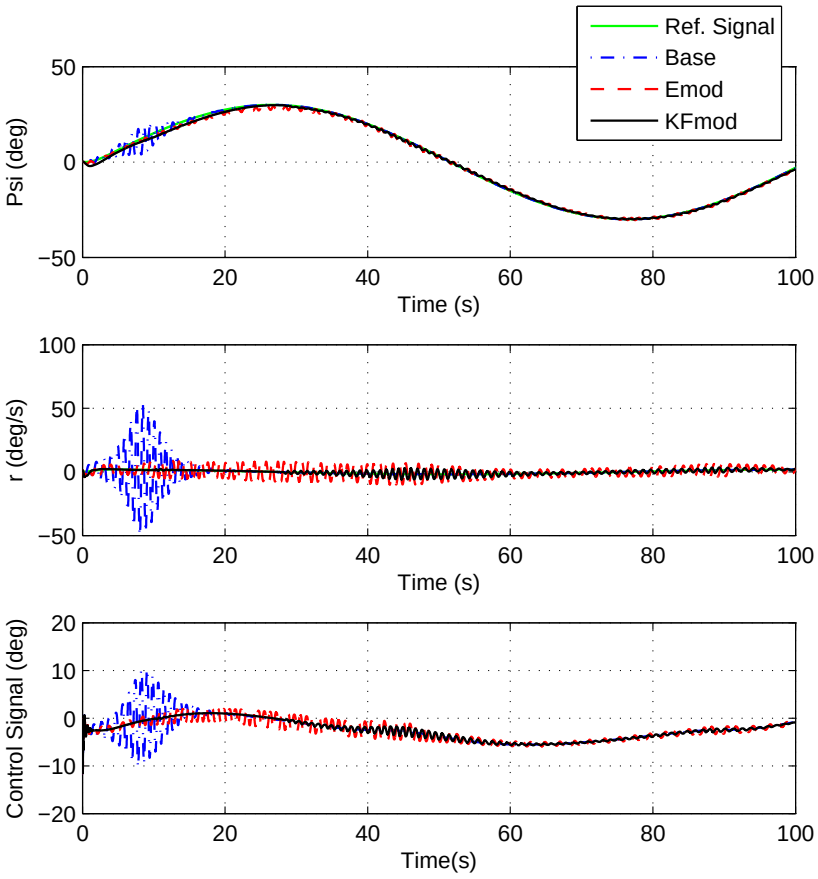


Figure 3.28: Performance Comparison of Adaptive Laws with Lateral Sine Input ($\gamma = \gamma\sigma_e = \gamma\sigma_{kf} = 20$)

System is analyzed with sensor noise for learning rate 20. Tracking and control effort performances are compared for baseline, standard e-modification and KF-based e-modification in Figure 3.29. Similar to the nominal case, KF-based e-modification provides the best results.

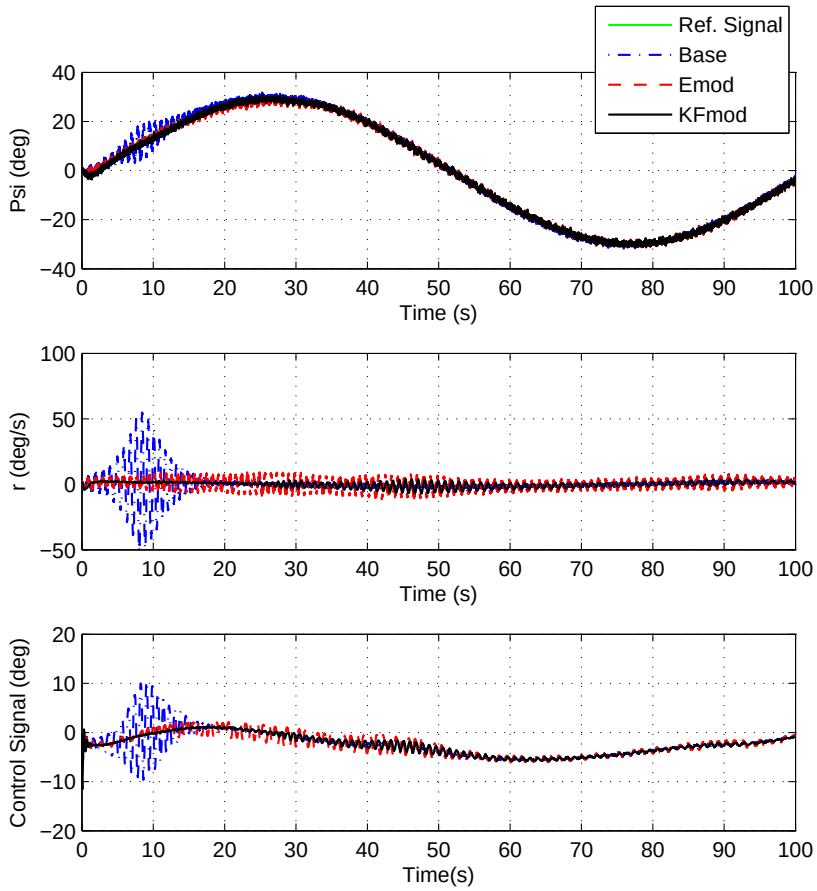


Figure 3.29: Performance Comparison of Adaptive Laws with Lateral Sine Input under Sensor Noise ($\gamma = \gamma\sigma_e = \gamma\sigma_{kf} = 20$)

Adaptive weight norms are compared for nominal case and the case with the sensor noise taken into consideration in Figure 3.30. It can be seen from the figure that control effort is less when the neural network is augmented with KF-based e-modification.

Body velocities of the helicopter during this maneuver are given in Figure 3.31.

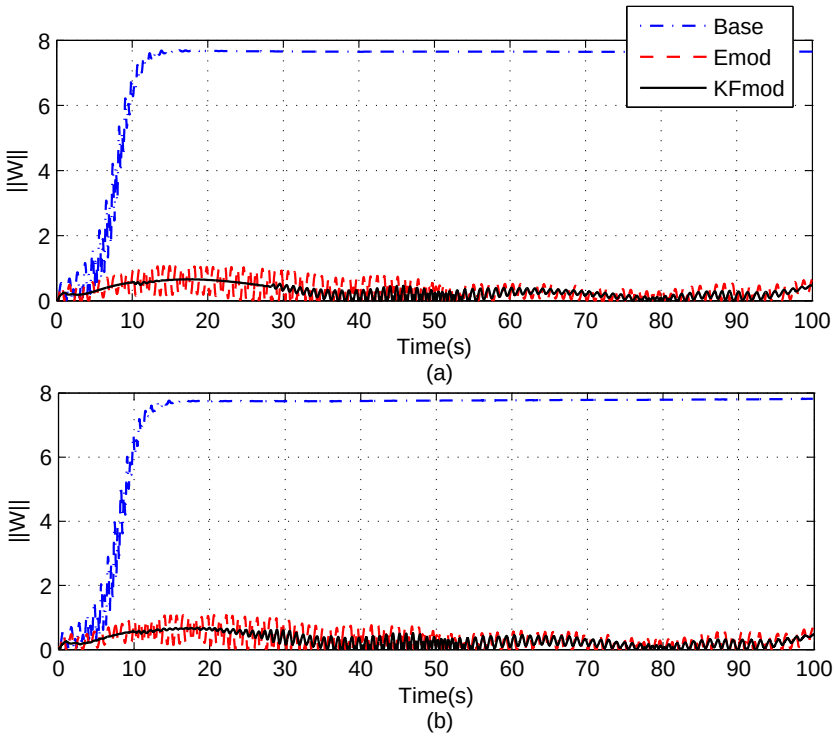


Figure 3.30: Comparison of Adaptive Weight Norms (a)Without Sensor Noise (b)With Sensor Noise

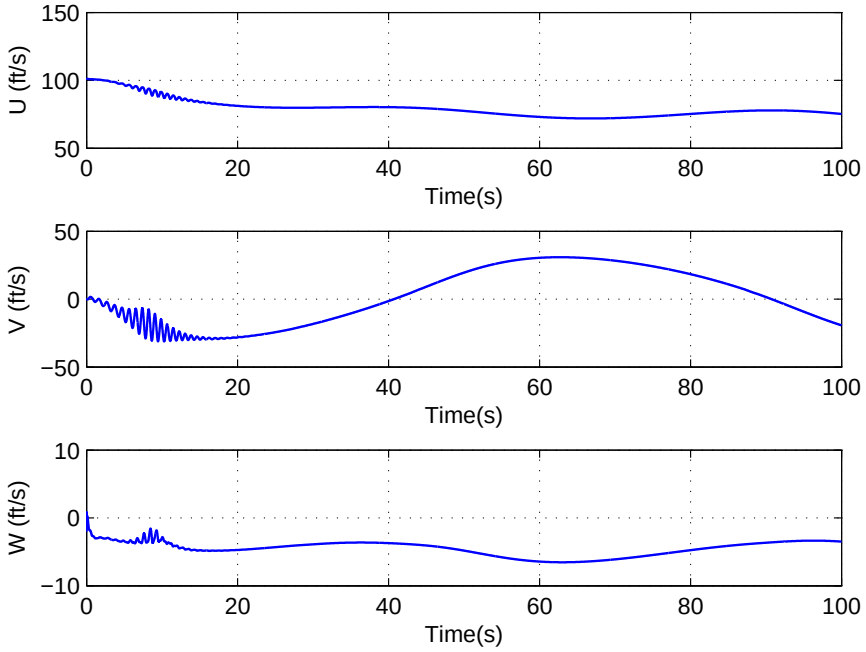


Figure 3.31: Body Velocities of the Helicopter with Lateral Sine Input

### 3.5.2.2 Results with SHL-NN

Adaptive controller constructed with single hidden layer neural network is implemented to the attitude control of the helicopter in this section. This structure of neural networks is preferred for more complex applications like multi-channel control since even one hidden layer improves the nonlinear function approximation significantly. The output of the adaptive control is a vector containing the adaptive elements of attitude channels $(\phi, \theta, \psi)$. With this structure, uncertainties in all three channels are compensated with a neural network. The system is illustrated with a block diagram in Fig. 3.32.

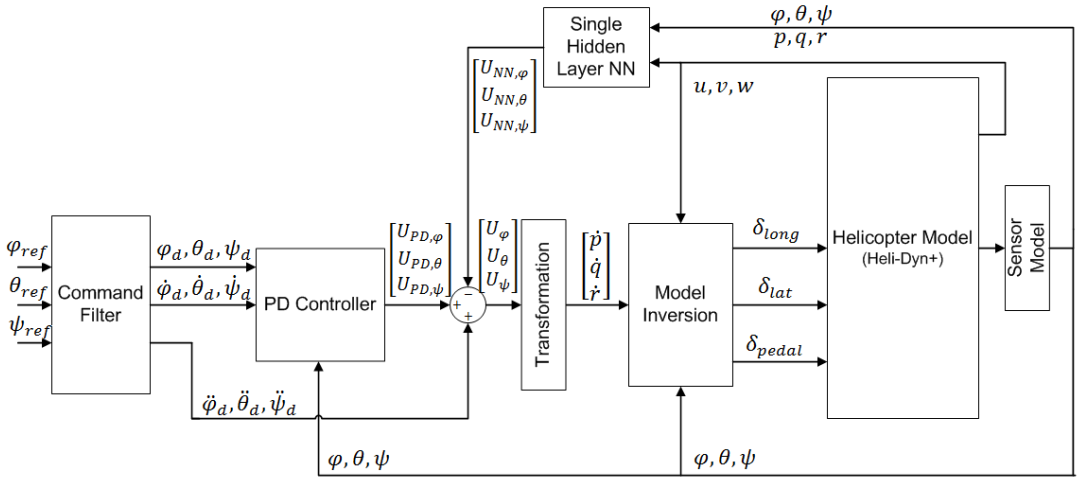


Figure 3.32: Block Diagram of the System with SHL

Input layer of SHL-NN is composed of 14 inputs including the bias term, and all the inputs are scaled to the same order. Number of hidden neurons are chosen to be 10 and there are 3 outputs which are adaptive control elements of roll, pitch and yaw channel. Neural network inputs are chosen to be;

$$\bar{x} = [\phi_{com} \quad \theta_{com} \quad \psi_{com} \quad \phi \quad \theta \quad \psi \quad u \quad v \quad w \quad p \quad q \quad r \quad ||Z|| \quad b_1]^T \tag{3.63}$$

where $||Z||$ represents the Frobenius norm of matrix Z, which is defined as

$$Z = \begin{bmatrix} W & 0 \\ 0 & V \end{bmatrix} \tag{3.64}$$

Activation potentials of the neurons are chosen to be:

$$a = [110 \;\; 100 \;\; 50 \;\; 20 \;\; 1 \;\; 0.1 \;\; 0.01 \;\; 0.001 \;\; 0.0001 \;\; 0.0001]$$

Feedback gains of the PD controller are chosen such that natural frequency of the desired dynamics is 1 rad/s and its damping ratio is 0.8. In addition, Kalman Filter parameters for SHL-NN structure are chosen to be $S_{10} = S_{20} = I, R_1 = R_2 = 0.1I$ and $Q_1 = Q_2 = 0.01I$ for all maneuvers.

Simulations are performed for longitudinal and lateral channels with step input similar to the case with LPNN.

**Longitudinal Channel**

15 degree step input is fed to the longitudinal channel which is the pitch channel. Other channels $(\phi, \psi)$ are kept at zero reference. Figure 3.33 shows the attitude channels and the pitch rate $(q)$ of the helicopter with baseline adaptive law, standard e-modification and KF-based e-modification. The improvement of the KF-based e-modification is clearly seen from the pitch angle $(\theta)$ and the pitch rate $(q)$ which is the result of the variable modification gain obtained with Kalman approach.

Helicopter control inputs (longitudinal, lateral and pedal inputs) are shown in Figure 3.34. Improvement of the KF-based e-modification on control effort is observed from the longitudinal control input. The result of KF-based e-modification is less oscillatory compared to its alternatives which relieves the load at the swashplate.

Sensor noise is taken into account and a performance evaluation is performed for longitudinal maneuver. The system responses are provided in Figure 3.35 and the control inputs are provided in Figure 3.36. Similar to the nominal case, results with KF-based e-modification are less oscillatory in terms of both system response and control effort. In addition, it achieves the required tracking.

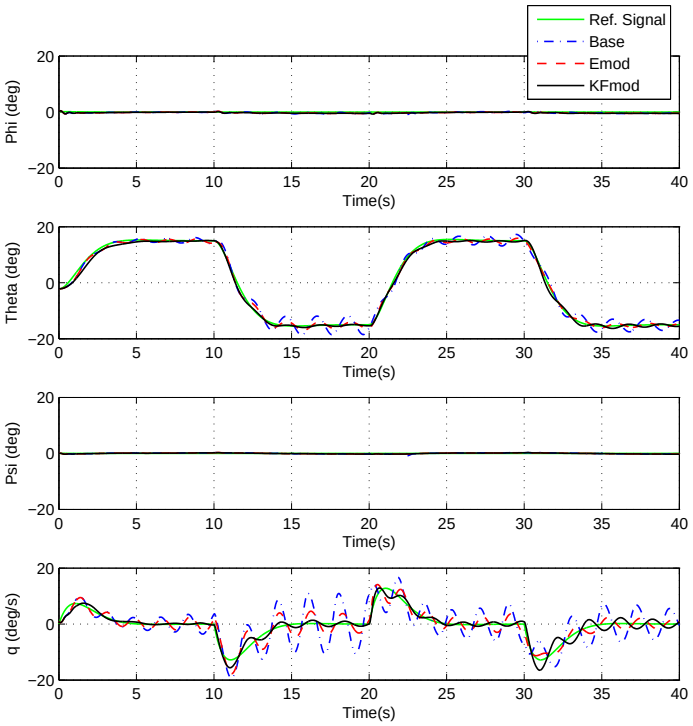


Figure 3.33: Helicopter Response to Longitudinal Input with and without Modification (SHL) ($\gamma = \gamma\sigma_e = \gamma\sigma_{kf} = 5$)

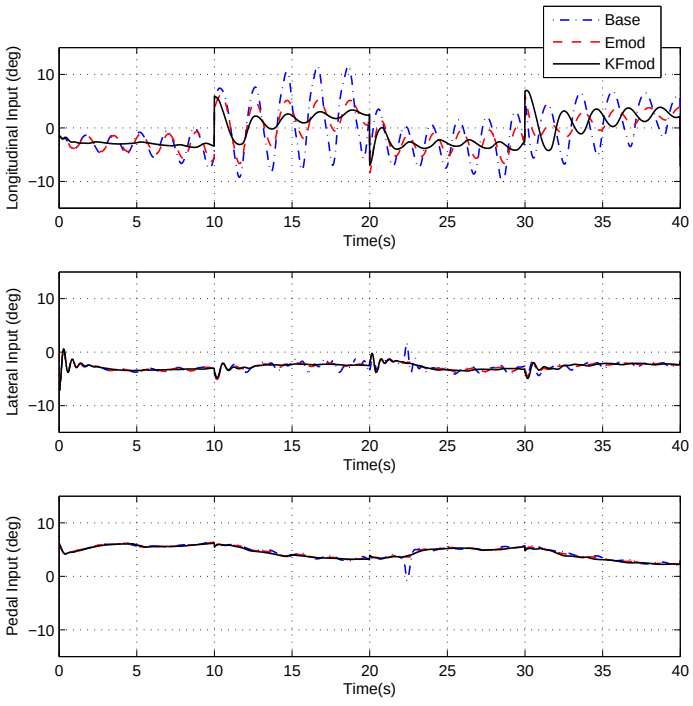


Figure 3.34: Helicopter Control Inputs with and without Modification for Longitudinal Maneuver (SHL)

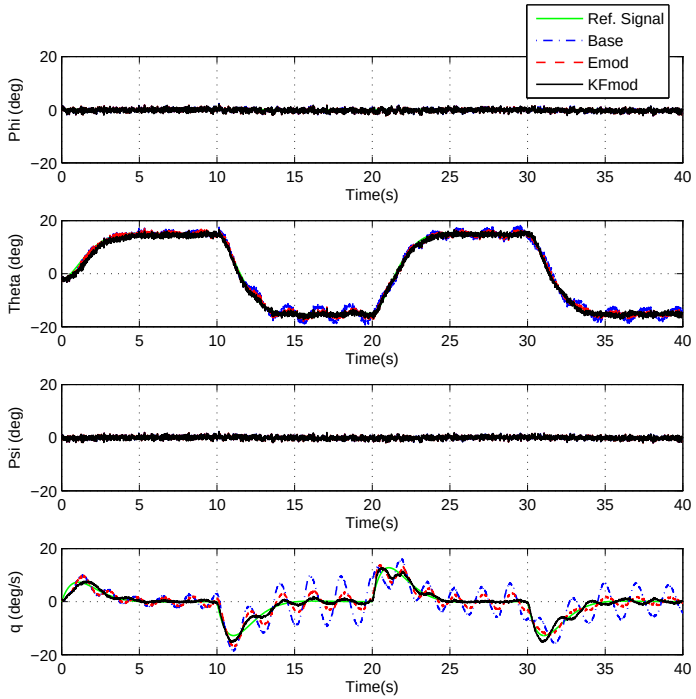


Figure 3.35: Helicopter Response to Longitudinal Input under Sensor Noise with and without Modification (SHL) ($\gamma = \gamma\sigma_e = \gamma\sigma_{kf} = 5$)

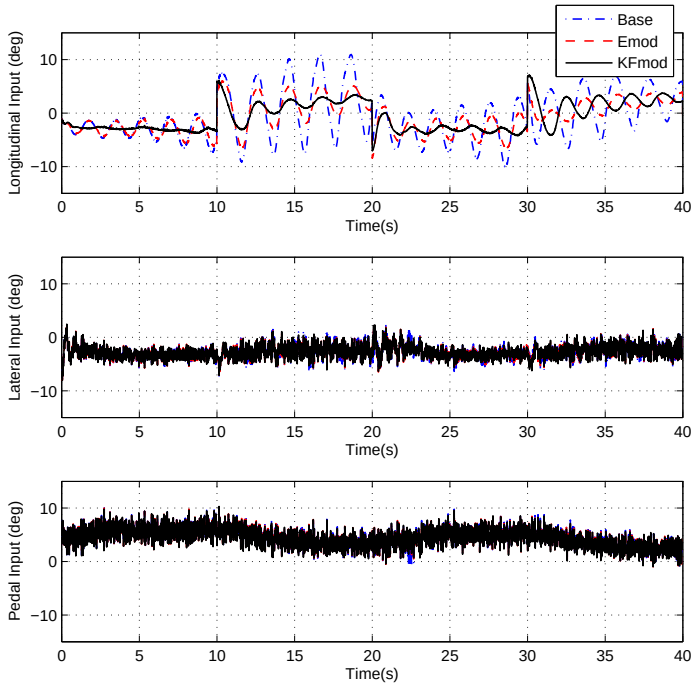


Figure 3.36: Helicopter Control Inputs under Sensor Noise with and without Modification for Longitudinal Maneuver (SHL)

Adaptive control effort is compared in terms of weight norms in Figure 3.37 for nominal case and when the system is under sensor noise. The norm of the neural network weights with KF-based e-modification is smaller compared to its alternatives illustrating its efficiency.

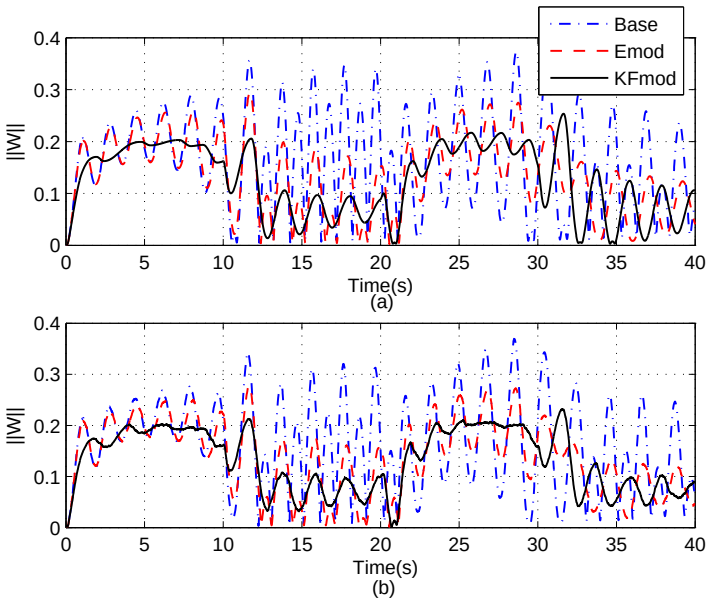


Figure 3.37: Comparison of Adaptive Weight Norms for SHL-NN (a)Without Sensor Noise (b)With Sensor Noise

Body velocities of the helicopter during longitudinal maneuver are given in Figure 3.38.

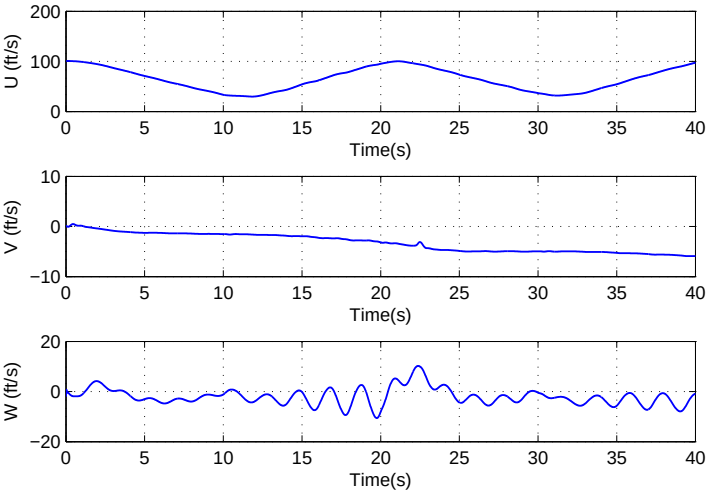


Figure 3.38: Body Velocities of the Helicopter During Longitudinal Maneuver (SHL)

**Lateral Channel**

In order to analyze the performance of KF approach in lateral channel, 15 degree step input is fed to the phi channel ($\phi$). Other channels ($\theta, \psi$) are kept at zero reference. Figure 3.39 shows the attitude channels and the roll rate ($p$) of the helicopter with baseline adaptive law, standard e-modification and KF-based e-modification. The difference between results are not very noticeable in this simulation compared to the longitudinal channel. However, oscillations occur in roll rate for baseline adaptive law and standard e-modification, whereas KF approach provides smooth system response without any oscillations. Figure 3.40 shows the helicopter control input comparison for different adaptive laws. It is observed from the figure that KF approach eliminates the oscillations for both longitudinal and lateral control inputs. This expresses the effectiveness of single hidden neural network over LPNN. Although the maneuver is lateral, neural network adapts the system also in longitudinal channel.

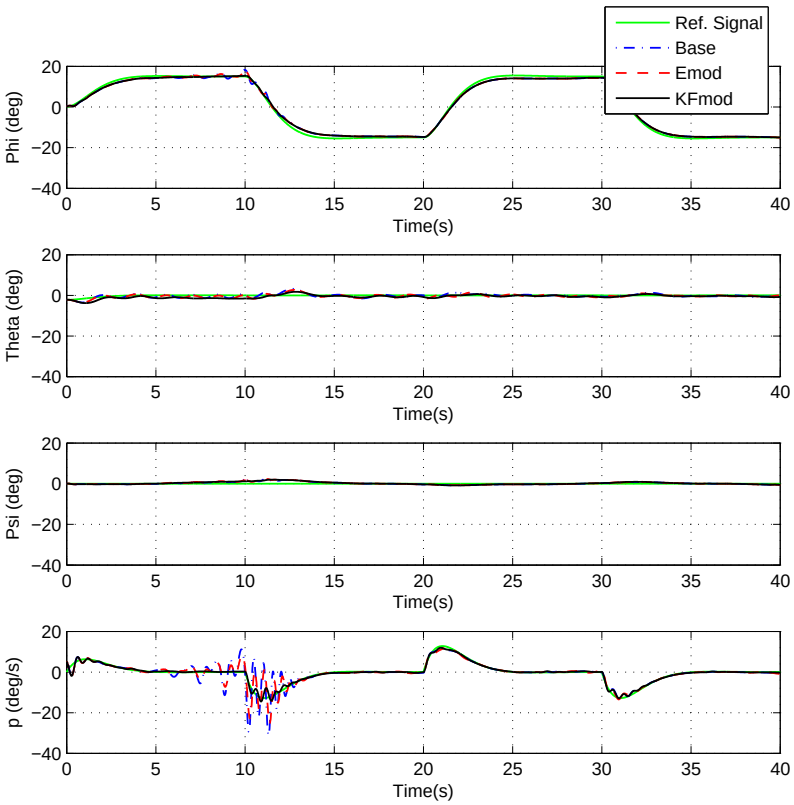


Figure 3.39: Helicopter Response to Lateral Input with and without Modification (SHL) ($\gamma = \gamma\sigma_e = \gamma\sigma_{kf} = 5$)

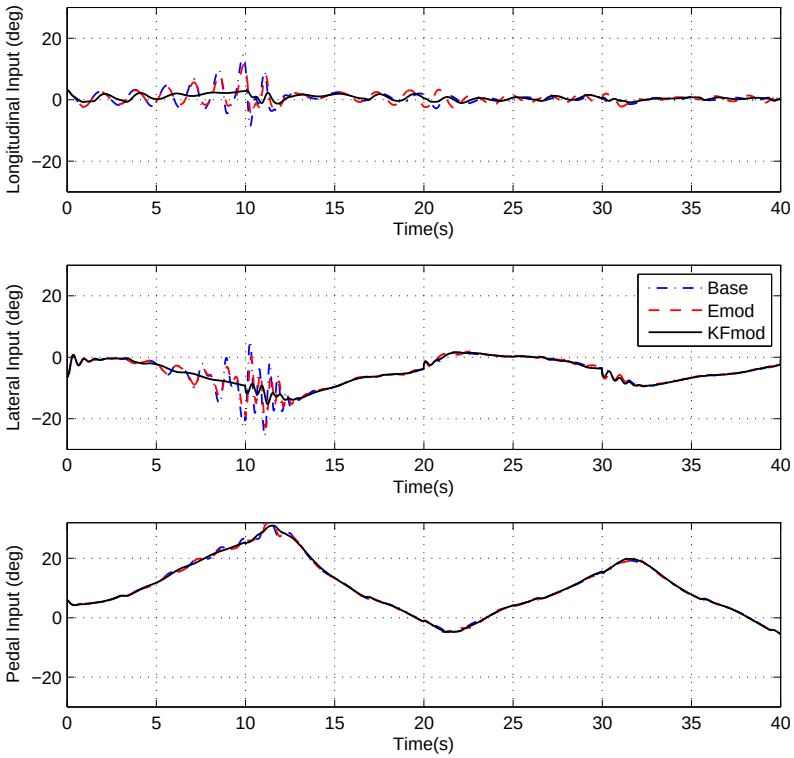


Figure 3.40: Helicopter Control Inputs with and without Modification for Lateral Maneuver (SHL)

Figures 3.41 and 3.42 show the results when the system is under sensor noise. However, no significant improvement of KF approach is observed in this scenario. On the other hand, KF-based e-modification does not perform worse than its alternatives. There are slight improvements in the results; however, they are not as obvious as the results of the other cases.

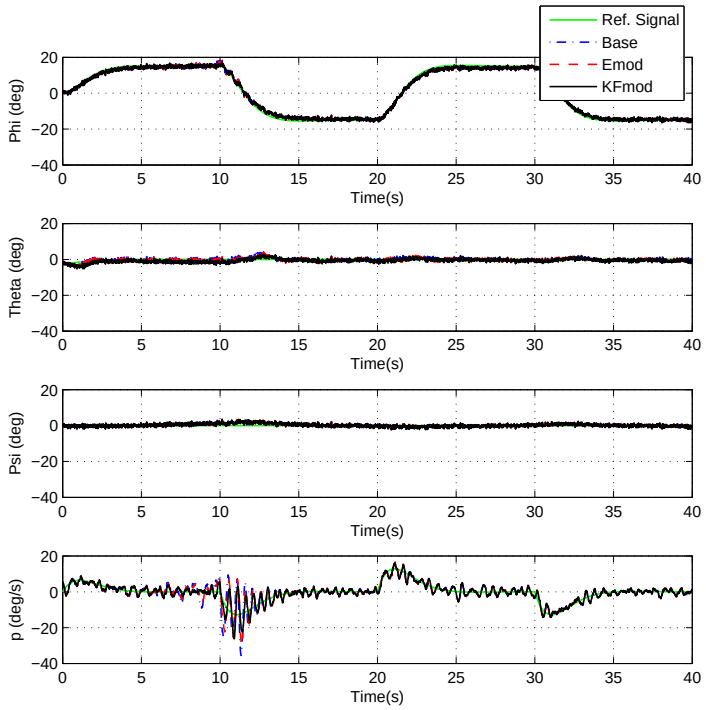


Figure 3.41: Helicopter Response to Lateral Input under Sensor Noise with and without Modification (SHL) ($\gamma = \gamma\sigma_e = \gamma\sigma_{kf} = 5$)

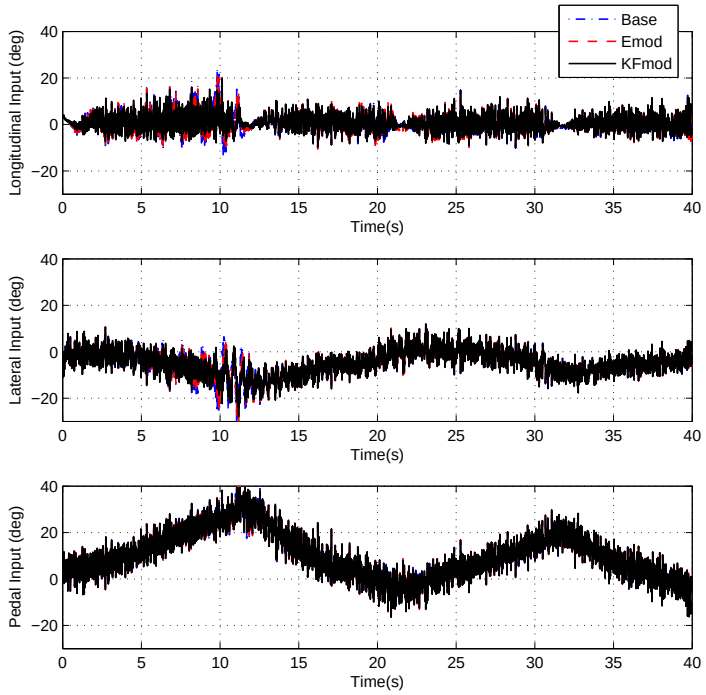


Figure 3.42: Helicopter Control Inputs under Sensor Noise with and without Modification for Lateral Maneuver

Adaptive control effort is compared in terms of weight norms in Figure 3.43 for nominal case and when the system is under sensor noise.

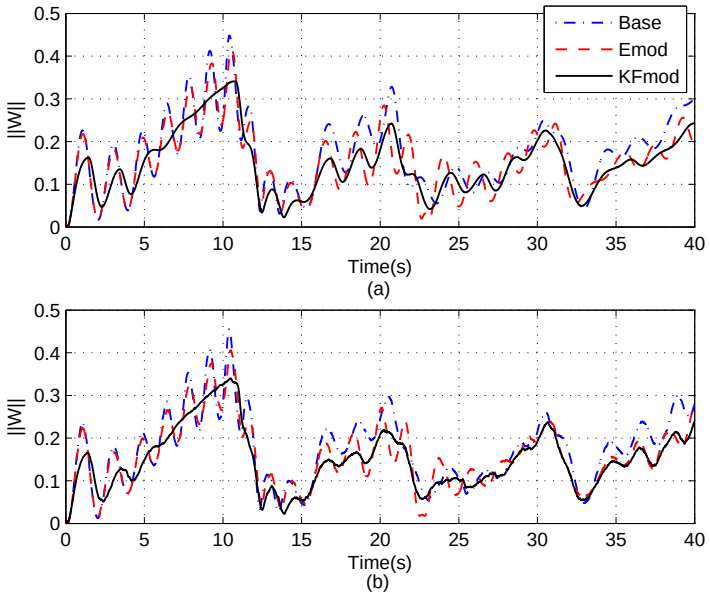


Figure 3.43: Comparison of Adaptive Weight Norms for Lateral Maneuver (a)Without Sensor Noise (b)With Sensor Noise

Body velocities of the helicopter during lateral maneuver are given in Figure 3.44.

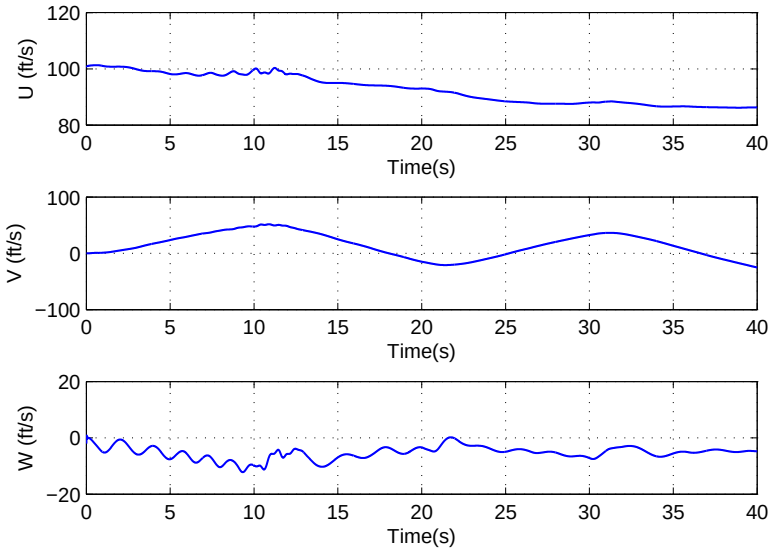


Figure 3.44: Body Velocities of the Helicopter During Lateral Maneuver (SHL)

Choosing the Kalman Filter parameters may need some tuning to obtain these results. If these paremeters are not tuned, tracking may not be satisfied in the required level. However, from the simulation analysis, it is seen that adaptive law with Kalman Filter based modification term does not induce extra oscillations to the system.

# CHAPTER 4

# CONCLUSION

In this thesis, two Kalman Filter based applications are implemented to a high-fidelity helicopter model. In the first application, a navigation filter using a Kalman Filter is designed. The objectives are to add a sensor model to the helicopter model, to simulate the inertial sensors' error characteristics (accelerometers and gyoscopes), to add a GNSS model to simulate the characteristics of GNSS solutions and to design INS/GNSS integration algorithm by using Kalman Filter to obtain an accurate navigation solution. The second application is the use of the Kalman Filter approach in adaptive control as a modification term. The objectives are to design an attitude controller for the helicopter, to augment it with neural networks to adapt for the uncertainties existing in the system and to use a Kalman Filter approach in the modification term of the update law.

In the first part, the error characteristics of a MEMS inertial sensors are modeled. Then inertial navigation algorithm is designed to obtain attitude, velocity and position of the helicopter from the inertial sensor outputs. Next, INS solution is aided with a GNSS to estimate the accumulated sensor errors in inertial navigation solution and correct them in the system to obtain a reliable navigation solution of the helicopter. A GNSS model is constructed with a typical position and velocity errors of the receivers on the market. Kalman filter is designed and navigation errors are estimated (position, velocity and attitude) as well as sensor bias errors.

The validation of the Kalman Filter algorithm is performed with simulations. Performance of the integration algorithm is studied with a flight scenario consisting of both longitudinal and lateral maneuvers. The results are analyzed in terms of estimation

errors and error covariances. It is observed that the stand-alone inertial navigation solutions diverge from the true solution with time. On the other hand, corrected navigation solutions of the Kalman Filter provides a solution with small and bounded errors. Errors between integrated navigation and true solutions are observed to be in covariances which are obtained through the Kalman Filter indicating that results are consistent. Thus, the accuracy of the Kalman Filter algorithm is validated. Furthermore, estimated sensor bias errors reach the actual sensor error values which also point to the accuracy of the Kalman filter. In addition, a significant disadvantage of the system is also studied, which is GNSS signal outage. This case is also simulated and the improvement of GNSS aiding is observed. Accumulated errors during the signal outage are estimated and compensated by Kalman Filter just after reacquisition. Moreover, performance of Kalman Filter is also investigated through the difference between actual observations and predicted observations. The difference between the measurements and estimated values by Kalman Filter is seen to be zero-mean. This means that estimation of the Kalman filter is consistent with the measurements indicating that Kalman filter works optimally throughout the simulation.

In the second part, a model inversion based controller with a neural network adaptive element is designed to control the attitude of the helicopter, namely Euler angles. Kalman Filter (KF) approach is used in the modification term of the neural networks. The rather well-known e-modification is reformulated with this approach and added to the baseline adaptation law. Linear-in-the parameter and single hidden layer neural networks are adopted as the structure to analyze the performance of the adaptive controller both in single channel and multi channel.

Performance is evaluated and compared with other traditional update laws in terms of system response, tracking performance and control effort with simulations. It is observed that the KF-approach results in a less oscillatory control input. This is a result of the variable modification gain obtained with KF approach. With variable modification gain, the network gain is adjusted while the tracking error is compensated for and becomes smaller. Thus, it eliminates the unnecessary control effort arising due to fixed modification gain. In existing modification terms, this fixed gain is selected higher in consideration of possible large modeling errors. To achieve the required tracking, high learning gains result in oscillatory control inputs. These os-

cillatory inputs can excite the unmodeled dynamics and may lead to instability. On the other hand, with KF approach, smoother control inputs with less oscillations are provided through variable modification gain. This is a significant improvement, since this would relieve control effort and therefore the loads at the swashplate of the helicopter. Moreover, as a result of smoother control input, the KF approach provides smoother system response than its alternatives and also achieves the required tracking. From all simulations with different maneuvers and neural network structures, similar results are observed using the KF-approach.

The performance of the KF-based e-modification is evaluated also when there is sensor noise. The system response, tracking performance and the control effort of the helicopter are compared for the baseline adaptive law, standard e-modification and KF-based e-modification. Similar to the cases where there is no sensor noise, it is observed that KF-based e-modification provides the best results with less oscillatory system response and control effort in all simulation scenarios.

It is seen that selection of Kalman Filter parameters influences the tracking and it may be necessary to tune these parameters for the required tracking performance. However, results have shown that Kalman Filter based modification term does not cause divergence of the system response.

As a conclusion, integrated navigation and control systems are developed for a high-fidelity helicopter. With the help of GNSS aiding, helicopter can navigate accurately with low cost sensors at both short- and long-term missions. Accurate navigation solution is also critical for the performance of the control system to provide the true system response to the controller so that the controller is able to produce the necessary control inputs. Attitude control of the helicopter is fulfilled and augmented with neural networks to sustain the performance of the helicopter under uncertainties. Kalman Filter approach is used in the design of the adaptive controller and less oscillatory system response and control effort are achieved. Similar results are also obtained when the system is under sensor noise.

## 4.1 Future Work

The research carried out in this thesis can be extended in the future as follows:

- Kalman Filter designed for INS/GNSS integration can be improved to handle non-linear system or measurements, unknown system or measurement noise standard deviations or non-Gausssian measurement distributions by extending the Kalman Filter to Extended KF, Unscented KF or Adaptive KF.
- Adaptive controller with KF approach can be challenged with different maneuvers
- KF approach in adaptive control can be implemented to the modification terms in literature other than e-modification.
- E-modification obtained in this work with KF approach can be combined with other adaptive control techniques such as Concurrent Learning.
- KF approach in adaptive control can be adopted not only for modification term but also for the whole adaptation law. Thus, learning rate of the neural networks would be variable and this improves the system response and control effort more effectively.

# REFERENCES


[1] I. Yavrucuk, O. Tarimci, M. Katircioglu, E. Kubali, and D. Yilmaz. A new Helicopter Simulation and Analysis Tool: Helidyn+. In *the Thirty-Sixth European Rotorcraft Forum*, 2010.

[2] M. Jun, S. I. Roumeliotis, and G. S. Sukhatme. State Estimation of an Autonomous Helicopter Using Kalman Filtering. In *IEEE/RSJ International Conference on Intelligent Robots and Systems*, 1999.

[3] D. Choukroun, I. Y. Bar-Itzhack, and Y. Oshman. A Novel Quaternion Kalman Filter. *IEEE Transactions on Aerospace and Electronic Systems*, 2006.

[4] S. Godha and M. E. Cannon. Integration of DGPS with a Low Cost MEMS - Based Inertial Measurement Unit (IMU) for Land Vehicle Navigation Application. In *ION GPS/GNSS*, 2005.

[5] T. Gao, Z. Gong, J. Lun, W. Ding, and W. Feng. An Attitude Determination System For a Small Unmanned Helicopter Using Low-Cost Sensors. In *IEEE International Conference on Robotics and Biomimetics*, 2006.

[6] C. Perez-D'Arphino et al. Development of a Low Cost Inertial Measurement Unit for UAV Applications with Kalman Filter based Attitude Determination. In *IEEE International Conference on Practical Robot Applications*, 2011.

[7] W. YongLiang, W. TianMiao, L. JianHong, W. ChaoLei, and Z. Chen. Attitude Estimation for Small Helicopter Using Extended Kalman Filter. In *IEEE Conference on Robotics, Automation and Mechatronics*, 2008.

[8] T. K. Lau, Y. Liu, and K. Lin. A Robust State Estimation Method Against GNSS Outage for Unmanned Miniature Helicopters. In *IEEE International Conference on Robotics and Automation*, 2010.

[9] S. Oh. Multisensor Fusion for Autonomous UAV Navigation Based on the Unscented Kalman Filter with Sequential Measurement Updates. In *IEEE International Conference on Multisensor Fusion and Integration for Intelligent Systems*, 2010.

[10] Y. Pan, P. Song, K. Li, Y. Zhou, and Y. Wang. Attitude Estimation of Miniature Unmanned Helicopter Using Unscented Kalman Filter. In *International Conference on Transportation, Mechanical and Electrical Engineering*, 2011.

[11] L. N. Hieu and V. H. Nguyen. Loosely Coupled GPS/INS Integration with Kalman Filtering for Land Vehicle Applications. In *IEEE International Conference on Control, Automation and Information Sciences*, 2012.

[12] H. Nakanishi, S. Kanata, and T. Sawaragi. GPS-INS-BARO Hybrid Navigation System Taking into Account Ground Effect for Autonomous Unmanned Helicopter. In *IEEE International Symposium on Safety, Security and Rescue Robotics*, 2012.

[13] K.S. Narendra and P. Kudva. Stable Adaptive Schemes for System Identification and Control: Part I,II. *IEEE Transactions on Systems, Man and Cybernetics*, 1974.

[14] K.S. Narendra and L.S. Valavani. Stable Adaptive Observers and Controllers. *Proceedings of the IEEE*, 1976.

[15] P. A. Ioannou and P. V. Kokotovic. Instability Analysis and Improvement of Robustness of Adaptive Control. *Automatica*, 20(5), 1984.

[16] K. S. Narendra and A. M. Annaswamy. A New Adaptive Law for Robust Adaptation Without Persistent Excitation. *IEEE Transactions on Automatic Control*, 32(2), 1987.

[17] K. Y. Volyanskyy, A. J. Calise, and B. Yang. A Novel Q-Modification Term for Adaptive Control. In *American Control Conference*, June 2006.

[18] N. T. Nguyen, K. Krishnakumar, and J. Boskovic. An Optimal Control Modification to Model-Reference Adaptive Control for Fast Adaptation. In *AIAA Guidance, Navigation and Control Conference*, August 2008.

[19] K. Kim, T. Yucelen, and A. J. Calise. K Modification in Adaptive Control. In *AIAA Infotech Conference*, 2010.

[20] K. Kim, T. Yucelen, and A. J. Calise. K Modification based H2 Adaptive Control. In *AIAA Guidance, Navigation and Control Conference*, August 2010.

[21] G.V. Chowdhary. *Concurrent Learning for Convergence in Adaptive Control Without Persistency of Excitation*. PhD thesis, Daniel Guggenheim School of Aerospace Engineering, 2010.

[22] G. Chowdhary and E. Johnson. Recursively Updated Least Squares Based Modification Term for Adaptive Control. In *American Control Conference*, June-July 2010.

[23] T. Yücelen and A. J. Calise. Kalman Filter Modification in Adaptive Control. *AIAA Journal of Guidance, Control and Dynamics*, 33(2), March-April 2010.

[24] A. S. Krupadanam, A. M. Annaswamy, and R. S. Mangoubi. Multivariable Adaptive Control Design with Applications to Autonomous Helicopters. *AIAA Journal of Guidance, Control and Dynamics*, 2002.

[25] G. N. Johnson and S. K. Kannan. Adaptive Flight Control for an Autonomous Unmanned Helicopter. In *AIAA Guidance, Navigation and Control Conference and Exhibit*, August 2002.

[26] A. J. Calise and R. T. Rysdyk. Adaptive Model Inversion Flight Control for Tiltrotor Aircraft. In *AIAA Guidance, Navigation and Control Conference*, 1997.

[27] O. Tarimci. Adaptive Control Applications for Rotary Wing Aircraft Models of Varying Simulation Fidelity. Master's thesis, Middle East Technical University.

[28] B. S. Kim and A. J. Calise. Nonlinear Flight Control using Neural Networks. *AIAA Journal of Guidance, Control and Dynamics*, 1997.

[29] J. Leitner, A. J. Calise, and J. V. R. Prasad. Analysis of Adaptive Neural Networks for Helicopter Flight Controls. In *AIAA Guidance, Navigation and Control Conference*, 1995.

[30] P. D. Groves. *Principles of GNSS, Inertial and Multisensor Integrated Navigation Systems*. Artech House, 2008.

[31] J. A. Farrell. *Aided Navigation: GPS with High Rate Sensors*. McGraw Hill Professional, 2008.

[32] H. D. Lopes, E. Kampen, and Q.P. Chu. Attitude Determination of Highly Dynamic Fixed-wing UAVs with GPS/MEMS-AHRS Integration. In *AIAA Guidance, Navigation and Control Conference*, 2012.

[33] A. J. Calise and R. T. Rysdyk. Nonlinear Adaptive Flight Control using Neural Networks. *IEEE Control Systems Magazine*, 1998.

[34] J.-J.E. Slotine and W. Li. *Applied Nonlinear Control*. Prentice Hall, 1991.

[35] E. Lavretsky. Adaptive Control. Lecture Notes of California Institute of Technology, 2005.

[36] R. Chandramohan, T. Yucelen, A. J. Calise, and G. Chowdhary. Experimental Results for Kalman Filter Modification in Adaptive Control. In *AIAA Infotech@Aerospace Conference*, 2010.

[37] S. Karsoliya. Approximating Number of Hidden Layer Neurons in Multiple Hidden Layer BPNN Architecture. *International Journal of Engineering Trends and Technology*, 2012.

[38] G. V. Chowdhary and E. N. Johnson. Theory and Flight-Test Validation of a Concurrent-Learning Adaptive Controller. *AIAA Journal of Guidance, Control and Dynamics*, 34(2), March-April 2011.

# APPENDIX A

# MATRICES IN KALMAN FILTER FOR NAVIGATION

Error Propagation Matrix:

$$F = \begin{pmatrix} F_{11} & F_{12} & F_{13} & 0_3 & C_b^n \\ F_{21} & F_{22} & F_{23} & C_b^n & 0_3 \\ 0_3 & F_{32} & F_{33} & 0_3 & 0_3 \\ 0_3 & 0_3 & 0_3 & 0_3 & 0_3 \\ 0_3 & 0_3 & 0_3 & 0_3 & 0_3 \end{pmatrix} \tag{A.1}$$

where

$$F_{11} = -\left[\omega_{in}^n \times\right] = \begin{bmatrix} 0 & \frac{V_{ib,E}\tan L}{R_0+h} & -\frac{V_{ib,N}}{R_0+h} \\ -\frac{V_{ib,E}\tan L}{R_0+h} & 0 & -\frac{V_{ib,E}}{R_0+h} \\ \frac{V_{ib,N}}{R_0+h} & \frac{V_{ib,E}}{R_0+h} & 0 \end{bmatrix} \tag{A.2}$$

$$F_{12} = \begin{bmatrix} 0 & -\frac{1}{R_0(L)+h} & 0 \\ \frac{1}{R_0(L)+h} & 0 & 0 \\ 0 & \frac{\tan L}{R_0(L)+h} & 0 \end{bmatrix} \tag{A.3}$$

$$F_{13} = \begin{bmatrix} 0 & 0 & \frac{V_{ib,E}}{(R_0+h)^2} \\ 0 & 0 & -\frac{V_{ib,N}}{(R_0+h)^2} \\ \frac{V_{ib,E}}{(R_0+h)\cos^2 L} & 0 & -\frac{V_{ib,E}\tan L}{(R_0(L)+h)^2} \end{bmatrix} \tag{A.4}$$

$$F_{21} = -\left[C_b^n f_{ib}^b \times\right] \tag{A.5}$$

$$F_{22} = \begin{bmatrix} \frac{V_{ib,D}}{R_0+h} & -\frac{2V_{ib,E}\tan L}{R_0+h} & \frac{V_{ib,N}}{R_0+h} \\ \frac{V_{ib,E}\tan L}{R_0+h} & \frac{V_{ib,N}\tan L+V_{ib,D}}{R_0+h} & \frac{V_{ib,E}}{R_0+h} \\ -\frac{2V_{ib,N}}{R_0+h} & -\frac{2V_{ib,E}}{R_0+h} & 0 \end{bmatrix} \tag{A.6}$$

$$F_{23} = \begin{bmatrix} -\frac{(V_{ib,E})^2\sec^2 L}{R_0+h} & 0 & \frac{(V_{ib,E})^2\tan L}{(R_0+h)^2} - \frac{V_{ib,N}V_{ib,D}}{(R_0+h)^2} \\ \frac{V_{ib,N}V_{ib,E}\sec^2 L}{R_0+h} & 0 & -\frac{V_{ib,N}V_{ib,E}\tan L+V_{ib,E}V_{ib,D}}{(R_0+h)^2} \\ 0 & 0 & \frac{(V_{ib,E})^2+(V_{ib,N})^2}{(R_0(L)+h)^2} - \frac{2g}{R_0} \end{bmatrix} \tag{A.7}$$

$$F_{32} = \begin{bmatrix} \frac{1}{R_0+h} & 0 & 0 \\ 0 & \frac{1}{(R_0+h)\cos L} & 0 \\ 0 & 0 & -1 \end{bmatrix} \tag{A.8}$$

$$F_{33} = \begin{bmatrix} 0 & 0 & -\frac{V_{ib,N}}{(R_0+h)^2} \\ \frac{V_{ib,E}\sin L}{(R_0+h)\cos^2 L} & 0 & -\frac{V_{ib,E}}{(R_0+h)^2\cos L} \\ 0 & 0 & 0 \end{bmatrix} \tag{A.9}$$

Noise Matrix:

$$G = \begin{pmatrix} 0_3 & C_b^n & 0_3 & 0_3 \\ C_b^n & 0_3 & 0_3 & 0_3 \\ 0_3 & 0_3 & 0_3 & 0_3 \\ 0_3 & 0_3 & I_3 & 0_3 \\ 0_3 & 0_3 & 0_3 & I_3 \end{pmatrix} \tag{A.10}$$

Initial Error Covariance Matrix:

$$P_0 = \begin{pmatrix} (\Delta_{Att0})^2 & 0_3 & 0_3 & 0_3 & 0_3 \\ 0_3 & (\Delta_{Vel0})^2 & 0_3 & 0_3 & 0_3 \\ 0_3 & 0_3 & (\Delta_{Pos0})^2 & 0_3 & 0_3 \\ 0_3 & 0_3 & 0_3 & (\Delta_{Acc0})^2 & 0_3 \\ 0_3 & 0_3 & 0_3 & 0_3 & (\Delta_{Gyr0})^2 \end{pmatrix} \tag{A.11}$$

where $\Delta_{Att0}$ :Initial Attitude Uncertainty,

$\Delta_{Vel0}$ : Initial Velocity Uncertainty,

$\Delta_{Pos0}$ : Initial Position Uncertainty,

$\Delta_{Acc0}$ : Initial Accelerometer Uncertainty,

$\Delta_{Gyr0}$ : Initial Gyroscope Uncertainty.

System Noise Matrix:

$$Q = \begin{pmatrix} \sigma^2_{Att} & 0_3 & 0_3 & 0_3 \\ 0_3 & \sigma^2_{Vel} & 0_3 & 0_3 \\ 0_3 & 0_3 & \sigma^2_{Acc} & 0_3 \\ 0_3 & 0_3 & 0_3 & \sigma^2_{Gyr} \end{pmatrix} \tag{A.12}$$

where $\sigma^2_{Att}$ : Random Noise in Gyroscopes,

$\sigma^2_{Vel}$ : Random Noise in Accelerometers,

$\sigma^2_{Acc}$ : Bias Drift in Accelerometers,

$\sigma^2_{Gyr}$ : Bias Drift in Gyroscopes.

Measurement Noise Matrix:

$$R = \begin{pmatrix} \sigma^2_{PosHor} & 0 & 0 & 0 & 0 & 0 \\ 0 & \sigma^2_{PosHor} & 0 & 0 & 0 & 0 \\ 0 & 0 & \sigma^2_{PosVer} & 0 & 0 & 0 \\ 0 & 0 & 0 & \sigma^2_{VelHor} & 0 & 0 \\ 0 & 0 & 0 & 0 & \sigma^2_{VelHor} & 0 \\ 0 & 0 & 0 & 0 & 0 & \sigma^2_{VelVer} \end{pmatrix} \tag{A.13}$$

where $\sigma^2_{PosHor}$ : GNSS Horizontal Position Uncertainty,

$\sigma^2_{PosVer}$ : GNSS Vertical Position Uncertainty,

$\sigma^2_{VelHor}$ : GNSS Horizontal Velocity Uncertainty,

$\sigma^2_{VelVer}$ : GNSS Vertical Velocity Uncertainty.